

Université du Québec  
Institut national de la recherche scientifique  
Centre Eau Terre Environnement

## **TESTS DE RÉPONSE THERMIQUE DISTRIBUÉS AVEC CÂBLES CHAUFFANTS**

Par  
Maria Isabel Vélez Márquez

Mémoire présentée pour l'obtention du grade de  
Maître ès sciences (M.Sc.)  
en sciences de la terre

### **Jury d'évaluation**

Président du jury et examinateur interne	Bernard Giroux INRS – Eau, Terre et Environnement
Examinateur externe	Mikael Philippe Division de georesources Bureau de recherches géologiques et minières (BRGM)
Directeur de recherche	Jasmin Raymond INRS – Eau, Terre et Environnement
Codirecteur de recherche	Daniela Blessent Universidad de Medellín



## **REMERCIEMENTS**

Tout d'abord je remercie mon directeur de recherche, Jasmin Raymond et ma codirectrice Daniela Blessent pour leurs conseils, leur disponibilité et leur soutien tout au long du projet. Je les remercie également pour leur ouverture d'esprit qui m'a permis d'effectuer ce projet entre le Québec, la Colombie et la France, et de participer au projet IGCP 636.

Je remercie Mikael Philippe d'avoir accepté de travailler avec nous, pour m'avoir accueilli au sein de la division de Georessources au BRGM, ainsi que pour toute sa collaboration lors de la réalisation du deuxième test de réponse thermique sans lequel ce travail n'aurait pas pu être accompli.

Merci à Nataline Simon, Nicolas L'avenant, Claude Hugo Koubikana, Olivier Bour, et Louis Lamarche pour leur contribution de grande importance pour mener à bien ce travail.

Je remercie aussi Claude Hugo Koubikana et Nehed Jaziri pour m'avoir accueilli à mon arrivée à l'INRS, pour toutes les séances d'études et pour leur patience envers mon français.

Un grand merci à Simon Gernez pour son soutien inconditionnel, pour sa patiente relecture et pour m'avoir aidé à voir les choses sous différentes perspectives, mais aussi à Oscar, Brillith et Sébastien pour toutes les aventures vécues entre Québec, Medellín et Bogotá.

Un merci spécial à ma famille et mes parents qui m'ont toujours accompagné malgré la distance, et à mes amis en Colombie et à Québec avec qui j'ai partagé des moments inoubliables au cours de ces dernières années.



## RÉSUMÉ

Les tests de réponse thermique (TRT) sont utilisés pour évaluer la conductivité thermique du sous-sol lors de la conception des systèmes de pompe à chaleur géothermique. Pour effectuer un test conventionnel, une source de haute puissance est requise pour chauffer l'eau qui circule dans l'échangeur de chaleur pilote. Une nouvelle méthode d'essai avec un câble chauffant a été développée comme une alternative pour effectuer le test avec une source d'énergie de basse puissance et un équipement compact. Deux tests de réponse thermique ont été réalisés dans des échangeurs de chaleur expérimentaux d'environ 100 m de profondeur. Le premier test a été effectué aux Laboratoires pour l'innovation scientifique et technologique de l'environnement (LISTE) de l'INRS à Québec, en utilisant un câble chauffant en sections. Le deuxième test a été réalisé à la plate-forme expérimentale de géothermie du Bureau de Recherche Géologique et Minières (BRGM) en France, localisé à Orléans, avec un câble chauffant continu.

Le suivi de l'évolution de la température au cours de deux essais a été fait à l'aide de capteurs submersibles et des mesures distribuées de la température avec fibre optique (FO-DTS). Les données de température des capteurs submersibles ont été utilisées pour estimer la conductivité thermique du sous-sol à différentes profondeurs et les données de température de la fibre optique ont été employées pour évaluer la présence de convection naturelle dans l'échangeur de chaleur pendant les tests. Les résultats obtenus ont été comparés aux TRTs conventionnels effectués dans les mêmes échangeurs de chaleur. Une différence maximale de 15 % entre la conductivité thermique moyenne estimée avec les câbles chauffants et avec les tests conventionnels a été trouvée.

La conductivité thermique estimée lors des tests de réponse thermique et le profil de température non perturbée mesuré dans le même forage ont été utilisés pour déduire le flux de chaleur terrestre près de la surface. Les profils de température non perturbée ont été reproduits avec un modèle numérique inverse de transfert de chaleur par conduction pour évaluer le flux de chaleur près de la surface défini comme la condition de frontière inférieure. Cette méthodologie est une alternative pour évaluer le flux de chaleur lors de l'exploration préliminaire des ressources géothermiques profondes des zones urbaines, où les tests de réponse thermique sont fréquents.



## TABLE DES MATIÈRES

REMERCIEMENTS.....	iii
RÉSUMÉ.....	v
TABLE DES MATIÈRES.....	vii
LISTE DES TABLEAUX.....	ix
LISTE DES FIGURES.....	xi
NOMENCLATURE.....	xiii
I. Synthèse .....	1
1 Introduction .....	3
2 Définition du problème .....	7
3 Objectifs .....	10
3.1 Objectif général .....	10
3.2 Objectifs spécifiques .....	10
4 Structure du mémoire.....	10
II. Articles.....	13
Article 1 .....	15
A new thermal response test with heating cable sections and fiber optic distributed temperature monitoring.....	15
1.1 Introduction.....	16
1.2 Field test.....	18
1.3 Test analysis .....	19
1.3.1 Thermal conductivity estimation.....	19
1.3.2 Free convection assessment .....	20
1.4 Results .....	22
1.4.1 Thermal conductivity estimation.....	24
1.4.2 Free convection assessment .....	25
1.5 Discussion and conclusions .....	27
Article 2 .....	29
Distributed thermal response tests using a heating cable and fiber optic temperature sensing .....	29
2.1 Introduction.....	31
2.2 Field test methodology .....	34
2.3 Test analyses .....	38
2.3.1 Thermal conductivity assessment.....	38
2.3.2 Uncertainty analysis .....	40

2.3.3	Free convection assessment inside GHE pipe .....	42
2.4	Results .....	44
2.4.1	Thermal conductivity estimation.....	47
2.4.2	Uncertainty analysis .....	50
2.4.3	Free convection assessment .....	52
2.5	Discussion.....	55
2.5.1	Thermal conductivity estimation.....	55
5.2.2	Uncertainty analysis .....	57
5.2.3	Comparison of TRT methods.....	58
2.6	Conclusions.....	59
Article 3 .....		61
Inferring terrestrial heat flow from thermal response test data combined with a temperature profile.....		61
3.1	Introduction.....	63
3.2	Methodology.....	65
3.2.1	<i>In situ</i> thermal conductivity assessment .....	65
3.2.2	Temperature measurements and paleoclimate correction .....	66
3.2.3	Numerical model development .....	68
3.3	Results .....	72
3.3.1	Paleoclimate correction.....	72
3.3.2	Numerical simulation.....	72
3.4	Discussion .....	74
3. 5	Conclusion.....	76
III.	Conclusions.....	77
1	Synthèse des résultats.....	79
2	Conclusions.....	83
RÉFÉRENCES.....		85

## **LISTE DES TABLEAUX**

### **Article 2**

Table 2.1 Experimental condition and configuration of TRT .....	46
Table 2.2. Error associated with the measured parameters .....	50
Table 2.3. Combined errors .....	50
Table 2. 4. Uncertainly of the punctual thermal conductivity assessment for the heating cable sections ..	51
Table 2.5. Uncertainly of the punctual thermal conductivity assessment for the test with a continuous heating cable .....	51
Table 2.6. Comparison of TRT methods for thermal conductivity profile assessment. ....	58

### **Article 3**

Table 3.1. Verification of the mesh independence and the bottom heat flow boundary position. ....	73
---	----



## **LISTE DES FIGURES**

### **I. Synthèse**

Figure 1. Schéma d'un système de pompes à chaleur géothermique .....	4
Figure 2. Unité mobile de TRT développé à l'Université de technologie de Luleå.....	5
Figure 3. Schéma d'un test de réponse thermique conventionnel .....	6
Figure 4. a) Unité pour TRT avec a) un câble chauffant en sections et b) un câble chauffant continu.....	8

### **II. Articles**

#### **Article 1**

Figure 1.1. Equipment to conduct a TRT with heating cable sections.....	19
Figure 1.2. Temperature evolution during the three stages of the TRT with heating cable sections. ....	22
Figure 1.3. Observed temperatures at the middle of a non-heating section.....	23
Figure 1.4. Observed and computed temperature increments during the recovery period .....	24
Figure 1.5. Subsurface thermal conductivity.....	25
Figure 1.6. Temperature distribution during the TRT around a typical heating section.....	26
Figure 1.7. Verification of the Rayleigh number stability criteria considering different critical lengths .....	27

#### **Article 2**

Figure 2.1. Stratigraphic description of the borehole located in a) Quebec City and b) Orléans .....	35
Figure 2.2. Apparatus for TRT with a) heating cable sections and b) a continuous heating cable .....	36
Figure 2.3. Junction box for TRT with a heating cable. ....	37
Figure 2.4. Temperature evolution during the three steps of the TRT.....	45
Figure 2.5. Observed temperature at the middle of a non-heating section .....	45
Figure 2.6. Temperature evolution during the three steps of the TRT at BRGM.....	47
Figure 2.7. Observed and computed temperature increments during the recovery period .....	48
Figure 2.8. Observed temperatures during the recovery period .....	48
Figure 2.9. Point subsurface thermal conductivity .....	49
Figure 2.10. Temperature distribution during the TRT around a typical heating section.....	53
Figure 2.11. Verification of the Rayleigh number stability criteria considering different critical lengths .....	54
Figure 2.12. Verification of the Rayleigh number stability criteria .....	54

## **Article 3**

Figure 3.1. Thermal conductivity profiles and mean thermal conductivity in Quebec City and Orléans.....	65
Figure 3.2. Example of the surface temperature variation assumed during a glacial period.....	66
Figure 3.3. Chronology of glacial periods in Canada.....	67
Figure 3.4. Chronology of glacial periods in Europe.....	67
Figure 3.5. Historic air and ground temperature variations considered.....	69
Figure 3.6. Simulation domain and boundary condition.....	71
Figure 3.7. Temperatures corrected for paleoclimate effects .....	72
Figure 3.8. Simulated temperature matched with observed temperature.....	74
Figure 3.9. The histogram of basal heat flow values .....	74

## **Conclusions**

Figure 1. Carte de flux de chaleur de l'est du Canada.. .....	79
Figure 2. Carte de flux de chaleur de la France.....	80

## NOMENCLATURE

[M L T t I] are used to denote units of mass, length, temperature, time and electric current, respectively

Fo	Fourier's number [-]
G	gravitational acceleration [L t <sup>-2</sup> ]
g	finite heat source function [-]
h	length of heat source [L]
H	height of the water column [L]
I	electric current intensity [I]
m	slope [-]
n	number of observations [-]
q	heat injection rate per unit length [M L t <sup>-3</sup> ]
R	electric resistance [M L <sup>2</sup> t <sup>-3</sup> I <sup>-2</sup> ]
r	radius [L]
Ra	Rayleigh number [-]
S	error of the estimate
t	time [t]
T	temperature [T]
U	electric potential difference [M L <sup>2</sup> t <sup>-3</sup> I <sup>-1</sup> ]

## Greek symbols

$\alpha$	thermal diffusivity [L <sup>2</sup> t <sup>-1</sup> ]
$\lambda$	thermal conductivity [M L T <sup>-1</sup> t <sup>-3</sup> ]
$\delta$	uncertainty
$\sigma$	standard deviation
$\nu$	cinematic viscosity [L <sup>2</sup> t <sup>-1</sup> ]

## **Subscripts**

a	aspect-ratio
c	calculated
cr	critique
h	heating
nh	non-heating
m	measured
off	end of heat injection
s	subsurface
t	critical height
tot	total
0	initial condition

# I. Synthèse



## 1 Introduction

Depuis environ 1850, l'utilisation mondiale des combustibles fossiles (charbon, pétrole et gaz) a augmenté et conduit à une croissance des émissions de dioxyde de carbone. La transition des combustibles fossiles vers des sources d'énergies renouvelables, dont l'énergie géothermique fait partie, est une étape indispensable dans le but d'utiliser nos ressources naturelles plus efficacement. Les avantages environnementaux de l'énergie géothermique sont nombreux. La réduction des émissions des gaz à effet de serre, comme le dioxyde de carbone ( $\text{CO}_2$ ), le dioxyde de soufre ( $\text{SO}_2$ ) et les oxydes d'azote ( $\text{NO}_x$ ) est l'un des principaux avantages (Sarbu & Sebarchievici, 2014, Self *et al.*, 2012). D'autres bénéfices comme la réduction de la consommation d'énergie pour le chauffage et la climatisation des bâtiments ainsi que l'utilisation d'une source d'énergie renouvelable (Mustafa Omer, 2008) sont des aspects environnementaux importants qui permettent de réduire la dépendance énergétique des combustibles fossiles. Néanmoins, le coût relié à la conception et la mise en œuvre des systèmes géothermiques est encore un obstacle pour son utilisation massive.

Les systèmes de pompe à chaleur géothermique (PACG) sont une technologie verte, couramment utilisée dans le monde entier pour le chauffage et la climatisation des bâtiments (Spitler & Gehlin, 2015). Ces systèmes utilisent le sous-sol comme une source de chaleur pendant l'hiver et comme un dissipateur thermique pendant l'été afin de chauffer et de climatiser les bâtiments. La température du sous-sol est presque constante lorsque comparée à celle de l'air extérieur, ce qui permet de bénéficier de l'inertie thermique du sous-sol pour maintenir la température d'espaces intérieurs (Sarbu & Sebarchievici, 2014).

Les PACG sont composés de trois systèmes principaux, soit (Figure 1) : (1) une pompe à chaleur géothermique, qui permet de transporter la chaleur entre le sous-sol et le bâtiment (Self *et al.*, 2012) ; (2) une connexion avec le sous-sol, qui facilite l'extraction et l'injection de la chaleur du milieu souterrain avec un échangeur de chaleur (Self *et al.*, 2012) ; et (3) un système de distribution de la chaleur dans le bâtiment (Sarbu & Sebarchievici, 2014).

L'échangeur de chaleur représente une partie importante du coût d'installation de ces systèmes et des procédures de conception méticuleuses sont nécessaires pour ne pas surestimer la longueur du forage, qui a un impact direct sur l'efficacité des PACG (Zhang *et al.*, 2014) ainsi que sur leur coût. En conséquence, la connaissance des propriétés thermiques du sous-sol est nécessaire pour optimiser la conception de ces systèmes géothermiques.

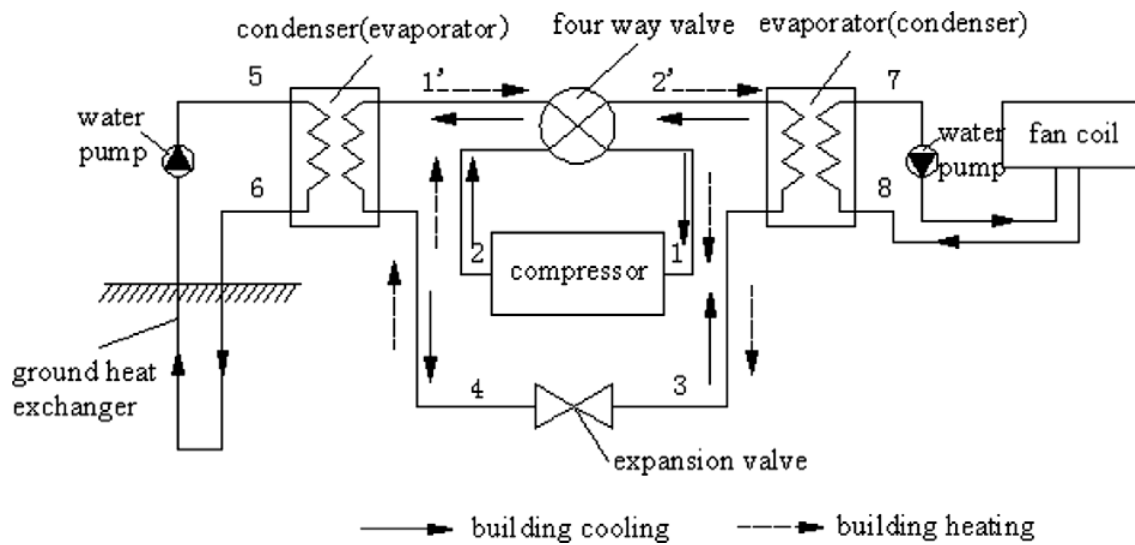


Figure 1. Schéma d'un système de pompes à chaleur géothermique (tirée de Bi et al, 2009).

Les tests de réponse thermique (TRT) sont une méthode *in situ* pour déterminer les propriétés thermiques du sous-sol et des forages. Cette méthode a été proposée pour la première fois par Mogensen (1983) pour déterminer la conductivité thermique du sous-sol et la résistance thermique des forages. Un système avec un refroidisseur et une pompe qui fait circuler un fluide caloporteur dans le tuyau d'un échangeur de chaleur a été utilisé à cette époque. Les données d'essai ont été analysées avec l'équation de la source de chaleur linéaire infinie (Carslaw, 1945).

Dès le milieu des années 1980 et au milieu des années 1990, plusieurs TRT (non-mobiles) ont été effectués sur des forages verticaux expérimentaux existants. Le besoin d'un dispositif de test qui pourrait être déplacé d'un site à l'autre est ensuite devenu clair (Spitler & Gehlin, 2015).

Entre 1995 et 1996, des équipements mobiles pour effectuer des TRT (Figure 2) ont été développés à l'Université de technologie de Luleå en Suède par Eklöf et Gehlin (1996) et à Oklahoma State University aux États-Unis par Austin III (1998). Dans les deux cas, les auteurs ont présenté le développement de l'équipement de terrain, la méthodologie d'analyse du test et les résultats expérimentaux obtenus. Au début des années 2000, Gehlin (2002) a présenté dans sa thèse de doctorat une synthèse de la méthode associée au TRT pour évaluer les caractéristiques thermiques des forages géothermiques. Des revues sur les différents équipements, procédures et méthodes d'analyse concernant les TRT dans différents pays ont été présentées par Gehlin (2002), Sanner et al. (2005), Sanner et al. (2013) et Spitler et Gehlin (2015).

La méthodologie conventionnelle des TRT consiste à reproduire les phénomènes de transfert de chaleur qui se produisent dans un échangeur de chaleur au sol (Mogensen, 1983). Lors d'un TRT conventionnel (Figure 3), l'eau qui circule dans un échangeur de chaleur est chauffée avec un élément électrique pour perturber l'équilibre thermique du sous-sol (Gehlin, 2002). La température et le débit à l'entrée et à la sortie de l'échangeur sont mesurés et l'augmentation de température observée est analysée pour estimer les propriétés physiques du sous-sol et du forage (Raymond *et al.*, 2011a).



**Figure 2. Unité mobile de TRT développé à l'Université de technologie de Luleå (tirée de Gehlin, 2002, photo: Peter Olsson).**

Le taux d'injection de chaleur recommandé pour un TRT conventionnel dans les guides de l'industrie géothermique en Amérique du Nord est de 50 à 80 W m<sup>-1</sup> afin de créer une différence de température d'environ 3 à 7 °C entre l'entrée et la sortie de l'échangeur de chaleur (Kavanaugh, 2001). Le courant électrique nécessaire pour produire cette variation de température est élevé et est souvent fourni par une génératrice ou par une connexion haute tension au réseau électrique. La mobilisation et l'opération de la génératrice, ou l'utilisation des câbles de haute tension et les mesures de sécurité nécessaires pour brancher l'unité TRT avec le réseau électrique, représentent le coût principal des TRTs effectués avec cette méthode conventionnelle (Raymond & Lamarche, 2014). De plus, l'équipement utilisé pour les TRT conventionnels est lourd et la préparation de l'essai est complexe puisqu'il faut s'assurer qu'il n'y ait pas de fuites dans le système soumis aux conditions de terrain.

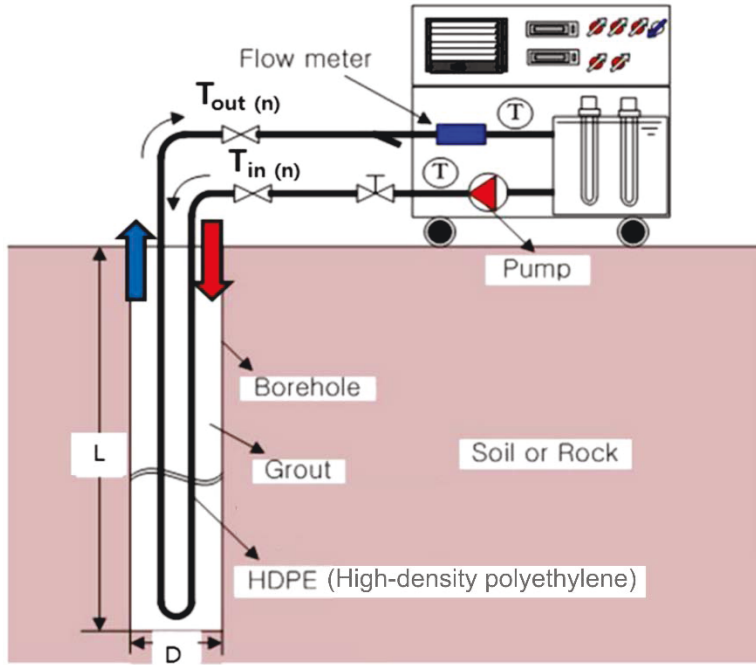


**Figure 3. Schéma d'un test de réponse thermique conventionnel (tirée de Chang et Kim, 2016).**

Avec la croissance des PACG au niveau mondial, les TRT sont devenus largement utilisés partout dans le monde (Zhang *et al.*, 2014). Il existe en Europe 70 plates-formes mobiles pour effectuer des TRT (Sanner *et al.*, 2013). Hors de l'Europe, le principal marché des TRTs se trouve aux États-Unis et au Canada (Zhang *et al.*, 2014).

Bien que la réalisation d'un TRT soit la méthode la plus utilisée pour déterminer les propriétés thermiques du sous-sol de façon *in situ*, cette méthode a des inconvénients qui ont fait l'objet de recherches pendant les dernières années. Les TRTs conventionnels, basés sur la mesure de l'augmentation de la température d'entrée et sortie du fluide, permettent seulement d'obtenir une valeur globale de la conductivité thermique du sous-sol pour toutes les formations géologiques interceptées par le forage exploratoire. Plusieurs développements ont récemment été effectués pour améliorer les TRT. Des tests en mode d'extraction de chaleur, en utilisant une pompe à chaleur ont été proposées par Witte *et al.* (2002). L'utilisation de fibres optiques pour mesurer la variation de la température à l'intérieur des forages s'est ensuite développée (Fujii *et al.*, 2006, Fujii *et al.*, 2009) afin d'évaluer la conductivité thermique du sous-sol à différentes profondeurs pour estimer un profil de conductivité thermique. La fibre optique a également été utilisée pour valider des modèles analytiques de l'évolution verticale de la température (Beier *et al.*, 2012) et pour mesurer les températures des parois des forages pendant les TRT (Acuña & Palm, 2013).

Le suivi de la restitution de la température après l'injection chaleur (Raymond *et al.*, 2011a, Raymond *et al.*, 2011c) est une autre approche qui permet réduire l'incertitude dans l'estimation de la conductivité thermique et de la résistance thermique du forage. Cette méthode permet d'inférer presque indépendamment la résistance thermique du forage et la conductivité thermique du sous-sol (Raymond *et al.*, 2011c). La période d'injection chaleur est utilisée pour estimer la résistance thermique et la période de restitution pour évaluer la conductivité thermique. La présence d'écoulement souterrain peut affecter l'estimation de la conductivité thermique lors d'un TRT (Bozdağ *et al.*, 2008). Des modèles numériques simulant l'écoulement souterrain et le transfert de chaleur incluant l'advection et la dispersion ont été développés (Raymond *et al.*, 2011b) pour analyser les essais sous de telles conditions. En revanche, une solution analytique simulant une source de chaleur en mouvement, soit la ligne source infinie et finie en mouvement, peut aussi être utilisée (Molina-Giraldo *et al.*, 2011).

Des TRT avec un câble chauffant continu (Raymond *et al.*, 2010) et en sections (Raymond & Lamarche, 2014, Raymond *et al.*, 2015) ont également été proposés pour faciliter la réalisation des essais sur le terrain qui ne requièrent pas de circulation d'eau dans l'échangeur de chaleur. Cette dernière méthode constitue l'objet de ce travail et est présentée dans la section suivante.

## 2 Définition du problème

Dans le but de réduire les coûts associés à la source d'énergie et à la mobilisation et l'installation des équipements de terrain, une méthode alternative avec un câble chauffant continu (Figure 4b) a été développée par Raymond *et al.* (2010) sur la base des travaux de Pehme *et al.* (2007a ; 2007b). La méthode consiste à injecter la chaleur dans le forage, en induisant un courant électrique à travers un câble chauffant. La température est mesurée à différentes profondeurs dans le forage en utilisant des capteurs de température submersibles. Ces mesures additionnelles de la température permettent d'évaluer les changements de la conductivité thermique du sous-sol qui ont une influence notable dans la conception des PACG (Raymond & Lamarche, 2014).

Cette méthode facilite la réalisation des travaux de terrain parce que l'équipement est plus léger et la circulation d'eau dans l'échangeur de chaleur n'est pas nécessaire (Raymond *et al.*, 2010). Néanmoins, la puissance électrique requise augmente avec la profondeur de forage, limitant l'utilisation du câble chauffant continu. Un câble composé de sections chauffantes et non chauffantes (Figure 4a), qui permet de réduire la puissance électrique nécessaire, a ensuite été développé par Raymond et Lamarche (2014) et Raymond *et al.* (2015). Un test à l'échelle du

laboratoire a été aussi effectué par Simon (2016), avec l'objectif de valider et optimiser la méthode à petite échelle.

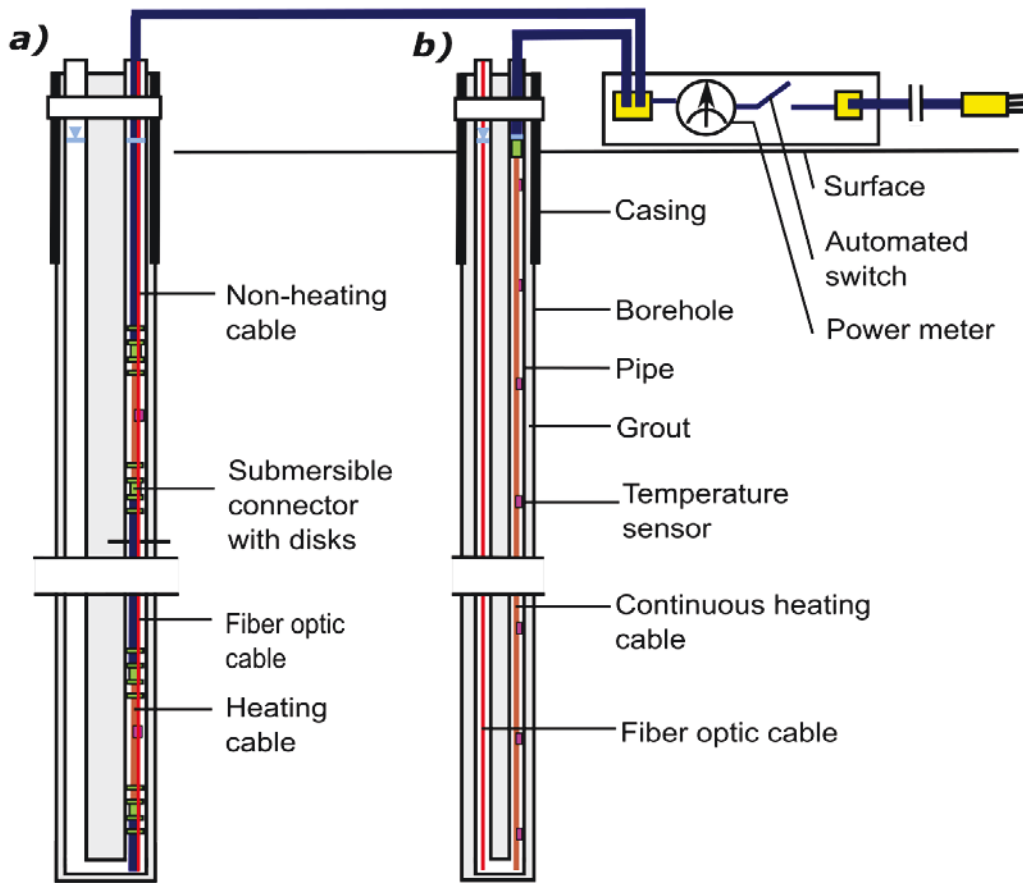


**Figure 4. a)** Unité pour TRT avec a) un câble chauffant en sections et b) un câble chauffant continu (modifiée de Raymond, 2018).

Lors des dernières années, la possibilité d'élargir le champ d'application des TRT à l'évaluation des ressources géothermiques profondes a été proposée par Sanner *et al.* (2013). La mesure de profils de température non perturbée couplée à l'information sur la conductivité thermique du sous-sol pourrait être utilisée pour estimer le flux de chaleur terrestre. L'utilisation de données provenant des TRTs apparaît d'autant plus intéressante puisque ces tests sont effectués dans les milieux urbains où il existe rarement des forages profonds dans lesquels le flux de chaleur est évalué. Les besoins en chaleur que pourraient combler les ressources géothermiques issues d'aquifères profonds se situent également dans les zones urbaines. Une analyse numérique basée sur le profil de température non perturbée d'un forage exploratoire utilisé pour un TRT, ainsi que l'évaluation de la conductivité thermique provenant du TRT, a été développée afin d'inférer le flux de chaleur terrestre sur les sites d'essais.

Ce travail est divisé en deux parties ayant pour but d'avancer l'état des connaissances en matière des TRTs pour simplifier son exécution, réduire son coût, et diversifier ses applications. La première partie cherche à valider la méthode des câbles chauffants continus et en sections et à mieux comprendre les phénomènes de transfert de chaleur qui s'y rattachent. À cet effet, deux sites expérimentaux ont été choisis pour effectuer les TRTs avec les deux types de câbles chauffants. Le site 1 est localisé aux laboratoires pour l'innovation scientifique et technologique de l'environnement (LISTE) de l'INRS, situés dans le Parc technologique du Québec métropolitain. Ce site a un forage géothermique de 150 m de profondeur aménagé avec un tuyau en U et deux puits d'observation de 42 m localisés à 10 m de distance au nord et au sud du forage géothermique. Un test avec un câble chauffant en sections a été effectué dans le site 1, en utilisant une fibre optique et un système de mesure distribuée de la température afin de faire un suivi de la température tout au long du forage jusqu'au 100 m de profondeur. Le but était d'évaluer la présence de convection naturelle dans le tuyau de l'échangeur de chaleur.

Le site 2 est la plate-forme expérimentale en géothermie du Bureau de Recherche Géologique et Minières (BRGM) en France, localisé à Orléans. Cette plate-forme est équipée avec deux sondes géothermiques (échangeurs verticaux) à 50 m de profondeur et une sonde à 100 m, associées à trois piézomètres de contrôle. La sonde géothermique verticale de 100 m de profondeur, aménagé avec un échangeur de chaleur à double boucle, a été utilisée pour effectuer le deuxième test en utilisant un câble chauffant continu et un taux d'injection chaleur faible. Ce test avait pour objectif de vérifier la possibilité d'utiliser le câble continu dans un forage aussi profond, en réduisant le taux d'injection de chaleur pour effectuer le test avec une source de basse puissance. Dans les deux tests, l'incertitude associée à l'estimation de la conductivité thermique a été déterminée.

La deuxième partie du mémoire décrit une nouvelle façon d'analyser les données d'un TRT afin d'estimer le flux de chaleur terrestre près de la surface. La conductivité thermique estimée lors de deux TRTs et des profils de température en équilibre mesurés avant les tests ont été utilisés pour évaluer le flux de chaleur terrestre près de la surface dans les forages. Le logiciel de modélisation COMSOL Multiphysics (COMSOL AB, 2016) a été utilisé pour construire le modèle numérique avec la méthode des éléments finis.

## **3 Objectifs**

Ce projet de maîtrise vise à valider et améliorer les tests de réponse thermique avec câbles chauffants pour évaluer la conductivité thermique du sous-sol en fonction de la profondeur, ainsi que d'évaluer le flux de chaleur terrestre en régions urbaines où les essais sont effectués.

### **3.1 Objectif général**

Améliorer la compréhension des phénomènes de transfert de chaleur lors des tests de réponse thermique (TRT) avec des câbles chauffants et diversifier ses applications pour les études sur les ressources géothermiques profondes.

### **3.2 Objectifs spécifiques**

- Valider la méthode du TRT avec un câble chauffant en sections et continu par comparaison avec les résultats des TRT conventionnels.
- Déterminer l'incertitude de l'estimation de la conductivité thermique lors d'un TRT avec un câble chauffant en sections et continu.
- Vérifier l'efficacité des disques en plastique pour bloquer les mouvements de convection naturelle dans le tuyau des échangeurs de chaleur, lors d'un TRT avec un câble chauffant en sections.
- Estimer le flux de chaleur près de la surface avec les résultats du TRT couplés à un profil de température à l'équilibre.

## **4 Structure du mémoire**

Ce mémoire de maîtrise est composé d'une synthèse des travaux de recherche et de 3 articles. Le chapitre 1 correspond à un article de conférence préparé à partir des résultats du premier test de réponse thermique qui a été mis en œuvre. L'article a été présenté à la soixante-dixième Conférence canadienne de géotechnique de la Société canadienne de géotechnique ayant eu lieu à Ottawa en octobre 2017. Le chapitre 2 est un article publié dans la revue Energies et décrivant les résultats des deux TRTs effectués pendant les travaux de maîtrise, incluant la comparaison des méthodes utilisées pour chaque test. Ce chapitre décrit la partie centrale de ce projet de maîtrise. Le chapitre 3 correspond à un article de conférence sur l'estimation de flux de chaleur terrestre près de la surface inférée à partir des TRTs et des profils de température. Cet article a été présenté à la vingt-sixième conférence annuelle du Computational

Fluid Dynamics Society of Canada ayant eu lieu à Winnipeg en juin 2018 puis soumis à la revue Physics and Chemistry of the Earth.

- Chapitre 1 : Velez, M. I., Raymond, J., Blessent, D., Simon, N., Bour O., 2017. A new thermal response test with heating cable sections and fiber optic distributed temperature monitoring. GeoOttawa, Oct 2017, Ottawa, Canada.
- Chapitre 2 : Article publié dans la revue Energies dans le numéro spécial *Geothermal Energy: Utilization and Technology*. Distributed thermal response tests using heating cables and fiber optic temperature sensing.
- Chapitre 3 : Article soumis à la revue Physics and Chemistry of the EarthTerrestrial heat flow evaluation from thermal response tests combined with temperature profiling



## **II. Articles**



# **Article 1**

## **A new thermal response test with heating cable sections and fiber optic distributed temperature monitoring**

### **Titre traduit**

Un nouveau test de réponse thermique avec câbles chauffants et suivi de la température par fibre optique

### **Auteurs**

Maria Isabel Vélez<sup>1</sup>, Jasmin Raymond<sup>1</sup>, Daniela Blessent<sup>2</sup>, Nataline Simon<sup>3</sup>, Olivier Bour<sup>3</sup>

<sup>1</sup> Centre-Eau Terre Environnement, Institut national de la recherche scientifique, Québec, Qc, Canada

<sup>2</sup> Programa de Ingeniería Ambiental, Universidad de Medellín, Medellín, Colombia

<sup>3</sup> Géosciences Rennes-OSUR, CNRS — University Rennes 1, Rennes Cedex, France

### **Publié**

Actes de la 70<sup>ème</sup> conférence canadienne de géotechnique (GeoOttawa 2017)

## **RESUMÉ**

Les tests de réponse thermique sont utilisés pour évaluer la conductivité thermique du sous-sol lors de la conception des systèmes de pompes à chaleur couplées au sol. Pendant un test conventionnel, une source de haute puissance est requise pour chauffer l'eau qui circule dans l'échangeur de chaleur pilote. Une nouvelle méthode d'essai avec un câble chauffant en sections installé dans la colonne d'eau stagnante d'un tuyau de l'échangeur de chaleur a été développée pour réduire la puissance électrique requise. Cette méthode, associée à des mesures de température distribuée avec fibre optique, a été utilisée pour effectuer un test de réponse thermique. La conductivité thermique du sous-sol à l'endroit des sections chauffantes a été inférée avec une équation simulant les transferts thermiques par conduction issue d'une ligne source finie. Les données de la fibre optique ont été utilisées pour évaluer les possibles transferts de chaleur par convection naturelle. La conductivité thermique estimée varie entre 1.72 et  $2.19 \text{ W m}^{-1}\text{K}^{-1}$ . L'analyse du critère de stabilité du nombre de Rayleigh suggère la présence de convection naturelle pendant l'injection chaleur.

## **ABSTRACT**

Thermal response tests are used to assess the subsurface thermal conductivity to design ground-coupled heat pump systems. Conventional tests require a source of high power to heat water circulating in a pilot ground heat exchanger. A new method using heating cable sections standing in the water column of a ground heat exchanger pipe has been developed to reduce the required power source. This method, coupled with fiber optic distributed temperature sensing, was used to conduct a thermal response test. The subsurface thermal conductivity near heating sections was inferred using a finite line source equation simulating conductive heat transfer. Temperature data provided by the fiber optic was used to evaluate possible heat transfer by free convection in the standing water column. The estimated thermal conductivity ranged between 1.72 to  $2.19 \text{ W m}^{-1}\text{K}^{-1}$ . The analysis of Rayleigh number stability criteria suggested the presence of free convention during the heat injection.

### **1.1 Introduction**

Thermal response tests (TRT) are commonly used to assess the subsurface thermal conductivity for the design of ground-coupled heat pumps systems (Raymond & Lamarche 2014). The fluid circulating in the ground heat exchanger (GHE) is heated using an electric

element to reproduce heat transfer phenomena occurring in the GHE during a conventional TRT (Mogensen, 1983). Inlet and outlet temperature and flow are recorded and then analyzed to determine the effective subsurface thermal conductivity (Gehlin, 1998; Raymond *et al.* 2011)

Conventional TRT requires a source of high power ( $50 - 80 \text{ W m}^{-1}$ , Kavanaugh 2001) to heat water circulating in the GHE and only allows to estimate the effective subsurface thermal conductivity (Sanner *et al.* 2013).

The use of fiber optic to measure the vertical temperature profile during TRT has been proposed by Fujii *et al.* (2009) in order to assess the vertical distribution of thermal conductivity in ground heat exchangers. Interchanging sections of heating and non-heating cables and submersible temperature sensors to measure temperature at depth have been proposed by Raymond and Lamarche (2014) as an alternative method to conduct TRT. This method allows to reduce the electric power required for the test and to evaluate thermal conductivity at different depths using a finite heat source solution to reproduce observed temperatures along the heating sections (Raymond *et al.* 2015). Heat transfer due to free convection can occur in the vertical pipe near heating sections during the heat injection. Numerical simulations carried out by Raymond and Lamarche (2014) indicated that perforated plastic disks located at the limits of heating sections can be sufficient to reduce convective heat transfer and suggested the need for a full-scale field experiment to determine the efficiency of perforated disks to reduce free convection.

This work aims to evaluate the heating cable sections methodology to estimate subsurface thermal conductivity and the effect of perforated plastic disks, to reduce free convection in the heat exchanger.

A TRT coupling heating cable sections and fiber optic distributed temperature sensing (FO-DTS) was carried out in a ground heat exchanger made with a single U-pipe, where a conventional TRT with water circulation had been conducted before. FO-DTS technology can be used to monitor temperature in boreholes at high frequency and spatial resolution along a fiber optic cable (Bense *et al.* 2016). Thermal conductivity was estimated at the depth of each heating section using the finite heat source solution. Temperature data provided by the FO-DTS were used to evaluate free convection inside the borehole using the Rayleigh number stability criteria proposed by Love *et al.* (2007) for a vertical cylinder filled with water.

## 1.2 Field test

The TRT coupling heating cable sections and distributed temperature sensing was carried out in a ground heat exchanger of 150 m made with a single U-pipe with a nominal diameter of 1.25 in (3.18 cm). The heat exchanger is located at INRS Laboratories for scientific and technological innovation in environment (LISTE) located in Quebec City. It was drilled in shales of the Les Fonds Formation in 2015, when a conventional TRT was conducted (Ballard *et al.* 2016).

The equipment required to conduct the TRT consisted of a cable assembly of 100 m in length, made of alternating heating and non-heating sections with length of 1.2 and 8.6 m, respectively; a junction box to link the cable assembly to the power supply; submersible temperature sensors to measure and record the temperature evolution and perforated plastic disks installed at the extremities of each heating section. The junction box is composed of a switch to start and stop heat injection, a voltage regulator, a power meter to monitor the power induced and circuit breakers to protect the electric circuits of the cable assembly and the power meter (Raymond *et al.* 2015).

The FO-DTS system consisted in a 250 m length of BruSens fiber optic cable, connected to a FO-DTS control unit, a Silixa XT-DTS instrument, in double-ended configuration with 2 km range. This 3.8 mm diameter fiber optic sensing cable, armoured with stainless steel, has a fast thermal response which allow to record efficiently thermal changes. To calibrate the DTS unit, two 20 m cable length sections were placed respectively in an ambient temperature calibration bath and in a cold calibration bath. In each bath, a Starmon mini probe ( $\pm 0.025^\circ\text{C}$ ) and a RBRduet probe ( $\pm 0.002^\circ\text{C}$ ) allowed to record the temperature and calibrate FO-DTS data. The last 100 m of fiber optic cable were attached to the cable assembly. The submersible temperature sensors were installed at the middle of each heating section. Four perforated plastic disks, separated by 10 cm approximately, were fixed at the extremities of the heating and non-heating sections delimiting the active heating length considered for analysis (1.6 m; Figure 1.1).

The whole assemblage was installed in a pipe of the ground heat exchanger reaching a depth of 100 m, with the heating sections located approximately 10 m from each other, from 5 until 95 m depth. The FO-DTS system was configured to collect data every 60 seconds with a 25 cm sampling interval along the fiber optic cable. The test started with a measure of the undisturbed subsurface temperature of 26 h. Then, heat was injected for a period of 73 h, at an average rate

of  $42.5 \text{ W m}^{-1}$  through the heating sections. Finally, temperature recovery was monitored during 70 h, for a total test duration of 169 h.

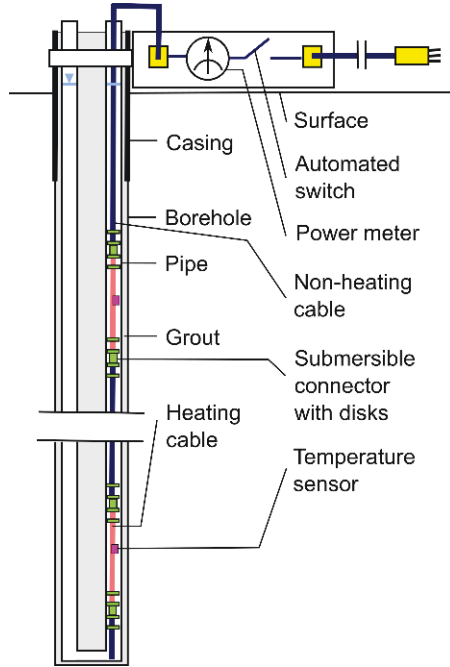


Figure 1.1. Equipment to conduct a TRT with heating cable sections (from Raymond and Lamarche, 2014).

### 1.3 Test analysis

#### 1.3.1 Thermal conductivity estimation

The test analysis was made according to the methodology proposed by Raymond *et al.* (2015). The thermal conductivity was estimated at the location of each temperature sensor according to recovery temperature measurements.

The recovery temperature increments ( $\Delta T = T - T_0$ ) at the middle of each heating section, defined as the increase in temperature with respect to the initial temperature  $T_0$ , are reproduced with a linear heat source solution of finite length using a dimensionless  $g$ -function (Eq. 1.1):

$$\Delta T = \frac{q}{2\pi\lambda_s} g \left[ \left( Fo, \frac{r}{H} \right) - \left( Fo', \frac{r}{H} \right) \right] \quad (1.1)$$

$$\text{with } Fo = \frac{\alpha_s(t)}{H^2} \quad (1.2)$$

$$\text{and } Fo = \frac{\alpha_s(t - t_{\text{off}})}{H^2} \quad (1.3)$$

where  $q$  ( $\text{W m}^{-1}$ ) is the heat injection rate per unit length,  $\alpha_s$  ( $\text{m}^2 \text{s}^{-1}$ ) and  $\lambda_s$  ( $\text{W m}^{-1}\text{K}^{-1}$ ) are the thermal diffusivity and conductivity of the subsurface,  $r$  (m) is the radial distance from the heat source,  $H$  (m) is the active heating length and  $t_{\text{off}}$  is the time when heat injection was stopped.

The heat capacity of the subsurface has to be assumed to determine the thermal diffusivity ( $\alpha_s$ ) and compute Fourier's number (Eq. 1.2 and 1.3). The same value as that assumed for the conventional TRT analysis and inferred from a description of geological materials obtained from drilled cuttings was used. The heat injection rate ( $q$ ) for each heating section was assumed similar and was determined according to Joules and Ohms laws:

$$q = \frac{R_h I^2}{nH} \quad (1.4)$$

where  $R_h = R_{\text{tot}} - R_{\text{nh}}$  (1.5)

$$\text{and } R_{\text{tot}} = \frac{U}{I} \quad (1.6)$$

In the above equations,  $R$  (Ohm) is the electric resistance,  $I$  (A) is the current intensity,  $U$  (V) is the potential difference and  $n$  is the number of heating sections. The subscripts h, nh and tot correspond to the electrical resistance of the heating sections, non-heating sections and the whole cable assembly.

The computed temperature increments of the late recovery period were matched with a non-linear solver to the observed temperatures increments by adjusting the thermal conductivity using least-squared fit. The analysis of the temperature measurements recorded with the submersible data loggers was performed using a spreadsheet program developed by Raymond *et al.* (2015).

### 1.3.2 Free convection assessment

Love *et al.* (2007) studied the diffusive transport induced by temperature variation in groundwater wells and formulated a Rayleigh number stability criteria. The stability criteria considers the cylindrical well geometry and allows assessing convection in a cylindrical well with a standing water column having temperature gradients between top to bottom.

Free convection can be a dominant heat transfer mechanism when the Rayleigh number (Eq. 1.7) exceeds a critical Rayleigh number (Eq. 1.8) according to this stability criteria:

$$Ra = \frac{g\beta H^3 \Delta T}{\nu k} \quad (1.7)$$

In the above equation,  $g$  ( $\text{m s}^{-2}$ ) is the gravity acceleration,  $\beta$  ( $\text{K}^{-1}$ ) is the thermal expansion coefficient of the fluid,  $H$  (m) is the height of water column,  $\Delta T$  ( $^\circ\text{C}$ ) is the difference in temperature between the top and bottom of the system,  $\nu$  ( $\text{m}^2 \text{s}^{-1}$ ) is the fluid cinematic viscosity and  $k$  ( $\text{m}^2 \text{s}^{-1}$ ) is the fluid thermal diffusivity.

The critical Raleigh number computed for comparison is determined according to the cylinder geometry:

$$Ra_c = \frac{215.6}{r_a^4} (1 + 3.84 r_a^2) \quad (1.8)$$

$$\text{with } r_a = \frac{r}{H_t} \quad (1.9)$$

where  $r$  (m) is the well radius and  $H_t$  (m) is the well height. The critical Rayleigh number is therefore a function of the well aspect ratio ( $r_a$ ) only and an increment in the well aspect ratio results in a reduction of the value of  $Ra_c$  (Love *et al.* 2007).

The Rayleigh number stability criteria was proposed by Love *et al.* (2007) to assess convection in groundwater wells in the presences of a geothermal gradient. In this study, the stability criteria is used to evaluate convection in a GHE where heat is injected using heating cable sections. Therefore, a similar approach to the proposed Rayleigh number stability criteria is applied in a system composed by a vertical pipe filled with water, where the temperature gradient is not uniform. Then,  $H_t$  is defined as a critical length around the heating sections, instead than the well height considered for groundwater wells with a geothermal gradient.

A segment of 5.6 m of the cable assembly in the GHE was used to evaluate convection near a typical heating section. The segment is formed by a section of 4.4 m of non-heating cable located above and below a heating cable section of 1.2 m. The FO-DTS was used to determine  $\Delta T$  in Eq. 1.7 and compute the actual Raleigh number at different heights of the water column in the pipe varying in a range of 0.25 to 5.8 m to verify the Rayleigh number stability criteria. The critical Rayleigh number was calculated for the pipe radius ( $r = 1.72 \text{ cm}$ ) and a critical length

( $H_t$ ) of 3, 6 and 9 m to represent the mean height of the water column considered to calculate actual Rayleigh numbers, the length of the maximum temperature difference between a heating and non-heating sections and the total length a system of a single heating and a non-heating section.

## 1.4 Results

Two methods to monitor temperature were used during the test: the submersible temperature sensors located in the middle of each heating section and the FO-DTS throughout the cable assembly. The punctual temperature data provided by the submersible sensors were used to estimate the thermal conductivity. The fiber optic data allowed to image the temperature evolution in the GHE during the whole test and to evaluate the efficiency of the perforated plastic disks to reduce free convection.

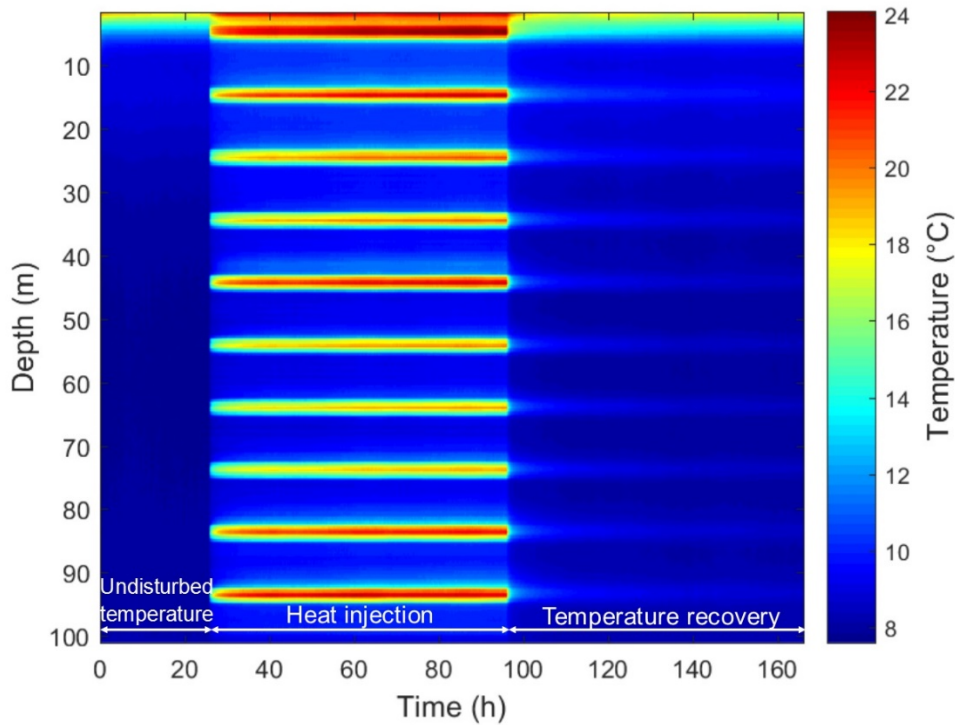


**Figure 1.2. Temperature evolution during the three stages of the TRT with heating cable sections.**

The initial undisturbed temperature was monitored during 26 h. Then, heat was injected for a period of 73 h (from 26 h to 99 h) and recovery temperatures were measured during the following 70 h, from 99 to 169 h (Figure 1.2). The total energy consumption during the test was 71.75 kWh and the average potential difference and current intensity were 113 V and 8.7 A,

respectively. During the heat injection, temperature increments reached at the depth of each heating section were variable. Those differences are related to variations in the subsurface thermal conductivity. High temperature increments indicate a low subsurface thermal conductivity and a slight temperature increases correspond to greater thermal conductivities.

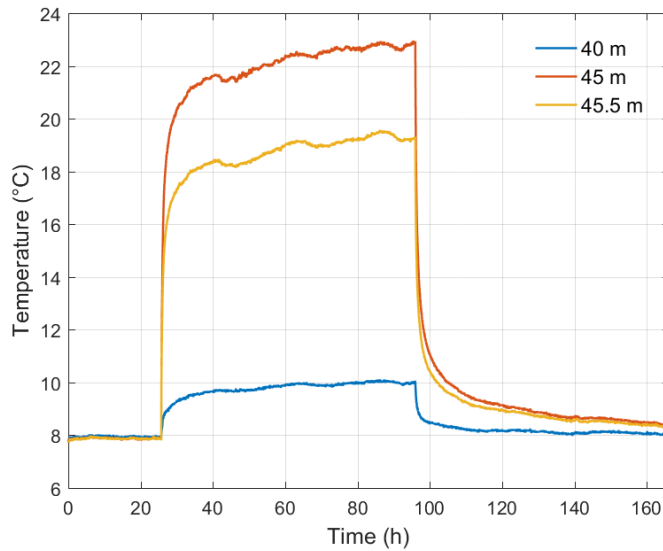


**Figure 1.3. Observed temperatures at the middle of a non-heating section (40 m) and at the top (45 m) and the middle (45.5 m) of a heating section.**

Some differences were observed between the temperature measured in the middle of the heating sections, using the submersible data loggers and the fiber optic. The submersible data logger measured temperature that ranged between 23 and 31 °C, while maximal temperature observed with the fiber optic ranged between 16 and 22 °C. Nevertheless, comparison between the punctual temperature measurements from the submersible data loggers and FO-DTS is difficult because fiber optic temperature measurements were not necessarily taken at the same place than that of the submersible data loggers, and a displacement of some centimeters can result in an important temperature difference. As it was mentioned before, temperature measurements from each method were used to analyze different phenomena, therefore further comparison was not carried out.

Temperature at the middle of non-heating sections increase approximately 2 °C from the initial undisturbed temperature (Figure 1.3, at 40 m depth). In the heating section (45 – 46.2 m) a difference of more than 2 °C is observed between the top and the middle of the section, indicating important temperature variations in a short distance.

### 1.4.1 Thermal conductivity estimation

A heat capacity of  $2.3 \text{ MJ m}^{-3} \text{ K}^{-1}$  associated with shales was assumed to compute the temperature increments. Numerical simulations carried out by Raymond *et al.* (2011) indicate that the temperature inside the borehole varies significantly according to measurement location during the heat injection, but not during heat recovery. Therefore, the first 30 h of the recovery period were neglected and the analysis was carried out using the last 40 h of recovery temperature measurements. Adjustment between observed and computed temperature increments (Figure 1.4) was achieved at the depth of each submersible temperature sensor tied to a heating section. However, to avoid repetition, just the curve matched at 45 m depth is presented as an example.

The thermal conductivity estimated with the heating cable methodology differs between -25.3% to 1.7% from bulk value estimated during the conventional TRT using the curve fitting analysis with the variable heat injection rate while it is near the upper range of the slope analysis assuming constant heat injection rate (Figure 1.5). The estimated thermal conductivity with the heating sections TRT is slightly higher than the value obtained with the conventional TRT depending on the methodology considered. This effect is studied in the next section.

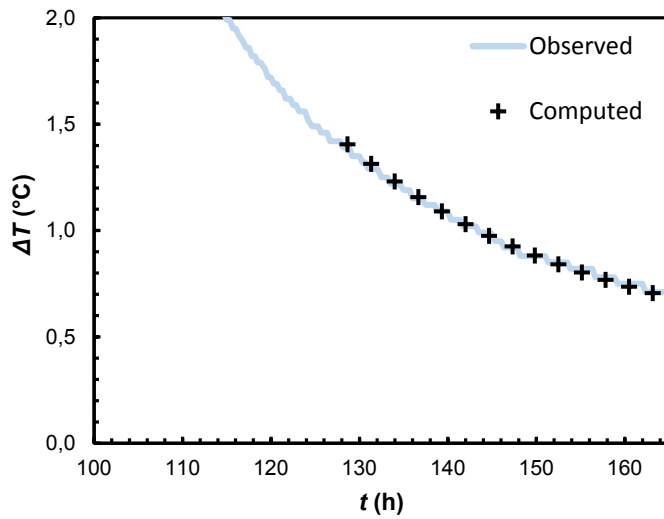


**Figure 1.4. Observed and computed temperature increments during the recovery period for the submersible sensor at 45 m depth.**

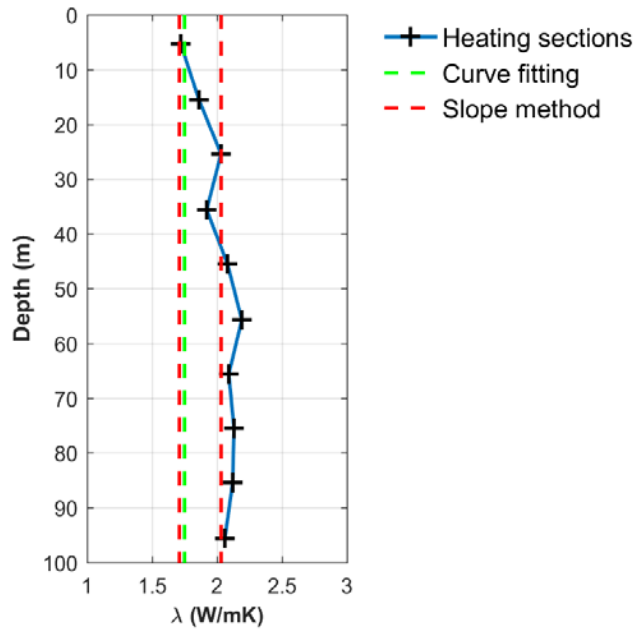


Figure 1.5. Subsurface thermal conductivity (crosses) obtained for the TRT with heating cable sections compared with the bulk values provided by the conventional TRT (green and orange dashed lines).

#### 1.4.2 Free convection assessment

The water temperature in the GHE pipe increased during the heat injection even in the areas far above from the heating cable sections. Increments of approximately 2 °C from the undisturbed temperature were observed (Figure 1.2). The highest recorded temperature is located in the upper part of the heating sections (Figure 1.6). The two observations suggest the presence of free convection in the GHE pipe water being heated.

The assessment of the Rayleigh number stability criteria is based on a heating section whose exact location is known and used as an example for all the other sections. The Rayleigh number was evaluated in the pipe water for the heating and non-heating sections located between 40 and 46 m depth. The top of the system was fixed at 40.6 m, a depth at which the minimum temperature during the heat injection was recorded.

The Rayleigh number calculations was done with temperature data recorded at 25, 95 and 121 hours, representing the beginning and the end of the heat injection and the recovery period respectively. The highest Rayleigh number occurs at the end of the heat injection period near the location of the heating section and up to 1.5 m above. The maximal Rayleigh value is located at the upper part of the heating section, agreeing with the temperature peak (Figure 1.7).

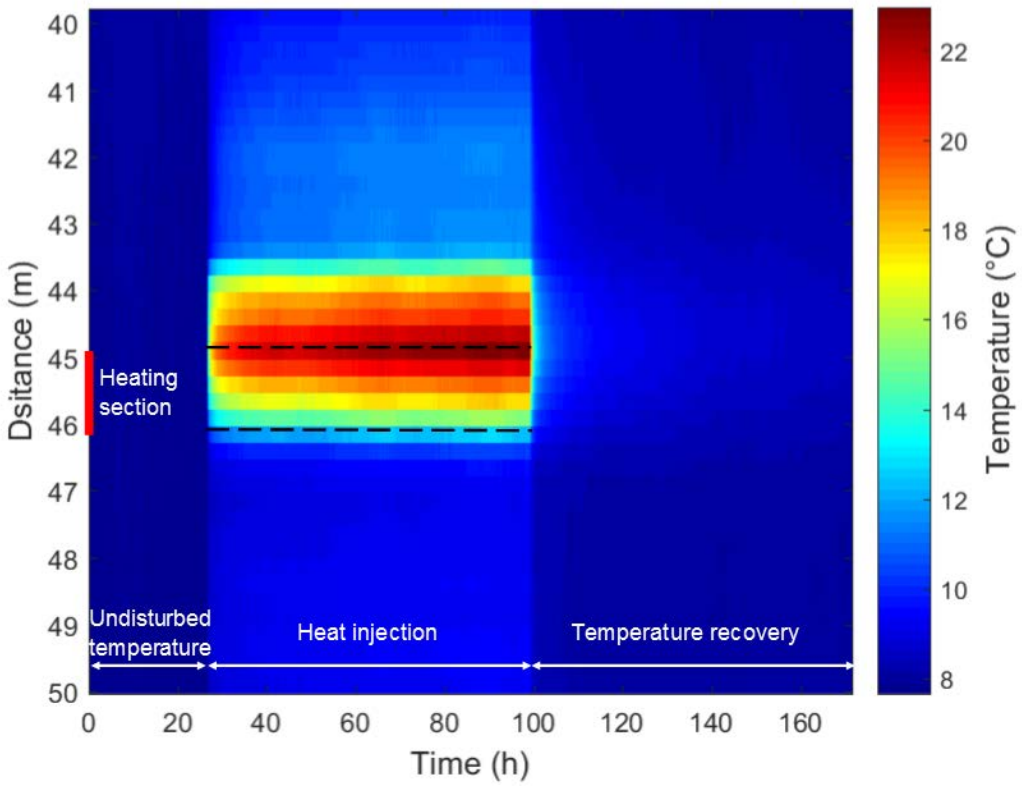


**Figure 1.6.** Temperature distribution during the TRT around a typical heating section at 45 to 46 m depth.

Three critical lengths 3, 6, and 9 m were used to calculate critical Rayleigh number with Eq. 1.8 and 9 and verify the stability criteria (Figure 1.7). When defining  $H_t$  equals 3 m, the actual Rayleigh number is larger than the critical Rayleigh number for all cases considered (28.5 h, 95 h, 121 h), suggesting the presence of significant heat transfer by free convection in all the water column. Nevertheless, recorded temperatures between 41 and 43 m depth did not have a great variation and free convection at this depth was not expected. The choice of  $H_t$  equals 3 can be too small for the studied system.

In the second case when defining  $H_t$  equals 6 m, the actual Rayleigh number at the beginning of the heat injection (28.5 h) and during the recovery period (121 h) did not exceed the critical value. However, the actual Rayleigh number exceeds the critical value at the end of the heating period (95 h) for a portion of the heating section and up to 1.5 m above, suggesting the presence of free convection.

The third case considering  $H_t$  equal to 9 m shows a critical Raleigh number that is always larger than actual Rayleigh number, suggesting the absence of free convection. Defining  $H_t$  equals

9 m can, however, overestimate Rayleigh's critical value since temperature increase far above from the heating section is a strong evidence for heat transfer due to free convection.

The effect of the perforated plastic disks to reduce free convection is difficult to evaluate. Nevertheless, the Rayleigh number reaches its maximal value at the top of the heating section (45 m) and decreases above heating sections where the perforated plastic disks were located. A similar effect occurs at the end of the heating section.

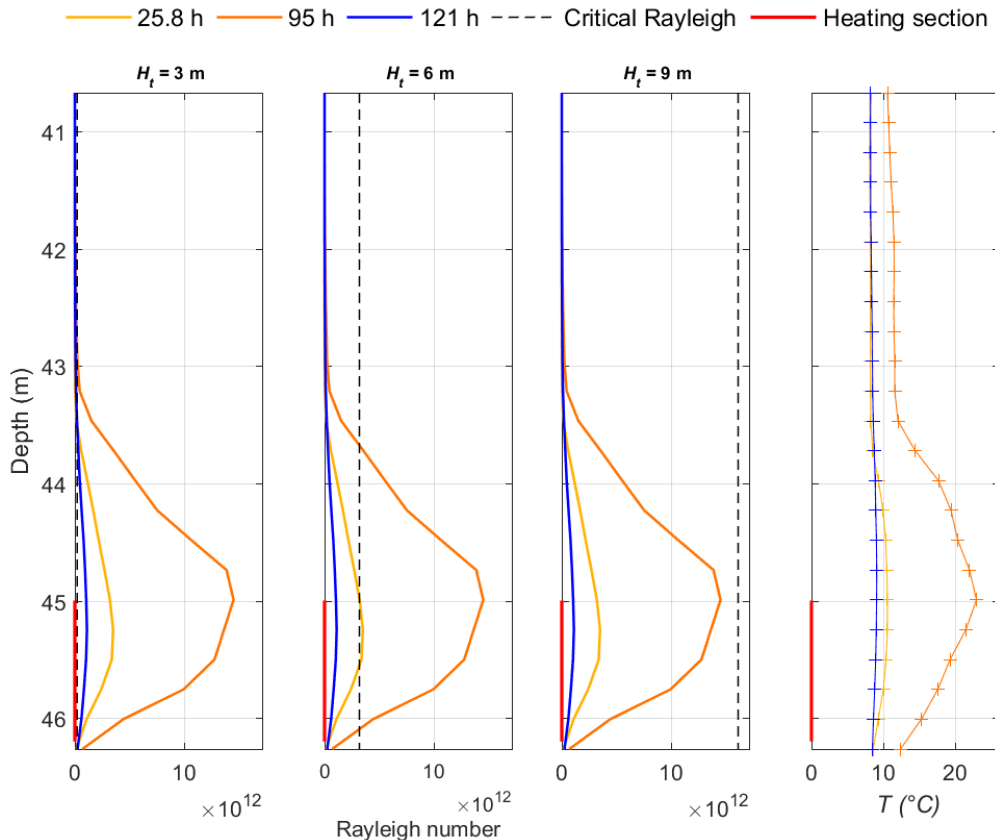


**Figure 1.7. Verification of the Rayleigh number stability criteria considering different critical lengths ( $H_t$ ) to calculate critical Rayleigh number (dashed lines).**

## 1.5 Discussion and conclusions

A new method to conduct thermal response tests (TRT) coupling heating cable section and fiber optic distributed temperature sensing (FO-DTS) has been presented. The monitoring in the whole cable assembly using FO-DTS allowed evaluating the temperature evolution beyond the submersible sensors near the heating sections extremities and the non-heating cable to better

understand the heat transfer phenomena occurring during the test. Such additional temperature measurements from the FO-DTS indicated small temperature increments in the middle of the non-heating cable sections and important temperature increases at the extremities of the non-heating cable section just above the heating sections.

The subsurface thermal conductivity was evaluated using a finite line source solution to simulate conductive heat transfer. The distributed thermal conductivity estimated is slightly higher than the maximum effective thermal conductivity evaluated during the conventional TRT. This overestimation can be explained by the fact that the analysis was done considering conductive heat transfer only and, as it was demonstrated by Raymond and Lamarche (2014), that free convection can occur beyond the interface between heating and non-heating cable sections.

Uncertainty of a TRT with a heating cable sections at the laboratory scale was evaluated by Simon (2016). Uncertainty of 25% about the estimated thermal conductivity was calculated using the standard rules of combination errors. A similar methodology adapted for the field test can be applied to evaluate the uncertainty about the estimated thermal conductivity.

The Rayleigh number stability criteria suggests the presence of free convection at the heating section and approximately 1.5 m above. The presence of free convection at the top of the heating sections can explain the difference between the thermal conductivity estimated using the heating cable section methodology and the conventional TRT.

The effect of free convection in the heating section extremities was already identified by Raymond and Lamarche (2014) with a numerical simulation of the borehole temperature evolution during a TRT. A first field demonstration of the heating cable methodology using submersible temperature sensors at the depth of each heating section and perforated plastic disks to reduce free convection was carried out by Raymond *et al.* (2015). Nevertheless, the temperature monitoring using FO-DTS had not been used before during a TRT with heating cable sections. The additional temperature data provided by the FO-DTS allow identifying important temperature increases at the top of the heating sections related to free convection.

Considering the significant temperature increase above the heating section, the active heating length used for the thermal conductivity estimation must be reevaluated. Further analysis is required to evaluate the ratio of conduction and convection heat transfer to adjust the test analysis methodology.

## **Article 2**

### **Distributed thermal response tests using a heating cable and fiber optic temperature sensing**

#### **Titre traduit**

Tests de réponse thermique distribués avec câbles chauffants et suivi de la température par fibre optique

#### **Auteurs**

Maria Isabel Vélez<sup>1</sup>, Jasmin Raymond<sup>1</sup>, Daniela Blessent<sup>2</sup>, Mikael Philippe<sup>3</sup>, Nataline Simon<sup>4</sup> Olivier Bour<sup>4</sup>, Louis Lamarche<sup>5</sup>

<sup>1</sup> Centre-Eau Terre Environnement, Institut national de la recherche scientifique, Québec, Qc, Canada

<sup>2</sup> Programa de Ingeniería Ambiental, Universidad de Medellín, Medellín, Colombia

<sup>3</sup> Georesources Division, BRGM, 3 avenue Claude Guillemin, BP 36009, 45060 Orléans Cedex 2, France

<sup>4</sup> Univ Rennes, CNRS, Géosciences Rennes - UMR 6118, F-35000 Rennes, France

<sup>5</sup> École de Technologie Supérieure, Département de génie mécanique, Montréal, Canada

#### **Publié**

*Energies* 2018, 11(11), 3059; <https://doi.org/10.3390/en11113059>

## **RESUMÉ**

Les tests de réponse thermique sont utilisés pour évaluer la conductivité thermique du sous-sol lors de la conception des systèmes de pompe à chaleur géothermique. Pour effectuer un test conventionnel, une source de haute puissance est requise pour chauffer l'eau qui circule dans l'échangeur de chaleur pilote. Une nouvelle méthode d'essai avec un câble chauffant a été développée comme une alternative pour effectuer le test avec une source d'énergie de basse puissance et un équipement compact. Deux tests de réponse thermique avec un câble chauffant en section et continu ont été réalisés dans deux échangeurs de chaleur expérimentaux sur des sites différents. Le suivi de l'évolution de la température au cours des essais a été fait à l'aide de capteurs submersibles et des mesures distribuées de la température avec fibre optique. La convection naturelle qui peut se produire dans l'échangeur de chaleur a été évaluée en utilisant le critère de stabilité du nombre de Rayleigh. Les équations de la ligne source finie et infinie ont été utilisées pour reproduire les variations de température le long du câble chauffant en sections et continu, respectivement. L'incertitude de l'estimation de la conductivité thermique avec chaque câble a aussi été évaluée. Une conductivité thermique moyenne supérieure de 15% que la valeur obtenue avec le test conventionnel a été estimée avec le câble chauffant en sections. La conductivité thermique évaluée à l'aide du câble chauffant continu correspond à la valeur estimée lors du test conventionnel. L'incertitude moyenne associée à l'essai de la section du câble chauffant était de 15,18%, tandis qu'une incertitude de 2,14% était estimée pour l'essai avec le câble chauffant continu. Selon le critère de stabilité du nombre de Rayleigh, la convection naturelle peut se produire pendant la période d'injection de chaleur lorsque des sections de câble chauffant sont utilisées. Le câble chauffant continu avec une source de puissance faible est une méthode prometteuse pour réaliser des tests de réponse thermique et des essais supplémentaires pourraient être effectués dans des trous de forage de plus de 100 m afin de vérifier son applicabilité dans les échangeurs de chaleur au sol couramment installés pour les systèmes de pompe à chaleur couplés au sol.

## **ABSTRACT**

Thermal response tests are used to assess the subsurface thermal conductivity to design ground-coupled heat pump systems. Conventional tests are cumbersome and require a source of high power to heat water circulating in a pilot ground heat exchanger. An alternative test method using heating cable was verified in the field as an option to conduct this heat injection experiment with a low power source and a compact equipment. Two thermal response tests

using heating cable sections and a continuous heating cable were performed in two experimental heat exchangers on different sites in Canada and France. The temperature evolution during the tests was monitored using submersible sensors and fiber optic distributed temperature sensing. Free convection that can occur in the pipe of the heat exchanger was evaluated using the Rayleigh number stability criterion. The finite and infinite line source equations were used to reproduce temperature variations along the heating cable sections and continuous heating cable, respectively. The thermal conductivity profile of each site was inferred and the uncertainty of the test was evaluated. A mean thermal conductivity 15% higher than that revealed with the conventional test was estimated with heating cable sections. The thermal conductivity evaluated using the continuous heating cable corresponds to the value estimated during the conventional test. The average uncertainty associated with the heating cable section test was 15.18%, while an uncertainty of 2.14% was estimated for the test with the continuous heating cable. According to the Rayleigh number stability criterion, significant free convection can occur during the heat injection period when heating cable sections are used. The continuous heating cable with a low power source is a promising method to perform thermal response tests and further tests could be carried out in deep boreholes to verify its applicability.

## 2.1 Introduction

Ground coupled heat pumps systems, made of a ground heat exchanger (GHE) and a heat pump, have been recognised as an efficient and environmentally friendly technology to cool and heat residential and commercial buildings. The thermal conductivity and the borehole thermal resistance are required to design such systems considering that an accurate estimation of these properties has a direct impact on their efficiency and cost (Marcotte & Pasquier, 2008, Zhang *et al.*, 2014).

Thermal response tests (TRTs) have been proposed by Mogensen (1983) as an in situ method to assess the subsurface thermal conductivity and the borehole thermal resistance. The first mobile TRT devices were developed by Eklöf and Gehlin (1996) and Austin III (1998) at Luleå Technical University and Oklahoma State University, respectively, and historic reviews of the TRT development has been published by Gehlin (2002), Sanner *et al.* (2013) and Spitler and Gehlin (2015). During a conventional test, the fluid circulating in the ground heat exchanger (GHE) is heated using an electrical element in the TRT ring to reproduce heat transfer phenomena occurring in the GHE. Inlet and outlet temperatures along with flow rates are recorded and then analysed to determine the bulk subsurface thermal conductivity over the

length intercepted by the borehole (Gehlin, 1998, Raymond *et al.*, 2011a). TRT analysis is usually performed using the infinite line source model, an analytical solution to the heat conduction equation (Carslaw, 1945, Ingersoll & Plass, 1948). This one dimensional conductive heat transfer solution describes the mean temperature increment at a radial distance from an infinite source of heat having a constant heat flow rate and assuming a constant temperature at an infinite radial distance from the source.

Conventional TRT requires a source of high power (50 - 80 W m<sup>-1</sup>; Kavanaugh, 2001) to heat the water circulating in the GHE and generate a temperature difference between 3 to 7 °C at the inlet and outlet of the GHE, reproducing the operation of a geothermal system. Only the bulk thermal conductivity can be estimated over the length intercepted by the borehole (Sanner *et al.*, 2005). Depending on the site properties, the estimated bulk thermal conductivity can be affected by the ground heterogeneity (Fujii *et al.*, 2006) and groundwater flow (Gehlin & Hellström, 2003, Gustafsson & Westerlund, 2011). The use of fiber optic distributed temperature sensing (FO-DTS), a technology to monitor temperature at high frequency and spatial resolution (Bense *et al.*, 2016), was proposed by Fujii *et al.* (2006; 2009) to measure the vertical temperature profile during TRT as an alternative method to assess the vertical distribution of the ground thermal conductivity and associated ground heterogeneity. Subsequently, fiber optic cables have been used to validate analytical models of the vertical temperature evolution (Beier *et al.*, 2012) and to measure borehole wall temperatures (Acuña & Palm, 2013) during TRTs. FO DTS and a heat trace cable was additionally used by Freifeld *et al.* (2008) to estimate the ground thermal conductivity as a function of depth and to infer ground surface temperature history.

To reduce the power requirements of TRTs, which is one of the main expenses estimated to be 10 to 30 % of the total test cost (Raymond & Lamarche, 2014), and to evaluate the thermal conductivity as a function of depth, an alternative method to perform TRTs using heating cables and submersible temperature sensors was proposed by Raymond *et al.* (2010, 2015). In locations where the ground is heterogeneous, the GHE can preferentially be drilled into lithological units with a high thermal conductivity (Fujii *et al.*, 2009). Obtaining the vertical distribution of the thermal conductivity may allow defining the most advantageous drilling conditions for the GHE in addition to better constrain the simulation of the system that can consider subsurface heterogeneity. Tests with heating cables are not affected by temperature variation at surface, such as atmospheric temperature changes and solar radiations, commonly influencing the heat injection rates of conventional TRT taking place at surface (Raymond *et al.*,

2010). The proposed method uses a cable standing in the water column of the GHE pipe to heat the ground, with several advantages, such as avoiding water circulation, removing the adverse effect of surface temperature fluctuations, reducing the required heat injection rate and simplifying the field manipulations. Two types of cable were used to perform the tests: a continuous heating cable and interchanging sections of heating and non-heating cable. The heat injection rate of heating cables used for previous tests varied from 20 to 40 W m<sup>-1</sup> (Raymond *et al.*, 2015; Raymond & Lamarche, 2014) and the required power of less than 1 kW was supplied by connecting the TRT unit to the electrical grid (Raymond *et al.*, 2015). Tests with a continuous heating cable were achieved in boreholes having a depth of approximately 30 m, while boreholes with more than 100 m in length have been the subject of tests with heating sections to keep a low power requirement (Raymond, 2018).

The test analysis conduct when using the continuous heating cable is similar to that of a conventional TRT, based on the infinite line source solution to reproduce the observed temperature increments in the GHE. A finite heat source solution must be used for the analysis of a test with heating cable sections to adequately reproduce observed temperatures along the heating sections that can be between 1 - 2 m in length (Raymond *et al.*, 2015). These mathematical solutions are based on the assumption of conductive heat transfer only, while natural convection can occur in the standing water column of the GHE pipe, especially near the limits of the heating and non-heating sections due to the temperature gradient created within the pipe upon heat injection. Numerical simulations conducted by Raymond and Lamarche (2014) and small-scale field experiments with one heating section (Simon, 2016) indicate that perforated plastic disks located between heating and non-heating sections can reduce convective heat transfer. It is, therefore, suggested that natural convection during full-scale TRT experiments conducted in the field with continuous and heating cable sections should be investigated.

The objectives of this work were to better understand free convection and conduction heat transfer mechanisms occurring during a TRT with a heating cable to estimate the subsurface thermal conductivity and its uncertainty, as well as to assess the effect of perforated plastic disks to reduce free convection when heating cable sections are used. Two TRTs using heating cables and FO-DTS were conducted at two experimental sites in Quebec City, Canada, and Orléans, France, with vertical heat exchangers. A first test was done with ten heating sections in a 100 m borehole using a heat injection rate of ~40 W m<sup>-1</sup> while, at the other site, a second test was achieved in a borehole of equivalent length with a continuous heating cable and a heat

injection rate of less than  $\sim 10$  W m<sup>-1</sup>. This paper describes first heating cable TRT combined with FO-DTS and a first continuous heating cable TRT in a long borehole with a low heat injection rate. Conventional TRT with water circulation was previously conducted at both sites and the results were used for comparison purposes. The Rayleigh number stability criterion, a methodology to evaluate convective heat transfer in vertical groundwater wells proposed by Love *et al.* (2007), was applied to assess convective heat transfer during the tests. FO-DTS technology used to monitor temperature in boreholes at high frequency and spatial resolution along a fiber optic cable (Bense *et al.*, 2016) provided the information needed to evaluate the Rayleigh number stability criterion. Thermal conductivity profiles were estimated using the infinite and finite heat source solution depending on the heating cable used and an uncertainty analysis of each test was performed.

## 2.2 Field test methodology

The TRT with heating cable sections was carried out at the Laboratories for scientific and technological innovation in environment of the Institut national de la recherche scientifique, located in Quebec City, Canada. A GHE made of a single U-pipe was used to perform the test to a depth of  $\sim 100$  m. The borehole intercepts backfill material down to a depth of 2 m, followed by 8 m of clay and then shale constituting the host rock (Figure 2.1a). This last geological unit is the Les Fonds Formation of the Sainte-Rosalie Group in the St. Lawrence Lowland sedimentary basin (Raymond *et al.*, 2017). The groundwater levels inside the borehole was approximately 2 m depth.

The second TRT with a continuous heating cable was carried out at the experimental geothermal test facility of the Bureau de Recherches Géologiques et Minière in Orléans, France. A GHE made of a double-U pipe was used for the test to a depth of  $\sim 100$  m. This borehole intercepts 8 m of sand and clays of the Sologne Basin succeeded by limestone formations (Figure 2.1b), mainly Calcaire de Pithiviers and Calcaire du Gatinais (Philippe, 2010).

The cable used for the test in Québec City is made of interchanging heating and no heating sections with length of 1.20 and 8.60 m, respectively (Figure 2.2a), while that for the test in Orléans was continuous (Figure 2.2b). The same field test methodology was applied to both sites, but the heat injection rate was adapted according to heating cable design to achieve a low power requirement.

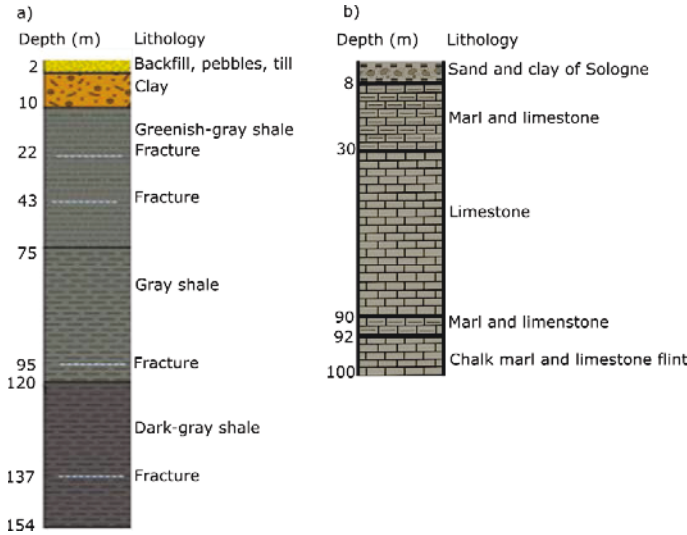


**Figure 2.1. Stratigraphic description of the borehole located in a) Québec City and b) Orléans (modified from a) Raymond et al., 2017 and b) Philippe, 2010).**

The equipment required to perform the tests consists of the heating cable assembly, a junction box to link the cable to the power supply (Figure 2.3), and submersible sensors to measure and record the temperature during the test. The junction box is composed of an automated switch to start and stop the heat injection, a voltage regulator, a power meter with an accuracy of +/- 0.02 W to monitor the power induced and circuit breakers to protect the electric circuits of the cable assembly and the power meter (Raymond et al., 2015). Additionally, when heating cable sections are used, perforated plastic disks are needed. Four disks separated by about 10 cm and defining the active heating length for analysis were installed at the interface between the heating and non-heating sections to reduce the possible convective heat transfer.

The temperature was measured in both tests using submersible sensors and a fiber optic cable. The submersible sensors are DST-centi temperature data loggers with an accuracy of +/- 0.10 °C and a resolution of 0.032 °C made by Star-Oddi. The FO-DTS system used for the test in Québec City consisted of a BruSens fiber optic cable of 250 m length and connected to a Silixa XT-DTS control unit in double-ended configuration with 2 km range (van de Giesen et al., 2012). This 3.80 mm diameter fiber optic sensing cable, armored with stainless steel, has a fast thermal response which allows for recording temperature changes efficiently. Two cable sections of 20 m long were placed in an ambient (37.40 °C) and cold (0.30 °C) temperature bath, respectively, to calibrate the DTS unit. A Starmon mini probe (+/- 0.025 °C) and a RBRduet probe (+/- 0.002 °C) were used in the bath to record the temperature for calibration purpose. The FO-DTS used in Orléans for the second test was an Orxy DTS in double-ended

configuration with a temperature resolution of +/- 0.05 °C (Philippe, 2010). The temperature measured with the fiber optic was corrected using a calibration bath at 0 °C.

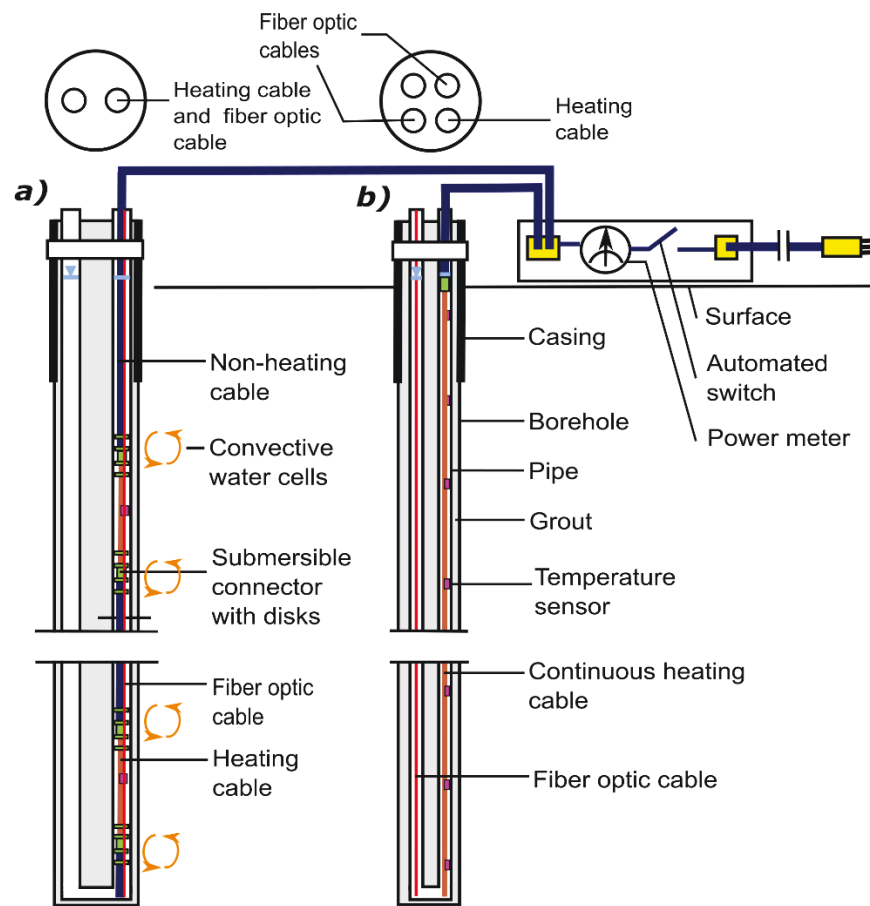


**Figure 2.2. Apparatus for TRT with a) heating cable sections and b) a continuous heating cable (modified from Raymond, 2018).**

In the first case, the submersible temperature sensors were placed in the middle of each heating section located approximately every 10 m, from 5 to 95 m depth. The fiber optic cable was attached to the cable assembly that was lowered in a pipe of the ground heat exchanger reaching a depth of 100 m. The FO-DTS system was configured to collect data every 60 s with a 25 cm sampling interval along the fiber optic cable while the submersible sensors recorded temperature every 10 minutes. The sampling interval of the temperature sensor and the fiber optic are different because the FO-DTS data are used to assess free convection during the TRT and the data from the submersibles sensors is used to infer the thermal conductivity. The test started with a measure of the undisturbed subsurface temperature followed by heat injection at an average rate of  $42.50 \text{ W m}^{-1}$ , after which the thermal recovery was monitored.



**Figure 2.3. Junction box for TRT with a heating cable.**

The double U-pipe heat exchanger in Orléans was equipped with a FO-DTS system that allows measuring the temperature in two of the pipes of the GHE. The test was implemented with a continuous heating cable of 95 m. The submersible temperature sensors were placed every 6 m, from 5.50 m to 83.60 m depth, and the FO-DTS system was programmed to collect data each meter, every 10 minutes. Due to the small pipe diameter, the heating cable and the fiber optic cables could not be placed in the same pipe. Thus, it was installed in other pipes located at a distance of 0.06 and 0.82 m from the pipes containing the fiber optic. The four pipes in this GHE are separated with spacers. The test started with the measurement of the undisturbed subsurface temperatures followed by heat injection at a rate of  $9.90 \text{ W m}^{-1}$  and, finally, thermal recovery monitoring. A test with a heat injection rate below  $10 \text{ W m}^{-1}$  was possible due to the improvement of temperature sensor resolution accomplished in recent years. Sensors with a resolution less than  $0.05 \text{ }^{\circ}\text{C}$  are able to measure small temperature changes allowing to perform the tests with a low heat injection rate, which was difficult to achieve with the previously available technologies.

## 2.3 Test analyses

### 2.3.1 Thermal conductivity assessment

The test analysis was done with the line source solution for conductive heat transfer. Two variations of this solution were used according to the cable deployed to perform the test. Heating cable sections were represented as finite line sources, whereas the infinite line source is used with a continuous heating cable. The methodology to analyse the TRT with both types of cable was previously described by Raymond and Lamarche (2014) and Raymond *et al.* (2010).

The temperature data collected with the submersible sensors were used to estimate the thermal conductivity at the depth of each sensor. The recovery temperature increments ( $\Delta T = T - T_0$ ), defined as the increase of temperature with respect to the initial temperature  $T_0$ , were reproduced with the analytical solutions using the temporal superposition principle to consider the recovery period where heat injection is zero. Numerical simulation results described by Raymond *et al.* (2011a) indicate that the temperature inside a slice of a borehole varies significantly according to the horizontal measurement location during the heat injection, making it necessary to consider the horizontal position of the temperature sensor to analyse the test. However during the recovery period the temperature becomes uniform and the position of the sensor does not influence the measurement. The horizontal position of the temperature sensor is difficult to determine, therefore the thermal conductivity was estimated using only the late recovery temperatures at each depth. A linear heat source solution of finite length with a dimensionless  $g$ -function (Eq. 2.1, Raymond and Lamarche, 2014; Raymond *et al.*, 2010), which depends on the Fourier number ( $Fo$ ), was used to analyse the test with heating sections:

$$\Delta T = \frac{q}{2\pi\lambda_s} g \left[ \left( Fo, \frac{r}{h} \right) - \left( Fo^{'}, \frac{r}{h} \right) \right] \quad (2.1)$$

$$\text{with } Fo = \frac{\alpha_s(t)}{h^2} \quad (2.2)$$

$$\text{and } Fo^{'} = \frac{\alpha_s(t - t_{\text{off}})}{h^2} \quad (2.3)$$

where  $q$  ( $\text{W m}^{-1}$ ) is the heat injection rate per unit length,  $\alpha_s$  ( $\text{m}^2 \text{s}^{-1}$ ) and  $\lambda_s$  ( $\text{W m}^{-1}\text{K}^{-1}$ ) are the thermal diffusivity and conductivity of the subsurface, respectively,  $r$  (m) is the radial distance from the heat source,  $H$  (m) is the active heating length, and  $t_{\text{off}}$  is the time when heat injection

was stopped. The heat capacity of the subsurface was assumed based on the rock type identified with drill cuttings and it was also used to determine the thermal diffusivity ( $\alpha_s$ ) and to compute Fourier's number (Eq. 2.2 and 2.3). The heat injection rate  $q$  ( $\text{W m}^{-1}$ ) for each heating section was assumed similar and determined according to Joule's and Ohm's laws:

$$q = \frac{R_h I^2}{nh} \quad (2.4)$$

where  $R_h = R_{\text{tot}} - R_{\text{nh}}$  (2.5)

$$\text{and } R_{\text{tot}} = \frac{U}{I} \quad (2.6)$$

where  $R$  (Ohm) is the electric resistance,  $I$  (A) is the electrical current intensity,  $U$  (V) is the potential difference,  $n$  is the number of heating sections and  $H$  (m) is the length of the heating sections. The subscripts h, nh, and tot correspond, respectively, to the electrical resistance of the heating sections, of the non-heating sections, and of the whole cable assembly.

The computed temperature increments of the late recovery period were matched with a non-linear solver (Lasdon et al., 1978) to the observed temperature increments by adjusting the thermal conductivity using a least-squared fit. The analysis of the temperature measurements recorded with the submersible data loggers was performed using a spreadsheet program developed by Raymond et al. (2015).

The infinite line source equation was used for the second test with a continuous heating cable to evaluate the temperature increase during the late recovery period. TRT theories indicate that, after a sufficiently long heat injection time ( $t$ ), the thermal conductivity can be estimated from the slope  $m$  of the graphic relating the temperature increases with the logarithmic time (Eq. 2.7; Beck et al., 1971):

$$m = \frac{\Delta T}{\Delta \ln(t)} = \frac{q}{4\pi\lambda_s} \quad (2.7)$$

A negative heat injection rate is introduced at time  $t_{\text{off}}$  to simulate the recovery period (Pehme et al., 2007b) and temperatures are plotted as a function of a normalized time  $t/(t-t_{\text{off}})$  to find thermal conductivity with the slope method:

$$m' = \frac{\Delta T}{\Delta \ln(t/t - t_{\text{off}})} = \frac{q}{4\pi\lambda_s} \quad (2.8)$$

The heat injection rate for the continuous heating cable was calculated from the electric potential difference and the electrical current intensity measurements (Eq. 2.9):

$$q = \frac{UI}{H} \quad (2.9)$$

where  $H$  (m) is now the total length of the continuous heating cable.

### 2.3.2 Uncertainty analysis

An analysis of the different sources of error influencing the test results was performed to determine the uncertainty associated with the tests. Witte (2013) proposed a methodology to evaluate the accuracy of the thermal conductivity estimated during TRT, taking into account the sources of error associated with the variables that are measured repeatedly during the test, measured once before or after the test or estimated independently. This methodology is based on the infinite line source equation, which is the model commonly used to analyse conventional TRT, and utilise the standard deviation and the confidence interval as the measure of the error. The general procedures described in the supplement 1 to the guide to the expression of uncertainty in measurement (BIPM *et al.*, 2008) and by Ellison and Williams (2012) are used to calculate the propagation of errors.

The methodology proposed by Witte (2013) was adapted in this study to calculate the uncertainty associated with the thermal conductivity estimated with both continuous and separated heating cable sections. The error analysis was applied to the finite line source equation for the test with heating cable sections while Witte (2013) theory could directly be used for the test with the continuous cable relying on the infinite line source equation.

The combined error of the cable electrical resistivity for the heating sections assembly  $\delta R_{\text{tot}}$  (Eq 2.10), the electrical resistivity of the heating section  $\delta R_h$  (Eq. 2.11) and the heat injection rate  $\delta q$  (Eq. 2.12) were determined using the accuracy of the individual parameters.

$$\frac{\delta R_{\text{tot}}}{R_{\text{tot}}} = \sqrt{\left(\frac{\delta V}{V}\right)^2 + \left(\frac{\delta I}{I}\right)^2} \quad (2.10)$$

$$\delta R_h = \sqrt{(\delta R_{\text{tot}})^2 - (\delta(R_{\text{nh}} L_{\text{nh}}))^2} \quad (2.11)$$

$$\text{with } \delta(R_{\text{nh}} L_{\text{nh}}) = R_{\text{nh}} L_{\text{nh}} \sqrt{\left(\frac{\delta R_{\text{nh}}}{R_{\text{nh}}}\right)^2 + \left(\frac{\delta L_{\text{nh}}}{L_{\text{nh}}}\right)^2} \quad (2.12)$$

$$\frac{\delta q}{q} = \sqrt{\left(\frac{\delta R_h}{R_h}\right)^2 + \left(\frac{\delta I}{I}\right)^2 + \left(\frac{\delta h}{h}\right)^2} \quad (2.13)$$

Then, the methodology was adapted to estimate the uncertainty associated with the  $g$ -function used to calculate the temperature increments (Eq. 2.1). This equation was simplified removing the constant value of  $2\pi$  (Eq. 2.14) and the equation was modified defining a variable  $Z = g(Fo) \Delta T^1$  (Eq. 2.15), allowing for determination of the error associated with the analytical solution. The uncertainty  $\delta Z$  was determined over a 95% of confidence (Eq. 2.16; Simon, 2016) by the generalization of the error estimation of non-linear regression (Eq. 2.17). From Eq. 2.1, we have;

$$\Delta T = \frac{q}{\lambda_s} [g(Fo) - g(Fo')] = \frac{q}{\lambda_s} f(Fo) \quad (2.14)$$

$$\frac{q}{\lambda_s} = \frac{g(Fo)}{\Delta T} = Z \quad (2.15)$$

$$\delta Z = 1.96 S_z \quad (2.16)$$

The standard deviation of  $S_z$  was determined similarly to the standard deviation of a slope (Eq. 2.17), considering the standard deviation of the calculated temperature increases ( $\Delta T_c$ ) and the measured temperature increases ( $\Delta T_m$ ; Eq. 2.18).

$$S_z = \sqrt{\frac{\sigma^2}{S_{xg}}} \quad (2.17)$$

$$\text{where } \sigma^2 = \frac{\sum (\Delta T_m - \Delta T_c)^2}{n - 2} \quad (2.18)$$

$$\text{and } S_{xg} = \sum (g - \bar{g})^2 \quad (2.19)$$

$$\frac{\delta \lambda}{\lambda} = \sqrt{\left(\frac{\delta q}{q}\right)^2 + \left(\frac{\delta Z}{Z}\right)^2} \quad (2.20)$$

In this set of equations,  $n$  represents the number of temperature data considered in the analysis,  $g$  is the finite heat source function calculated at each time at the depth of each temperature sensor and  $\bar{g}$  is the mean value of the function at each depth ( $S_{xg}$ , Eq. 2.19). Finally, the

uncertainty of the thermal conductivity estimation  $\delta\lambda$  was calculated taking in account the error of the heat injection rate and the error of  $Z$  (Eq. 2.20).

The accuracy of the individual parameters measured during the test with the continuous heating cable was used to calculate the combined error of the heat injection rate (Eq. 2.21) and the combined error of the slope of the graph relating the temperature increases with the logarithmic time  $\delta m'$  (Eq. 2.22). The uncertainty of the slope is expressed in terms of the regression residuals  $\sigma_T^2$  (Eq. 2.23) and the sum of the squared deviation from the sample mean ( $S_{xt}$ ; Eq. 2.24). Finally, the uncertainty of the thermal conductivity  $\delta\lambda$  is calculated as a function of the error of the heat injection rate and the slope (Eq. 2.25).

$$\frac{\delta q}{q} = \sqrt{\left(\frac{\delta U}{U}\right)^2 + \left(\frac{\delta I}{I}\right)^2 + \left(\frac{\delta H}{H}\right)^2} \quad (2.21)$$

$$\delta m' = \sqrt{\frac{\sigma_T^2}{S_{xt}}} \quad (2.22)$$

$$\text{where } \sigma_T^2 = \frac{\sum(T_m - T_c)^2}{n-2} \quad (2.23)$$

$$\text{and } S_{xt} = \sum(t - \bar{t})^2 \quad (2.24)$$

$$\frac{\delta\lambda}{\lambda} = \sqrt{\left(\frac{\delta q}{q}\right)^2 + \left(\frac{\delta m'}{m'}\right)^2}$$

(2.25)

### 2.3.3 Free convection assessment inside GHE pipe

Love *et al.* (2007) studied the diffusive transport induced by temperature variation in groundwater wells and formulated a Rayleigh number stability criterion to assess free convection in cylindrical wells. The stability criterion considers the well geometry and allows assessing convection in a standing water column having temperature gradients between top and bottom. Free convection can be a dominant heat transfer mechanism when the Rayleigh number  $Ra$  calculated with equation 2.26 exceeds a critical Rayleigh number  $Ra_c$  identified with Eq. 2.27.

$$Ra = \frac{g\beta H^3 \Delta T}{\nu \alpha_w} \quad (2.26)$$

where  $g$  ( $\text{m s}^{-2}$ ) is the gravitational acceleration,  $\beta$  ( $\text{K}^{-1}$ ) is the thermal expansion coefficient of the fluid,  $H$  (m) is the height of the water column,  $\Delta T$  ( $^\circ\text{C}$ ) is the difference in temperature between the top and the bottom of the system,  $\nu$  ( $\text{m}^2 \text{s}^{-1}$ ) is the fluid cinematic viscosity and  $\alpha_w$  ( $\text{m}^2 \text{s}^{-1}$ ) is the fluid thermal diffusivity. The critical Raleigh number computed for comparison is determined according to the cylinder geometry:

$$Ra_c = \frac{215.6}{r_a^4} (1 + 3.84 r_a^2) \quad (2.27)$$

$$\text{with } r_a = \frac{r}{H_t} \quad (2.28)$$

where  $r$  (m) is the well radius and  $H_t$  (m) is the height of the water column. The critical Rayleigh number is therefore a function of the well aspect ratio  $r_a$  (-) only and an increment in the well aspect ratio results in a reduction of the  $Ra_{cr}$  value (Love et al., 2007).

The Rayleigh number stability criterion was proposed by Love et al. (2007) to assess convection in groundwater wells in the presence of a geothermal gradient. In this study, the stability criterion was used to evaluate convection in GHE pipe where heat is injected using heating cables. Therefore, a similar approach based on the Rayleigh number stability criterion was applied to a system composed by a vertical pipe filled with water, where the temperature gradient is not uniform. Thus,  $H_t$  was defined as a critical length along the heating cable, rather than the well depth considered for groundwater well with a geothermal gradient. Nevertheless, defining a representative value for this variable is complicated because the critical Rayleigh number depends on the well aspect ratio. Increasing the well aspect ratio (larger radius and shorter height) results in a reduction of the critical Rayleigh number. Consequently, three different values of  $H_t$  were defined to evaluate its influence on the results of Rayleigh number stability criterion assessment.

A segment of 5.60 m of the cable assembly in the GHE was used to evaluate convection near a typical heating section. The segment is formed by a section of 4.40 m of non-heating cable located above a heating cable section of 1.20 m. The FO-DTS was used to determine  $\Delta T$  in Eq. 2.26 and compute the actual Raleigh number at different heights of the water column in the pipe varying over a range of 0.25 - 5.80 m to verify the Rayleigh number stability criterion.

The critical Rayleigh number was calculated for the pipe radius ( $r = 1.72$  cm) and a critical length  $H_t$  of 3.00, 6.00 and 9.00 m. These values represent the mean height of the water column used to calculate actual Rayleigh numbers, the length of the maximum temperature difference between heating and non-heating sections and the total length of a system of a single heating and a non-heating section, respectively.

In the tests with a continuous cable, free convection is not expected because the heat injection rate is roughly uniform along the cable. Nevertheless, the Rayleigh criterion was evaluated to verify the absence of this effect. The shortest section showing the maximum temperature difference was selected, avoiding the first 5 m near the surface where the ambient temperature had an influence on the temperature measured in the pipe during the TRT. The criterion was evaluated between 18 m depth (minimal temperature of 12.30 °C) and 42 m depth (maximal temperature of 16.30 °C).

The actual Rayleigh numbers were computed considering a water column varying from 1 to 24 m. The pipe had a radius 1.31 cm and the critical Rayleigh number was first evaluated using a minimal critical length of 2 m. This value was defined as the minimal length because the sampling resolution of the fiber optic data was 1 m.

## 2.4 Results

The fiber optic measurements allowed visualizing the temperature evolution in the GHE during the whole test to better illustrate and understand heat transfer mechanisms. The undisturbed temperature was monitored during 26 h for the test in Québec City. Then, heat was injected for a period of 73 h (from 26 h to 99 h) and thermal recovery was monitored during the following 70 h, from 99 to 169 h (Table 2.1, Figure 2.4). The total energy consumption during the test was 71.75 kWh and the average potential difference and electrical current intensity were 113 V and 8.7 A, respectively. The maximum temperature increase reached at the depth of each heating section was variable. Those differences are related to the variation in the subsurface thermal conductivity. High temperature increments at the depth of a heating section indicate a low subsurface thermal conductivity and a slight temperature increase corresponds to a greater thermal conductivity. The electric current during the field tests was fixed with a variable transformed allowing to reduce changes in heat injection rates. However, the heat injection rate was affected by the variation of the current intensity of the electrical grid. Then local variation in the heat injection rate could also influence the temperature increases. This effect was

attenuated by analysis of recovery temperature measurements, where we know that heat injection is zero.

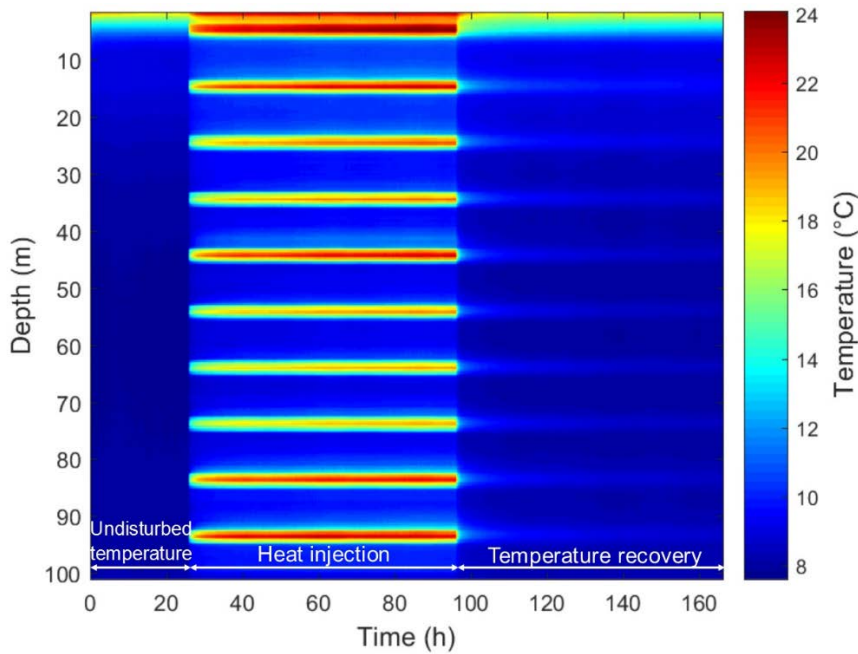


**Figure 2.4. Temperature evolution during the three steps of the TRT in Quebec City with heating cable sections.**

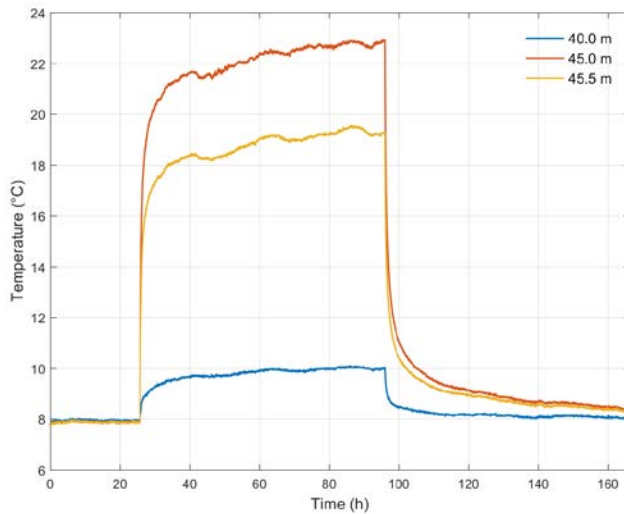


**Figure 2.5. Observed temperature at the middle of a non-heating section (40 m) and at the top (45 m) and the middle (45.5 m) of a heating section.**

The distributed temperature measurement reveals an increase of approximately 2 °C from the initial temperature at the middle of non-heating sections, with measurements at 40.0 m depth provided as an example (Figure 2.5). Differences of more than 2 °C were also observed

between the top and the middle of the heating sections, which are 45.0 and 45.5 m in the example (Figure 2.5), indicating important temperature variations over a short distance.

**Table 2.1 Experimental condition and configuration of TRT**

Parameter	Quebec City	Orléans
Heating cable type	Heating section	Continuous heating cable
Test analysis method	Finite line source	Infinite line source
Borehole configuration	Single U-bend	Double U-bend
TRT start date	2016-08-31	2017-07-03
TRT start time	11:20:00	13:00:00
TRT end date	2016-09-07	2017-08-02
TRT end time	12:11:00	10:00:00
Borehole depth (m)	150	100
Heating cable length (m)	100	95
Borehole diameter (mm)	114	180
Pipe diameter (mm)	32.00	26.20
Duration of undisturbed temperature monitoring (h)	26.00	100.00
Heat injection period (h)	73.00	135.70
Thermal recovery period (h)	70.00	481.30
Total test duration (h)	169.00	717.00
Initial temperature (°C)	8.20	13.10
Heat injection rate (W m <sup>-1</sup> )	42.50	9.90
Temperature sensors vertical distance (m)	10	6

The undisturbed temperature was monitored during 100 h for the second test in Orléans. Then, heat was injected for 135.60 h and a recovery period of 481.30 h was monitored (Figure 2.6 and Table 2.1). A geothermal gradient was observed at the Orléans site before conducting the TRT (Figure 2.6). A uniform temperature increase occurred during the heat injection period but ground temperature initially varied with depth such that the temperature increase was affected by the geothermal gradient, reaching a higher temperature at the bottom of the GHE (Figure 2.6). The heat injection rate was 9.90 W m<sup>-1</sup>, a lower rate compared to the first test. This rate was defined for the 100 m heating cable to cope with the potential difference provided by the electrical grid (120 V) and respecting the limits of the voltage regulator (140 V and 10 A). The total energy consumption during the test was 127.60 kWh and the average potential difference and electrical current intensity were 104 V and 8.99 A, respectively.

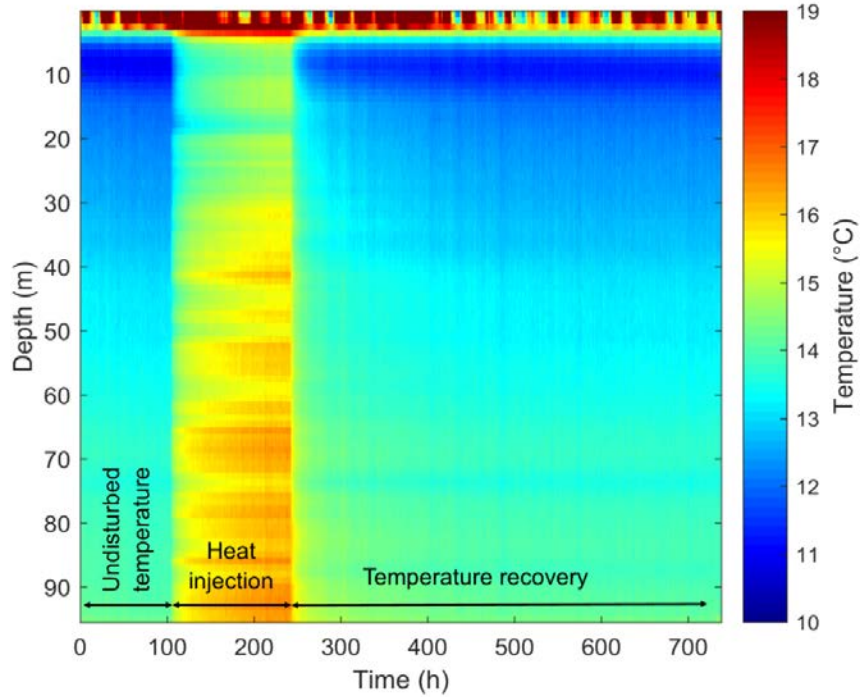


**Figure 2.6.** Temperature evolution during the three steps of the TRT at BRGM with a continuous heating cable.

#### 2.4.1 Thermal conductivity estimation

The analysis described below is based on submersible temperature measurements. A heat capacity of  $2.3 \text{ MJ m}^{-3} \text{ K}^{-1}$  associated with shales was assumed to compute the temperature increments and reproduce observations recorded for the first test in Québec City. The first 30 h of the recovery period were neglected and the analysis considered only the last 40 h to avoid the influence of the sensor location in the temperature measurement.

Adjustment between observed and computed temperature increments was achieved at the depth of each submersible temperature sensor tied to a heating section (Figure 2.7). However, to avoid repetition, only the curve matched at 45 m depth is provided as an example.

The first 20 h of the recovery period was neglected for the assessment of the thermal conductivity for the second test in Orléans. The temperature during the late recovery period was plotted as a function of the logarithmic time (Figure 2.8) and the slope of this line was used to determine the thermal conductivity at each measurement depth with submersible sensors according to Eq. 2.8.

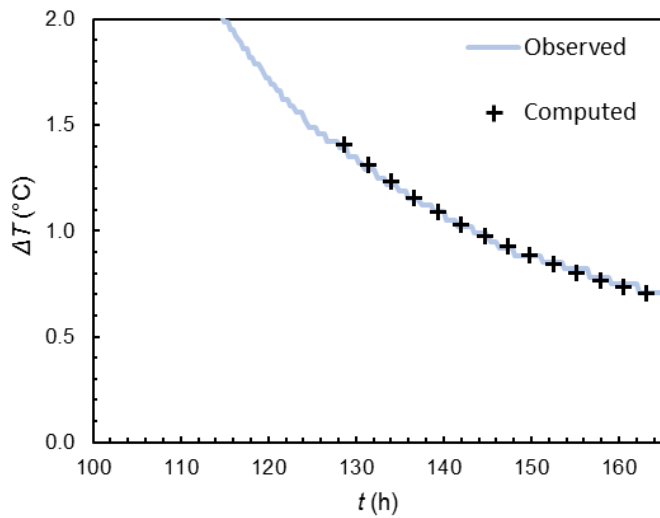


**Figure 2.7. Observed and computed temperature increments during the recovery period for the submersible sensor located at 45 m depth.**

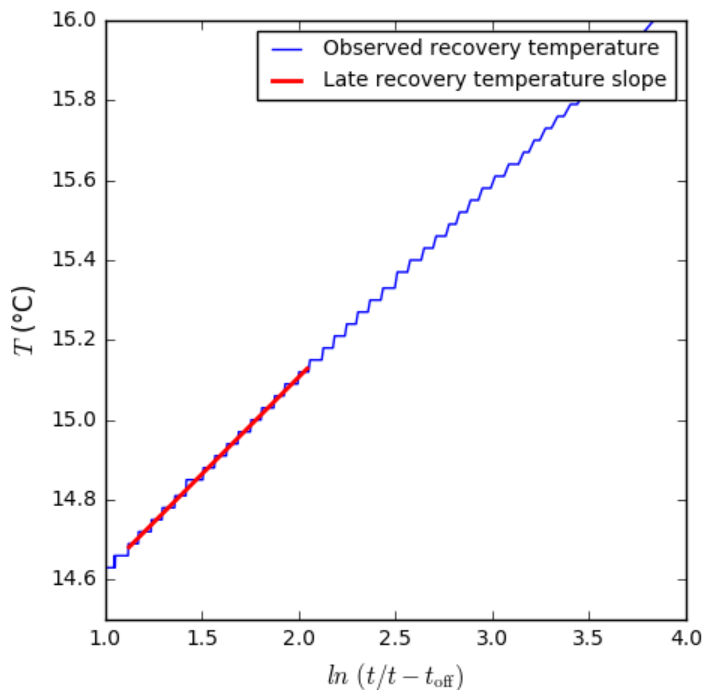


**Figure 2.8. Observed temperatures during the recovery period for the submersible sensor located at 53.6 m depth.**

The estimated thermal conductivity in Québec City ranged between  $1.72$  to  $2.19 \text{ W m}^{-1}\text{K}^{-1}$ , with an average value of  $2.02 \text{ W m}^{-1}\text{K}^{-1}$  (Figure 2.9a). A minimal and a maximal thermal conductivity of  $1.71 \text{ W m}^{-1}\text{K}^{-1}$  and  $2.03 \text{ W m}^{-1}\text{K}^{-1}$  were estimated in the conventional TRT with water circulation using the slope method and considering a constant heat injection rate. The maximal

value was estimated during a TRT with a constant flow rate, and the minimal value during a second TRT in which the flow rate was reduced after 30 h of heat injection. A thermal conductivity of  $1.75 \text{ W m}^{-1}\text{K}^{-1}$  was further obtained with analysis of the conventional TRT using the line source model with the superposition principle to consider variations in the heat injection rate (Ballard et al., 2016, Raymond et al., 2017). The thermal conductivity points estimated with the heating cable section methodology differs between -25.30 % to 1.70 % from the bulk value estimated during the conventional TRT, using the line source model with the variable heat injection rate, while it is closer to the upper range of the slope analysis assuming constant heat injection rate.

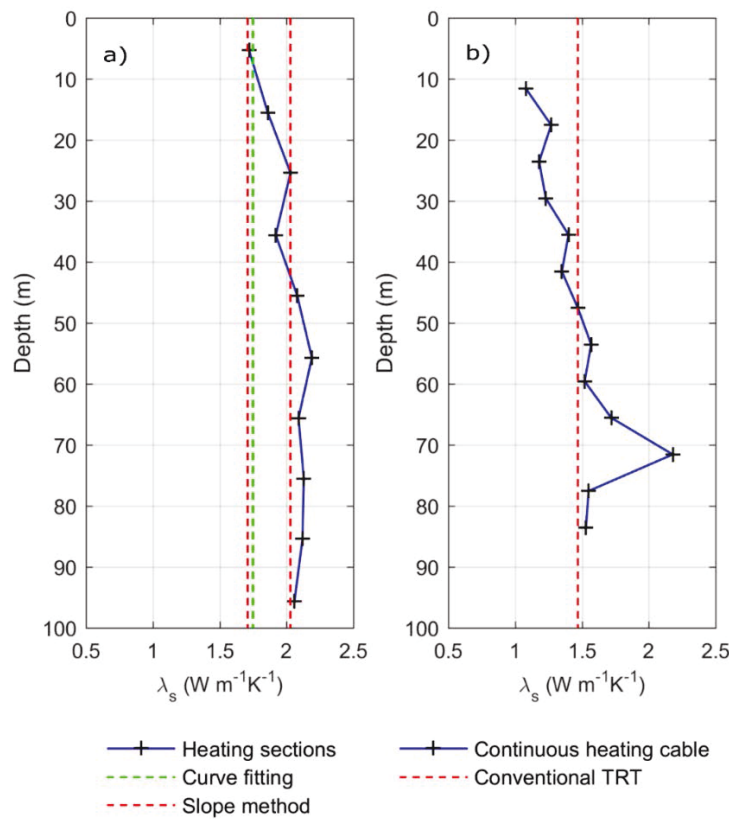


**Figure 2.9. Point subsurface thermal conductivity (crosses) obtained with the a) heating cable sections in Québec City and b) the continuous heating cable in Orléans. The results are compared to the bulk values provided by the conventional TRT with water circulation (green and red dashed lines).**

The bulk thermal conductivity estimated with the conventional TRT in Orléans was  $1.47 \text{ W m}^{-1}\text{K}^{-1}$  (Maragna, 2014), while thermal conductivity points identified with the heating cable methodology varied from  $1.08$  to  $2.18 \text{ W m}^{-1}\text{K}^{-1}$  with a mean value of  $1.47 \text{ m}^{-1}\text{K}^{-1}$ . Differences varying from 48.30 to 26.53 % were found when comparing the thermal conductivity

profile with the bulk result of the conventional test. The maximal difference was found at 71.60 m depth, where the maximal thermal conductivity was estimated (Figure 2.9b).

## 2.4.2 Uncertainty analysis

The absolute error of the measured parameters was determined from the accuracy associated with the measurement instruments (Table 2.2), except for the electrical resistance of the non-heating cable section, which was measured in the laboratory during previous work (Asselin, 2014) and where the standard deviation of the measurements was used for the absolute error.

**Table 2.2. Error associated with the measured parameters**

Parameter measured repeatedly during the test	Absolute error	Relative error (%)	Reference value - Quebec City	Reference value - Orléans
Temperature $T$ (°C)	0.10			
Electric power $P$ (W)	0.02	0.002	985.13	940.45
Electric current intensity $I$ (A)	0.02	0.17	8.71	8.99
Electric potential difference $U$ (V)	0.02	0.01	113.12	104.70
<b>Parameter measured once and separately</b>				
Length of the heating cable $H$ (m)	0.01		-	95.00
Length of the heating section $L_h$ (m)	0.01	0.81	1.24	-
Electrical resistance of the non-heating section $R_{nh}$ ( $\Omega \text{ m}^{-1}$ )	0.0002	0.50	0.04	-

**Table 2.3. Combined errors**

Continuous heating cable	Absolute error	Relative error (%)	Reference value
Heat injection rate $q$ ( $\text{W m}^{-1}$ )	0.21	2.12	9.91
Slope $m'$ (-)	0.001	0.23	0.55
<b>Heating cable section</b>			
Total electrical resistance of the cable assembly $R_{tot}$ ( $\Omega$ )	0.12	0.94	12.99
Electrical resistance of the heating cable sections $R_h$ ( $\Omega$ )	0.13	14.26	0.90
Heat injection rate $q$ ( $\text{W m}^{-1}$ )	6.07	14.29	42.50
Analytical model $Z$ (-)	1.06	5.00	21.14

**Table 2. 4. Uncertainly of the punctual thermal conductivity assessment for the heating cable sections test in Québec City**

Depth (m)	Thermal conductivity (W m <sup>-1</sup> K <sup>-1</sup> )	Relative error $\delta k$ (W m <sup>-1</sup> K <sup>-1</sup> )	Absolute error (%)
5.3	1.72	0.27	15.61
15.5	1.86	0.31	16.38
25.4	2.03	0.30	14.85
35.6	1.91	0.29	15.02
45.5	2.07	0.30	14.62
55.7	2.19	0.33	14.95
65.6	2.08	0.32	15.44
75.5	2.12	0.33	15.31
85.4	2.12	0.32	14.88
95.6	2.06	0.30	14.73
Average	2.02	0.31	15.18

**Table 2.5. Uncertainly of the punctual thermal conductivity assessment for the test with a continuous heating cable in Orléans**

Depth (m)	Thermal conductivity (W m <sup>-1</sup> K <sup>-1</sup> )	Relative error $\delta k$ (W m <sup>-1</sup> K <sup>-1</sup> )	Absolute error (%)
11.6	1.08	0.02	2.13
17.6	1.27	0.03	2.13
23.6	1.18	0.03	2.13
29.6	1.23	0.03	2.13
35.6	1.4	0.03	2.13
41.6	1.35	0.03	2.13
47.6	1.47	0.03	2.14
53.6	1.57	0.03	2.14
59.6	1.52	0.03	2.13
65.6	1.72	0.04	2.14
71.6	2.18	0.05	2.15
77.6	1.55	0.03	2.13
83.6	1.53	0.03	2.14
Average	1.47	0.03	2.14

Errors in Table 2.2 provided the basis to calculate combined errors in Table 2.3 to identify the accuracy of the heat injection rate ( $q$ ) and the uncertainty of the analysis method, whether it is the finite line source equation ( $Z$ ) or the slope ( $m'$ ) with the infinite line source equation. The parameters  $Z$  and  $m$  were calculated using the data of each temperature sensor such that the values presented in Table 3 are the mean of all the sensors.

The uncertainty of the point thermal conductivity assessment estimated for each profile was calculated from the combined errors. An uncertainty varying from 0.27 to 0.33  $\text{W m}^{-1}\text{K}^{-1}$  was determined for the test with heating cable sections (Table 2.4) with a mean value of 0.31  $\text{W m}^{-1}\text{K}^{-1}$  (15.18 %). An uncertainty varying from 0.02 to 0.05  $\text{W m}^{-1}\text{K}^{-1}$  was obtained for the continuous heating cable test (Table 2.5), with a mean value of 0.03  $\text{W m}^{-1}\text{K}^{-1}$  (2.14 %).

#### 2.4.3 Free convection assessment

The FO-DTS measurements enlarged for a heating section taken as example indicate that the highest recorded temperature is located in the upper part of the heating sections (Figure 2.10). This observation combined with the temperature increments of about 2 °C far from the heating sections and highlighted in Figure 2.5 suggest the presence of free convection in the GHE pipe water during TRT with heating sections even though perforated plastic disks were used to reduce convection.

The Rayleigh number was evaluated with temperature recorded in the pipe water for the heating section example from approximately 40 to 46 m depth (Figure 2.10 and 2.5). The top of the system was fixed at 40.6 m, a depth at which the minimum temperature during the heat injection was recorded. The Rayleigh number calculation was done with temperature data recorded at 25, 95 and 121 h, representing the beginning and the end of the heat injection, and the recovery period respectively. The highest Rayleigh number occurs at the end of the heat injection period near the location of the heating section and up to 1.5 m above. The maximal Rayleigh value is located at the upper part of the heating section, agreeing with the temperature peak (Figure 2.11).

In the second case, defining  $H_t = 6$  m,  $\text{Rayleigh}_{\text{actual}}$  at the beginning of the heat injection (28.5 h) and during the recovery period (121 h) did not exceed the critical value. However,  $\text{Rayleigh}_{\text{actual}} > \text{Rayleigh}_{\text{critical}}$  at the end of the heating period (95 h) for a portion of the heating section and up to 1.50 m above, suggesting the presence of free convection. The third case, considering  $H_t = 9$  m, shows a critical Raleigh number that is always larger than the actual Raleigh number, suggesting the absence of free convection. Defining  $H_t = 9$  m can, however,

overestimate Rayleigh's critical value, since temperature increases far above from the heating section is a strong evidence of heat transfer due to free convection.

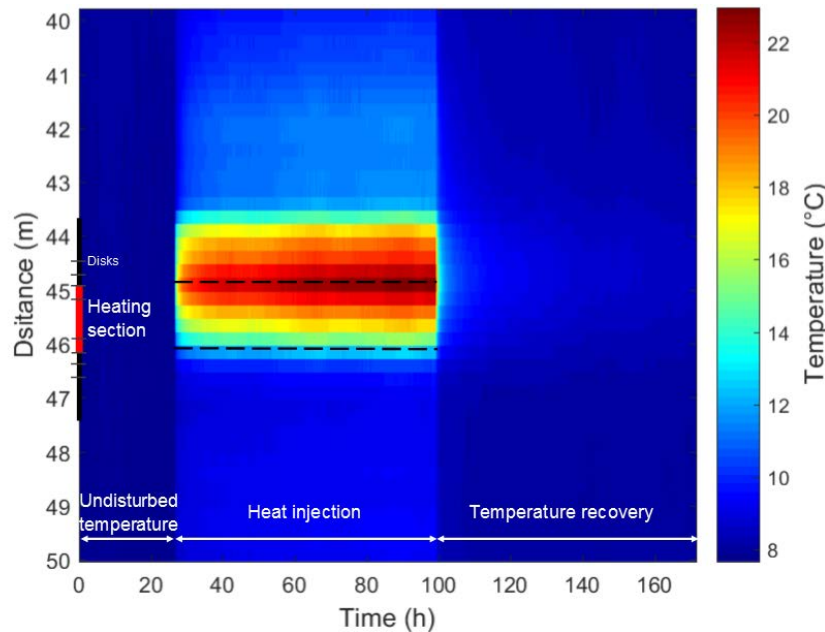


**Figure 2.10. Temperature distribution during the TRT around a typical heating section at 45 to 46 m depth.**

The effect of the perforated plastic disks to reduce free convection is difficult to evaluate. Nevertheless, the Rayleigh number reaches its maximal value at the top of the heating section (45 m) and decreases above heating sections where the perforated plastic disks were located. A similar effect occurs at the end of the heating section.

A similar analysis was done for the test with the continuous heating cable at 98.6 h, 234.6 h and 404.6 h, corresponding to the beginning of the heating period, the end of the heating period, and the end of recovery period, respectively. The critical Rayleigh number was evaluated with a minimum critical height of 2 m. In this case, the critical Rayleigh number was not exceeded during any of the three selected times (Figure 2.12). A difference of approximately one order of magnitude was observed between the actual Rayleigh number and its critical value, showing that free convection is not a dominant heat transfer mechanism during the test with the continuous heating cable. The analysis was not repeated with higher critical length because it will result in higher critical Rayleigh number, increasing the difference with the actual Rayleigh number.

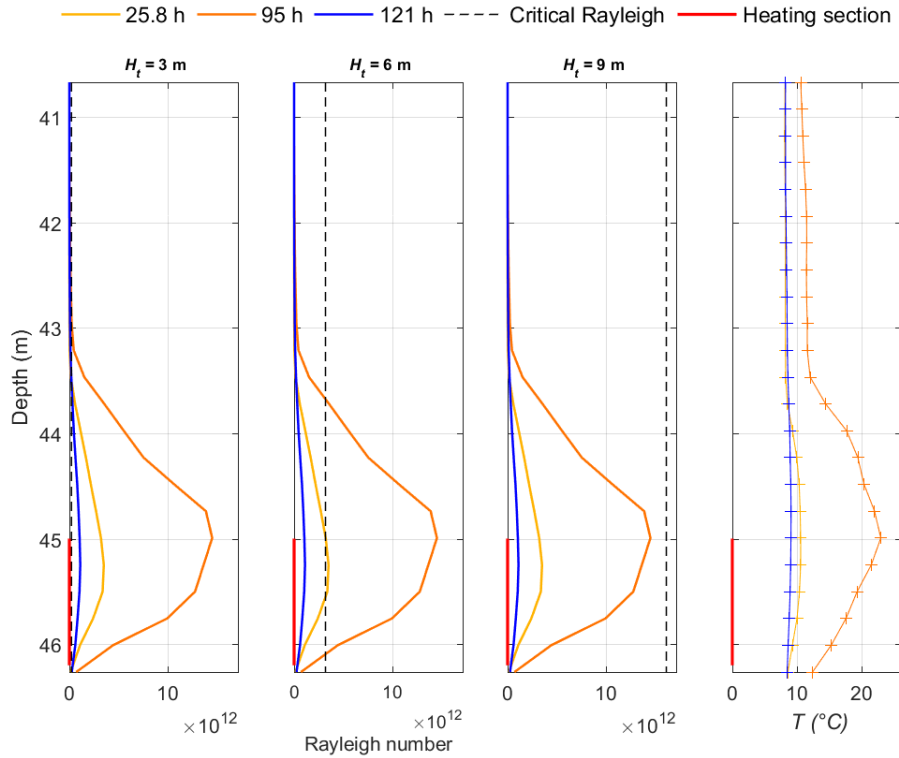


**Figure 2.11. Verification of the Rayleigh number stability criteria considering different critical lengths  $H_t$  to calculate the critical Rayleigh number (dashed lines) for the test with heating cable sections.**

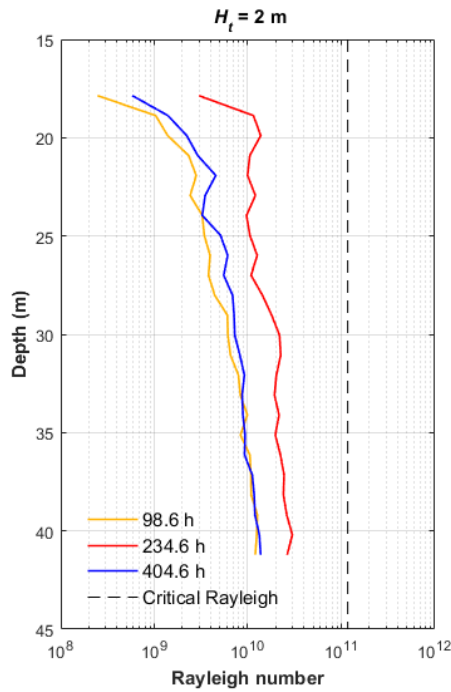


**Figure 2.12. Verification of the Rayleigh number stability criteria for the test with a continuous heating cable in Orléans.**

## 2.5 Discussion

The monitoring of temperature for the whole cable assemblies using FO-DTS allowed evaluating the temperature evolution beyond the submersible sensors to better understand the heat transfer phenomena occurring during both TRTs in addition to assessing thermal conductivity profiles of the ground. Thermal conductivity values are provided with error estimation for each case. In the case of the heating cable sections, it was particularly important to evaluate the temperature increases near the heating section extremities and along the non-heating sections. The additional temperature data provided by the FO-DTS allowed to identify significant temperature increases at the top of the heating sections and slight temperature increments at the middle of the non-heating sections, where temperature changes were not expected.

### 2.5.1 Thermal conductivity estimation

The subsurface thermal conductivity was evaluated using the finite and infinite line source solutions, to simulate conductive heat transfer at both tests with heating cable sections and a continuous heating cable. A thermal conductivity profile with a mean value of  $2.02 \pm 0.31 \text{ W m}^{-1}\text{K}^{-1}$  was estimated from the test with heating cable sections conducted in Quebec City, Canada. This value is 15.45 % higher than the thermal conductivity evaluated during a conventional TRT made on the same GHE with water circulation analysed with the infinite line source model and considering variations in the heat injection rate (Ballard *et al.*, 2016, Raymond *et al.*, 2017). Analysis of a conventional TRT can, however, depends on the analysis method itself. The mean thermal conductivity estimated with the heating section TRT carried out in Quebec City differs only -0.47 % when compared to the maximum bulk thermal conductivity evaluated with the slope method for a conventional TRT performed in the same GHE (Ballard *et al.*, 2016, Raymond *et al.*, 2017). A previous field test with heating cable sections reported by Raymond *et al.* (2015) indicated a mean thermal conductivity 12 % higher than that estimated with a conventional TRT. These results suggest that TRT with heating cable sections can slightly overestimate the ground thermal conductivity when compared to a conventional TRT. Free convection generated above the heating cable section can explain this difference since TRT analysis is made considering conductive heat transfer only. Free convection in a TRT using heating cable sections was identified by Raymond and Lamarche (2014), through numerical simulation of the borehole temperature evolution during a TRT. The use of perforated plastic disks placed at the extremities of the heating section had been

suggested to reduce the possible free convection. Nevertheless, the effect of natural convection was still identified during the full-scale test with heating cable sections, indicating that the four perforated plastic disks are not sufficient to totally control free convection during the heat injection period. A test with a reduced heat injection rate could be performed to evaluate if natural convection induced by the heating sections decreases.

The analysis of the Rayleigh number stability criteria for the GHE in Quebec City, made of a single U-pipe and drilled in sedimentary rocks, was conducted in a section of the GHE pipe considering half of a non-heating section (40.0 – 45.0 m) and a heating section (45.0 - 46.2 m), in order to have a temperature gradient increasing with depth as it is expected in analogous ground water well (Love *et al.*, 2007). Considering the significant temperature increase above the heating section and the results of the Rayleigh number stability criterion with a critical height of 6 m, the presence of free convection is likely to be significant along the heating section and approximately 1.5 m above it.

A mean thermal conductivity of  $1.47 \pm 0.03 \text{ W m}^{-1}\text{K}^{-1}$  was estimated for the test with a continuous heating cable carried out in the GHE made of a double U-pipe drilled in limestone in Orléans, France. This value corresponds exactly to the bulk thermal conductivity estimated with the conventional TRT (Maragna, 2014). Previous comparison between TRT using continuous heating cable and a conventional TRT has not been made before. A constant initial temperature increase with depth, influenced by the natural geothermal gradient was observed before the TRT and seems to remain during the heat injection period with the continuous heating cable. Free convective heat transfer due to the geothermal gradient or caused by anthropogenic heat sources is possible since it has been observed in groundwater wells (Love *et al.*, 2007) and in the water column of open boreholes (Klepikova *et al.*, 2018; Berthold & Resagk, 2012). However, this weak convection mechanism can be neglected for TRTs analysis, where heat conduction triggered upon heat injection is assumed more important than any natural convection. The actual Rayleigh number for the test performs with the continuous heating cable did not exceed the critical Rayleigh number evaluated between 18 m and 42 m depth, indicating that convective heat transfer can be neglected in this case. In future works, the thermal conductivity could be evaluated using the FO-DTS to allow an increase in the spatial resolution currently limited by the number of temperature sensors and to provide an additional independent estimation of the thermal conductivity.

## 5.2.2 Uncertainty analysis

Uncertainty of TRT with heating cable sections conducted at a small scale was initially evaluated by Simon (2016), which reported an accuracy of approximately 25 % of the estimated thermal conductivity. A similar methodology adapted for the field test had been applied here. The highest uncertainty for the test is the error associated with the heat injection rate ( $\delta q = 6.07 \text{ W m}^{-1}$ ). The estimate of the electric resistance of the heating sections is the parameter with the most important uncertainty when calculating the heat injection rate. The uncertainty of the heat injection rate corresponds to 76 to 96 % of the total test uncertainty. The remaining proportion of uncertainty corresponds to the error associated with the analytical model ( $\delta Z$ ). The final test uncertainty ranged between 14.6 and 16.4 %, showing a reduction of approximately 10 % compared to the uncertainty estimated during the laboratory tests performed in three 10 m wells (Simon, 2016). The power injected underground for the laboratory tests was divided into three heating cable sections using a power switching supplies because three single heating section tests were carried out at the same time. The efficiency of this switch influenced the uncertainty of the heat injection rate, increasing the total uncertainty of the test. The electric current transmitted to the cable inducing the thermal power injected underground for the full-scale test presented in this study was controlled by a voltage regulator and measured using a power meter at the entry of the cable assembly, allowing to reduce the uncertainty associated to the evaluation of the heat injection rate. To adapt error calculation for conventional TRT to continuous heating cable TRT, both of which are using the slope analysis methods, some modifications were introduced to the approach proposed by Witte (2013). The error of the heat injection rate and the slope of the regression of the temperature increments were calculated as a combination of errors for the continuous heating cable TRT. It was not necessary to calculate the average temperature, as in a conventional TRT, because the analysis was based on the temperature increments measured at the depth of each temperature sensor. The error associated with the heat injection rate only depended on the electric current intensity and the electric potential difference that are measured with accuracy in the field. Thus, the accuracy of the temperature sensors only influences the error attributed to the slope when plotting the temperature response.

The parameter with the highest uncertainty for the continuous heating cable TRT is the heat injection rate, with an error of  $0.21 \text{ W m}^{-1}$ , which corresponds to 99 % of the total uncertainty. The remaining 1 % corresponds to the uncertainty of the slope. The final uncertainty of the thermal conductivity profile was 2.14 %, a lower value than the 5.10 % estimated for a

conventional TRT by Witte (2013). The accuracy of the heat injection rate appears to be the key factor, in any TRT method, that directly affects the uncertainty of the thermal conductivity estimate. Achieving an accurate assessment of the heat injection rate for TRTs with flowing water based on flow rate and temperature measurements tend to be more difficult than evaluating the heat injection rate transmitted through a continuous heating cable with potential difference and current intensity measurements. However, these measurements become complex for heating sections TRT, increasing the uncertainty associated with the analysis performed with the finite line source solution. This last analysis method with the finite line source solution requires assuming the heat capacity of the geological formation (Raymond & Lamarche, 2014), adding an additional uncertainty to the analysis.

### 5.2.3 Comparison of TRT methods

The assessment of thermal conductivity as a function of depth achieved using the heating cable methodology allows to define the most advantageous drilling conditions for the GHE according to the ground thermal conductivity variations. The ground thermal properties inferred with a high spatial resolution, also obtained with TRTs coupled to FO-DTS, are valuable when detailed simulations of the GHE performance with several thermal conductivity layers are considered.

Both heating cable sections and a continuous heating cable allowed reducing the power required to perform a TRT, as well as avoiding issues associated with water circulation, when compared to conventional tests (Table 2.6). The test error is reduced with a continuous heating cable compared to conventional TRT (Witte *et al.*, 2002) and heating sections TRT (Simon, 2016), for which the estimation of the heat injection rate has most influence on the test error that is increasing when comparing the three methods (Table 2.6).

**Table 2.6. Comparison of TRT methods for thermal conductivity profile assessment.**

	Continuous heating cable	Heating cable sections	Conventional with FO-DTS
Power requirement	Low	Low	High
Test time	+++	++	++
Equipment complexity	+	++	+++
Cost	\$	\$\$	\$\$\$
Measured parameters	$T_0, \lambda_s$	$T_0, \lambda_s$	$T_0, \lambda_s, R_b$
Surface disturbances	No	No	Yes
Analysis method	Infinite line source solution	Finite line source solution	Infinite line source solution

The time required to perform a TRT with a continuous heating cable and a low power source can be longer than TRT with heating sections (Raymond and Lamarche, 2014; Raymond *et al.*, 2015) or a conventional TRT with FO-DTS. However, the equipment is left on site and there is no need for follow up, which reduces the time spent in the field and the cost of operations.

The temperature monitoring during the recovery period is necessary in all cases, when trying to infer the thermal conductivity at depth (Raymond and Lamarche, 2014), making the test longer than the 50 to 80 h recommended for conventional heat injection TRTs (Kavanaugh, 2001) assessing the bulk thermal conductivity only. However, the estimation of the thermal conductivity based on the recovery temperature is more appropriate than using the heat injection period only Raymond *et al.*, 2011b. The heat injection rate per unit length has to be considerably low with a continuous heating cable of approximately 100 m in length, resulting in an increase of the heat injection period to achieve a minimum temperature increase of at least 3 °C in the GHE pipe. However, the reduction of the test uncertainty and the simplified field manipulations make the continuous heating cable test a reliable alternative to perform TRT. In boreholes of more than 150 m, the increase of the cable weight can be a challenge to install and remove the cable that could be done with a winch. The test time could further be reduced with the improvement of the resolution of submersible temperature sensors that could detect smaller temperature perturbations to decrease the minimum temperature increase and, consequently, test time.

## 2.6 Conclusions

Thermal conductivity profiles and the errors associated were estimated at two different experimental sites using alternative heating cable methods to conduct the thermal response tests (TRT). The assessment of free convection in the standing water of the GHE pipe suggested the presence of significant convection inside the pipe of the ground heat exchanger during the heat injection period when the heating cable sections were used. This analysis indicates that the perforated plastic disks installed at the interface between the heating and the non-heating sections do not remove all free convection during the heat injection period. However, the uncertainty range of the subsurface thermal conductivity estimated with heating section TRT was within the value inferred for a conventional TRT with water circulation. Considering the significant temperature increase observed above the heating section in the TRT carried out in Quebec City, the active heating length used to estimate the thermal conductivity can be reevaluated. Further analysis is required to evaluate the ratio of conduction and

convection heat transfer to adjust the test analysis methodology. Laboratory tests, comparing a standing water column with a column in which free convection is prevented using additives to make water become a gel, could be performed in future work to assess the temperature decrease caused by free convection movements. Convective heat transfer could additionally be taken into account for the analysis process through numerical simulations including free convective heat transfer mechanism.

The field tests performed, including the free convection and the uncertainty analysis, indicates that the TRT with the continuous heating cable has a better accuracy than the heating sections TRT. The assumption of dominant conductive heat transfers is valid when using the continuous heating cable and the total uncertainty of the test is lower than that obtained for both, the heating sections TRT and a conventional TRT with water circulation carried out under typical circumstances. The TRT with heating cable sections provides advantages to perform tests in deep boreholes (more than 100 m), without increasing the heat injection rate and the power requirement. However, the analysis of the heating section TRT is limited by the effect of free convection that is not included in the analytical modeling approach. The limiting factor associated with the continuous heating cable TRT in deep boreholes is the electric resistance of the cable that increases with its length. The heat injection rate can be reduced maintaining a low power requirement, as shown in this study, but the use of high resolution temperature sensors to measure small temperature differences becomes necessary. TRT with a continuous heating cable and a low power source is a promising method and further tests could be carried out in boreholes of more than 100 m to verify the applicability of this methodology in ground heat exchangers commonly installed for ground-coupled heat pump systems.

## **Article 3**

# **Inferring terrestrial heat flow from thermal response test data combined with a temperature profile**

### **Titre traduit**

Estimation du flux de chaleur terrestre à partir des tests de réponse thermique combinés avec un profil de température

### **Auteurs**

Maria Isabel Vélez<sup>1</sup>, Jasmin Raymond<sup>1</sup>, Daniela Blessent<sup>2</sup>, Mikael Philippe<sup>3</sup>

<sup>1</sup> Centre-Eau Terre Environnement, Institut national de la recherche scientifique, Québec, Qc, Canada

<sup>2</sup> Programa de Ingeniería Ambiental, Universidad de Medellín, Medellín, Colombia

<sup>3</sup> Georesources Division, BRGM, 3 avenue Claude Guillemin, BP 36009, 45060 Orléans Cedex 2, France

### **Soumis**

*Physics and Chemistry of the Earth*

## RÉSUMÉ

La densité du flux de chaleur terrestre, une information essentielle à l'évaluation des ressources géothermiques profondes, est rarement définie au niveau des zones urbaines où les besoins énergétiques sont pourtant importants. Afin de palier à ce manque d'information, la conductivité thermique estimée lors d'un test de réponse thermique, couplée à une mesure d'un profil de température non perturbée dans le même forage, a été utilisée pour évaluer le flux de chaleur terrestre près de la surface. Le profil de température non perturbé est reproduit avec un modèle numérique inverse de transfert de chaleur par conduction. L'optimisation de la condition frontière inférieure du modèle permet de déduire le flux de chaleur près de la surface. Les données de deux tests de réponse thermique effectués dans des échangeurs de chaleur au sol d'une profondeur d'environ cent mètres ont été analysées avec des simulations numériques inverses présentées à titre d'exemple. Les profils de température mesurés sur les sites et corrigés selon l'influence paléoclimatique des glaciations quaternaires ont été reproduits avec le modèle numérique. La méthodologie présentée offre une alternative pour évaluer le flux de chaleur lors de l'exploration préliminaire des ressources géothermiques des zones urbaines, où les tests de réponse thermique sont fréquents tandis que les puits profonds pour évaluer le flux de chaleur sont rares.

## ABSTRACT

The terrestrial heat flux density, an essential information to evaluate the deep geothermal resource potential, is rarely defined over urban areas where energy needs can, however, be important. In an effort to fill this gap, the subsurface thermal conductivity estimated during two thermal response tests was coupled with undisturbed temperature profiles measure in the same borehole to infer terrestrial heat flow near the surface. The undisturbed temperature profiles were reproduced with an inverse numerical model of conductive heat transfer, where the optimization of the model bottom boundary condition allows determining the near-surface heat flow. Data from two thermal response tests in ground heat exchangers of about hundred meters depth were analyzed with inverse numerical simulations provided as examples for the town of Québec City, Canada, and Orléans, France. The temperature profiles measured at the sites and corrected according to the paleoclimate effects of the quaternary glaciations were reproduced with the model. The presented methodology offers an alternative to assess heat flow in the preliminary exploration of deep geothermal resources of urban areas, where it is easier to conduct thermal response tests than to have deep wells available to assess heat flow.

### 3.1 Introduction

Heat flow is the main source of information about the Earth's thermal state (Golovanova *et al.*, 2014). Nevertheless, measuring the Earth's heat flow is difficult and only disperse data are available, especially in urban areas. Terrestrial heat flow is estimated by combining temperature profile and thermal conductivity data sets from deep boreholes (Bodri & Cermak, 2007; Sass & Beardmore, 2011), typically more than 300 m depth (Jessop, 1990; Beck, 1977). The temperature gradient is derived from point measurements of temperature at two or more discrete depths and thermal conductivity is commonly evaluated on core samples at the surface, either in the field or in the laboratory. As exploratory drilling for petroleum and minerals became widespread, temperature profiles measured in boreholes became the most common means of determining temperature gradients within the Earth (Sass & Beardmore, 2011). This information has been analyzed to estimate local heat flow values and produce regional maps. Such interpolation of heat flow estimates has since been carried out worldwide as a tool to better understand the thermal structure of the near surface that plays a role in the exploration of hydrocarbons, geothermal and mineral resources (Davies, 2013). The information given on heat flow map is particularly useful for the exploration of geothermal resources, with work now being conducted over urban areas where energy needs are important but deep mineral or hydrocarbon exploration wells to measure temperature almost nonexistent. This created a data gap evidencing the needs to adapt methods to assess heat flow over urban areas at the early stage of geothermal exploration projects before pursuing deep drilling.

For example, the heat flow map of Easter Canada has been built analyzing available heat flow data for the Canadian Shield and the Appalachians. There are actually more than 300 reliable heat flow values in the Canadian Shield, including 150 heat flow evaluations around Lake Superior, with boreholes usually deeper than 100 m (Mareschal & Jaupart, 2004). Nevertheless, none of the locations with heat flow assessments are located over urban areas such as Quebec City, Montreal or Toronto with significant energy demand. The heat flow map of France was inferred interpolating 479 heat flow assessments inside the country combined with additional data from Spain, Switzerland, German and Italy (SIG Mines France, 2007). Again, heat flow assessments over cities are rare, although they can be more common in Europe than North-East America. In fact, heat flow observations are non-uniformly distributed (Davies, 2013) and information is far from being completed in urban areas. Nevertheless, the development of geothermal heat pump systems manly taking place in populated cities is creating opportunities

to possibly estimate heat flow from subsurface thermal conductivity and temperature data obtained in shallow boreholes.

Thermal response tests (TRT) are commonly used to assess the subsurface thermal conductivity to design shallow geothermal systems (Raymond & Lamarche, 2014), like ground-coupled heat pumps including boreholes of 100 to 200 m depth. The ground temperature and thermal conductivity estimated during a TRT could be useful to infer the terrestrial heat flow (Sanner *et al.*, 2013), filling data gaps over urban areas. Inverse numerical modeling was previously achieved by Raymond *et al.* (2016) to reproduce temperature profiles measured in ground heat exchangers and estimate heat flow to spatially extend a TRT assessment, which was believed to be useful when designing large ground-coupled heat pumps systems enclosing several heat exchangers. The proposed method could similarly be used to evaluate heat flow through the scope of deep geothermal resource assessment, but needs to be improved by taking into account surface temperature changes as climate warming can significantly affect temperature profile measured in shallow ground heat exchangers.

Heat flow estimations, based on depth-temperature measurements, generally require corrections for paleoclimate effects (Westaway & Younger, 2013). Paleoclimate correction account for temperature changes at the Earth's surface that slowly propagates downward into the subsurface and appear as tiny temperature deviations imposed on the geothermal gradient (Bodri & Cermak, 2007). The past variations in surface temperature relative to its present value can be approximated as a series of steps changes, each starting at a particular time before the present day to correct temperature profiles. This is especially important for shallow boreholes affected by ground surface temperature variations. The objective of this work was, therefore, to evaluate the use of TRT field data that can be combined with an undisturbed temperature profile to estimate the heat flow. TRT data are relatively abundant in urban regions where shallow geothermal resources are exploited and, although collected in shallow wells of 100 to 200 meters depth, could be useful to complement sparse heat flow assessment from deeper wells. Thermal conductivity profiles estimated during TRT with heating cables at two experimental sites in Canada and France were used to build an inverse transient heat transfer 1D model with the finite element method implemented in COMSOL Multiphysics (COMSOL AB). The optimization of the model bottom boundary condition to reproduce the undisturbed temperature profiles measured in the boreholes, taking into account historic temperature measurement at the surface, allowed estimating the Earth heat flow in two cities.

## 3.2 Methodology

In situ thermal conductivity evaluated at depth during two TRT performed with heating cables were used as inputs to define the numerical model properties. Inverse transient heat transfer simulations were carried out with COMSOL Multiphysics to reproduce the undisturbed temperature profiles measured in the ground heat exchangers before the TRT.

### 3.2.1 *In situ* thermal conductivity assessment

The first TRT was carried out in an experimental borehole of approximately 100 m depth at the Laboratoires for scientific and technological innovation in environment (LISTE) of the Institut national de la recherche scientifique, located in Quebec City, Canada (Experimental site 1). The test was performed using heating cable sections and the finite line source solution was used to reproduce the temperature evolution along the heating section and estimated the thermal conductivity.

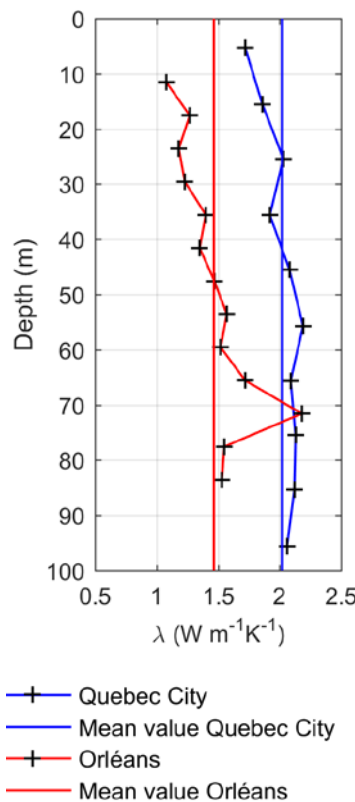
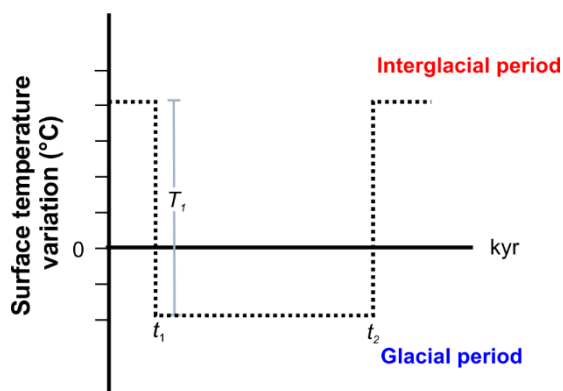


Figure 3.1. Thermal conductivity profiles and mean thermal conductivity in Quebec City and Orléans.

The second TRT was completed in the experimental geothermal test facility of the French geological survey (Bureau de Recherches Géologiques et Minières) in Orléans, France (Experimental site 2), with a continuous heating cable. This test was analyzed using the infinite line source solution (Velez *et al.*, 2018). The equipment required to perform the tests consists of the heating cable, a junction box to link the cable to the power supply and submersible sensors to measure and record the temperature during the test (Velez *et al.*, submitted). In Quebec City, the thermal conductivity was evaluated every 10 m and allowed to define 10 thermal conductivity layers in the model domain. The estimated thermal conductivity ranged between  $1.72$  to  $2.19 \text{ W m}^{-1}\text{K}^{-1}$ , with an average value of  $2.02 \text{ W m}^{-1}\text{K}^{-1}$  (Figure 3.1). In Orléans, thermal conductivity was assessed every 6 m in a borehole of similar depth allowing to define 13 thermal conductivity layers in the model domain. The thermal conductivity varied from  $1.08$  to  $2.18 \text{ W m}^{-1}\text{K}^{-1}$  with a mean value of  $1.47 \text{ m}^{-1}\text{K}^{-1}$  (Figure 3.1).

### 3.2.2 Temperature measurements and paleoclimate correction

The temperature profile at experimental site 1 was measured using a submersible temperature and pressure data logger (RBRduet) with an accuracy of  $0.002 \text{ }^{\circ}\text{C}$ . The logger was attached to a wire and gradually lowered in the borehole achieving a spatial resolution of approximately 2.4 m. The ground heat exchanger in Orléans was equipped with a fiber optic distributed temperature sensing (FO-DTS) system and the temperature profile was measured using the fiber optic cable with a temperature resolution of  $\pm 0.05 \text{ }^{\circ}\text{C}$  and a spatial resolution of 1 m.



**Figure 3.2. Example of the surface temperature variation assumed during a glacial period (kyr = thousand years).**

The initial temperature measured in the ground heat exchangers before conducting the TRT was corrected according to the influence of the paleoclimate temperature variations due to the

last Quaternary glaciations (Eq. 3.1). The correction is computed at each depth  $z$  (m), and depends on the duration of the glacial periods ( $t_1$ ,  $t_2$ , Figure 3.2), the temperature drop with respect to the present surface average temperature ( $T_1$ , Figure 3.2) and the thermal diffusivity of the rocks (Jessop, 1990). The corrected temperature is

$$T_c = T_m - \sum_i (T_{i_1}) \cdot \left[ erf\left(\frac{z}{2\sqrt{\alpha_s t_{i_1}}}\right) - erf\left(\frac{z}{2\sqrt{\alpha_s t_{i_2}}}\right) \right] \quad (3.1)$$

where  $T_m$  (K) is the temperature measured at each depth and  $\alpha_s$  ( $m^2 s^{-1}$ ) is the thermal diffusivity.

The last four glaciations in North America were considered for paleoclimate corrections at experimental site 1 (Figure 3.3). The temperature during the interglacial periods was assumed as the present day mean annual ground temperature (Allis, 1978, Jessop, 1990) and a temperature step of 5 K was supposed (Jessop, 1990). The last five glaciations in Europe and a temperature amplitude of 7 K were assumed for the experimental site 2 (Figure 3.4), according to the surface temperature history and a temperature step of 7 K proposed by Majorowicz and Šafanda (2008) and Majorowicz and Wybraniec (2011).

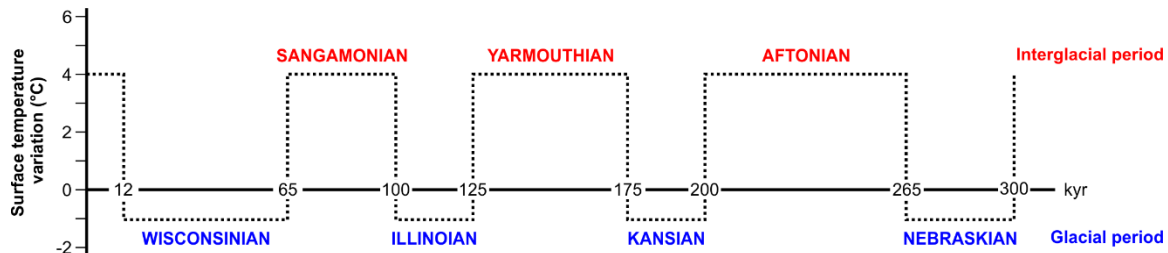


**Figure 3.3. Chronology of glacial periods in Canada considered at the experimental site 1 in Quebec City (modified from Bédard et al, 2017, kyr = thousand years).**

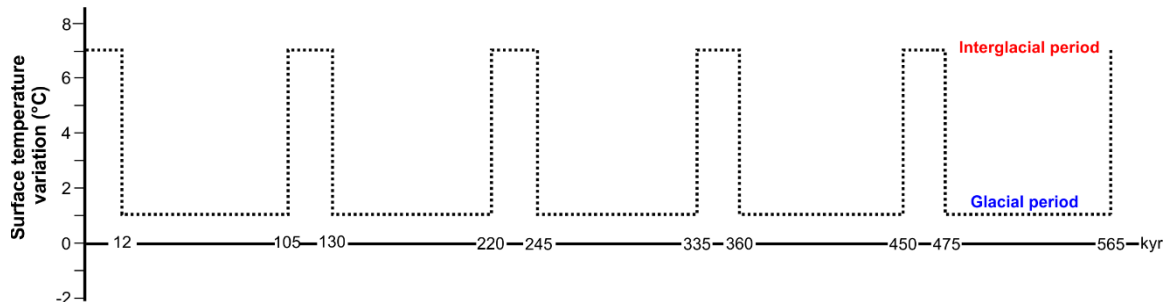


**Figure 3.4. Chronology of glacial periods in Europe and considered at the experimental site 2 in Orléans (kyr = thousand years).**

### 3.2.3 Numerical model development

Transient conductive heat transfer was simulated in one dimension to reproduce corrected for glaciation effects using the finite element program COMSOL Multiphysics solving the equation:

$$\frac{\partial}{\partial x} \left( \lambda \frac{\partial T}{\partial x} \right) = \rho c \frac{\partial T}{\partial t} \quad (3.2)$$

where  $\lambda$  ( $\text{W m}^{-1} \text{K}^{-1}$ ) is the thermal conductivity,  $\rho$  ( $\text{kg m}^{-3}$ ) is the density and  $c$  ( $\text{J kg}^{-1} \text{K}^{-1}$ ) is the heat capacity. The thermal properties of the subsurface of each layer were assumed to be uniform and constants in time. The heat generation rate due to the decay of radioactive elements in the subsurface was neglected since the simulated domain is relatively shallow (Raymond *et al.*, 2016).

The bottom boundary condition was a constant heat flow, which represents the Earth natural heat flow towards the surface. The model had a length of 700 m in the vertical direction to minimize the effect of the bottom boundary condition that can influence the propagation of temperature changes at the surface if located too close to the surface. A historical surface temperature varying with time was applied at the top of the domain as boundary condition taking into account the recent climate warming of the last century. Air temperature measurements at the Jean Lesage airport from 1943 to 2016 and available from the web site of Environment Canada (<http://climate.weather.gc.ca/>) were used at experimental site 1 in Quebec City to define the magnitude of historical temperature changes (Figure 3.5). Three sources of surface temperature were used at experimental site 2 in Orléans (Figure 3.5). Air and land surface temperature measured at the weather station of the experimental geothermal platform from January to Mai 2017 were used for the last period with data available at <http://plateforme-geothermie.brgm.fr/fr/suivi/METEO>. Air temperature measurements from 1996 to 2016 at a weather station in Tours, located 118 km from Orléans, were used for the middle period with data available at <https://donneespubliques.meteofrance.fr> (station ID: 07240). In the absence of temperature data near Orléans before 1996, the mean air temperature in France was used from 1901 to 1996 for the initial period with data available at: <http://sdwebx.worldbank.org/climateportal/>.

Air temperature was converted to ground surface temperature (Figure 3.4), defining the magnitude of the temperature changes at the top boundary of the model. The conversion of air to ground temperature was made using an empirical relationship developed by Ouzzane *et al.* (2015) defined as:

$$T_g = 17.898 + 0.951T_{\text{amb}} \quad (3.3)$$

where  $T_g$  (K) is the ground surface temperature and  $T_{\text{amb}}$  (K) is the ambient air temperature. The relation is based on the fact that among the parameters controlling the ground surface temperature (ambient temperature, sky temperature, wind velocity and solar radiation), the ambient temperature is the dominant parameter, therefore  $T_g$  can be correlated as a function of the ambient temperature only (Ouzzane *et al.*, 2015). The use of this empirical relationship resulted in an estimated ground surface temperature that is approximately 4 K higher than the air temperature (Figure 3.5). The resulting temperature evolution was used to define the relative temperature changes at the model upper boundary, adjusting the historic temperature curve to beginning at an initial temperature characteristic of the measured temperature profile.

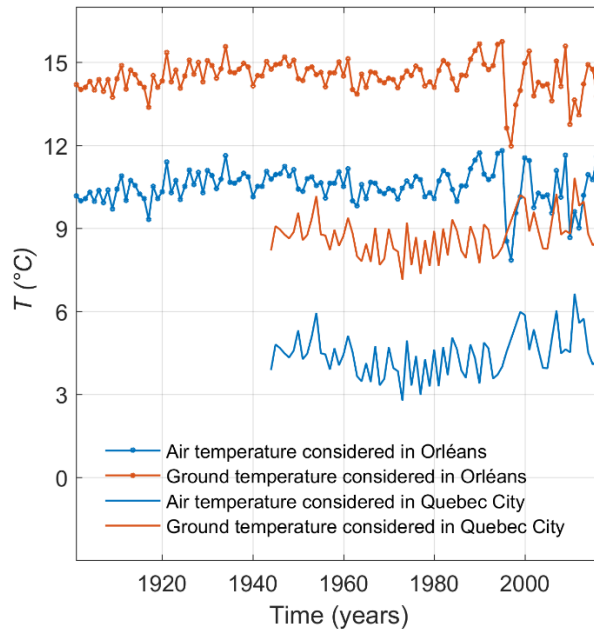


**Figure 3.5. Historic air and ground temperature variations considered in Quebec City and Orléans.**

The exact value of the initial temperature for the boundary condition at the surface ( $T_s$ ) was inferred from the undisturbed geothermal gradient measured at the bottom of the boreholes (last 40 m), which are less influenced by the ground surface temperature variations than the temperature in the upper section of the GHEs. These temperatures were extrapolated upward according to the equilibrium geothermal gradient to set the initial temperature at the surface according to (Raymond *et al.*, 2016):

$$T_s = \frac{-b}{m} \quad (3.4)$$

where  $b$  and  $m$  are the y-intercept and the slope of the graphic of temperature at depth in the last 40 m of the boreholes. The initial temperature condition needed to run the transient simulations was then calculated according to the basal heat flow  $q$  ( $\text{W m}^{-2}$ ) for temperature distribution to follow the equilibrium geothermal gradient:

$$T_i = T_s + \left( \frac{q}{\lambda_s} \right) \cdot z \quad (3.5)$$

where  $\lambda_s$  ( $\text{W m}^{-1} \text{K}^{-1}$ ) is the subsurface thermal conductivity and  $z$  (m) is the depth. The basal heat flow was optimized and therefore changed every simulation such that the initial temperature distribution was recalculated automatically with equation 3.5 every simulation.

The transient simulations to reproduce the observed temperature profiles were carried out for a duration of 72 and 116 years for Quebec City and Orléans experiment sites, respectively, with monthly time steps. The simulation times were equal to the available historic air temperature data.

A sensitivity analysis was carried out to define the depth at which the basal heat flow should be imposed and the mesh resolution to make sure the obtained temperature solution is reliable. The position of the bottom heat flow boundary condition and the mesh resolution were gradually increased to verify the model independence with respect to the position of the bottom boundary and the mesh size.

A uniform coarse mesh was initially defined in all the domain, then the mesh was gradually refined using the predefined COMSOL meshes until achieve a constant temperature in a given depth to verify the model independency from the mesh resolution. This initial refinement did not allow to reproduce the upper part of the profile affected by the seasonal temperature variation. A finer mesh was needed in the first 30 m of the profile to achieve a reliable reproduction of the temperature profiles. However, this finer mesh was only applied in the upper part of the profile to keep the calculation time short.

The position of the bottom boundary condition was increased each 50 m, from 100 to 700 m depth until an insignificant relative difference between the simulated temperature at a given depth was achieved. The thermal conductivity after 100 m is unknown. A sensitivity analysis varying the thermal conductivity in this last layer within the interval of thermal conductivity estimated in the TRT was made. The modification of the thermal conductivity results in a fluctuation of less than 10% in the simulated temperature and the inferred heat flow. Therefore,

the average thermal conductivity estimated in the TRT (Figure 3.1) was assumed from 100 to 700 m depth.

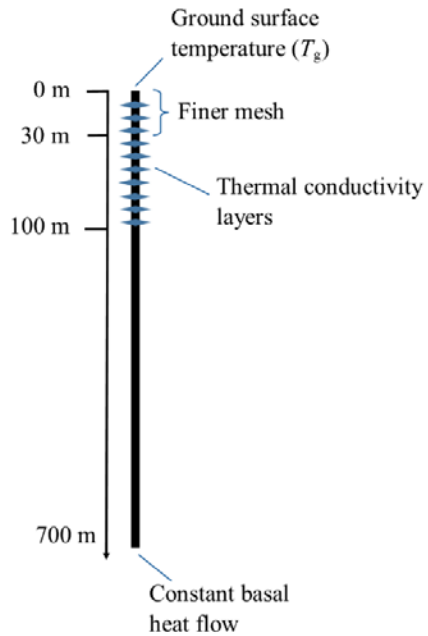


**Figure 3.6. Simulation domain and boundary condition.**

Inverse numerical simulations to optimize the basal heat flow and reproduce the observed temperature were made once the model was proven to be independent of boundary location and mesh. The sum of squared residuals between the observed and simulated temperature profiles was minimized with the coordinate search method (Conn *et al.*, 2009) in order to find the Earth heat flow (Figure 3.6). The Coordinate search solver aims at improving the objective function along the coordinate directions of the control parameter space (heat flow, in this case). The step lengths are decreased or increased according to the values of the objective function (COMSOL AB, 2013). The Coordinate search, method stop iterating as soon as no improvement over the current best estimate can be made with steps of relative size larger than or equal to the optimality tolerance (COMSOL AB, 2013). The optimality tolerance of the solver was defined at  $1 \times 10^{-6}$  and the maximum number of objective evaluation was set to 100. The convergence was achieved at 34 and 43 iteration in Quebec City and Orléans, respectively.

### 3.3 Results

#### 3.3.1 Paleoclimate correction

The paleoclimate correction of the measured temperature profiles achieved for the glaciations resulted in an increase of the temperature at depth. Considering the last four glaciations and a temperature step of 5 K, the average temperature increase for the profile in Quebec City was 0.14 K, with a maximal increase of 0.31 K at the bottom of the profile (Figure 3.7a). The average temperature increase, for the profile measured in Orléans, where the last five glaciations and a temperature step of 7 K were considered, was 0.31 K with a maximal value of 0.60 K at the bottom of the profile (Figure 7b). The corrected temperature was used observation to reproduce with the numerical model.

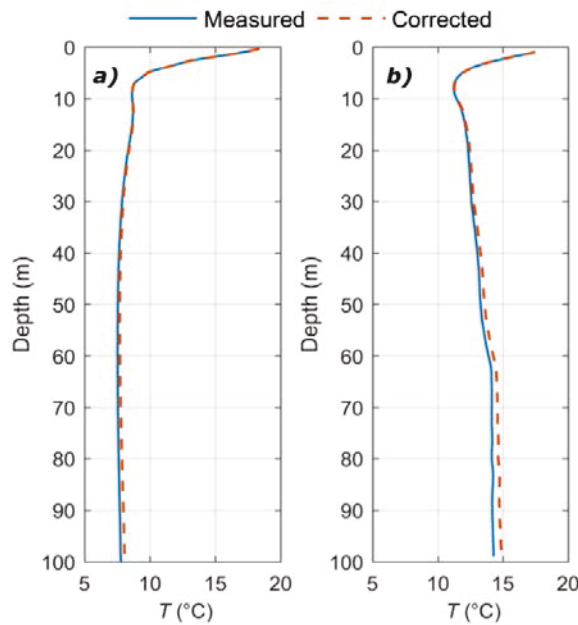


Figure 3.7. Temperatures corrected for paleoclimate effects for the sites a) in Quebec City and b) in Orléans.

#### 3.3.2 Numerical simulation

The sensitivity analysis indicated the mesh resolution and the model depth have an influence on the simulated temperature. A mesh with 60 and 140 elements was needed to achieve accurate simulation of the temperature profile with little temperature difference in between simulation cases for the models representing the experimental site in Quebec City and Orléans, respectively (Table 1). The bottom boundary was defined at 700 m depth in both cases to reduce its influence on the simulated temperature (Table 1). Temperature extracted at 30 m

depth is given to show the impact of the model mesh and bottom boundary position, evidencing the model independence.

**Table 3.1. Verification of the mesh independence and the bottom heat flow boundary position.**

<b>Number of elements</b>		
<b>Site 1</b>	<b>Temperature at 30 m depth</b>	<b>Relative difference (%)</b>
53	8.5061	-
58	8.4445	0.7293
60	8.4445	0.0000
<b>Site 2</b>		
71	12.4230	-
90	12.9881	0.5651
140	13.0961	0.1080
<b>Bottom boundary location (m)</b>		
<b>Site 1</b>		
600	8.1266	-
650	8.1260	0.0076
700	8.1260	0.0000
<b>Site 2</b>		
600	12.9666	-
650	13.2534	2.1639
700	13.0961	1.2009

An initial manual optimization of the heat flow was carried out, in order to reduce the heat flow range to optimize with the solver. The lower and upper bound for the heat flow optimization of the model representing the site in Quebec City were 10 and 40 mW m<sup>-2</sup>, respectively, while a range varying from 30 to 70 mW m<sup>-2</sup> was defined for the site in Orléans. Then, the least-squares function and the coordinate search method were used to optimize the heat flow bottom boundary condition and reproduce the measured temperature profile. The optimization started at the lowest heat flow value.

The least-square residuals for optimization of the heat flow at experimental site 1 decreased from 20 to 7.97 for the best fit scenario (Figure 3.8a), where the basal heat flow was 29 mW m<sup>-2</sup> (Figure 3.9). A heat flow of 47.4 mW m<sup>-2</sup> was found for experimental site 2 (Figure 3.9), with a reduction of the least-square residuals from 571 to 13.57 (Figure 3.8b).

Equilibrium heat flow estimations in the study areas located in cities are not available. Heat flow map of the Quebec Province indicates a heat flow in the range of 30 to 40 mW m<sup>-2</sup> for the Quebec City area (Mareschal *et al.*, 2010). The heat flow estimated with the numerical

simulations in Quebec City correspond to the lower value of this interval. A value varying from 100 to 110 mW m<sup>-2</sup> characterizes the Orléans site according to the heat flow map of France (SIG Mines France, 2007). The estimated heat flow in Orléans is lower than the reported value for the area. Nevertheless, the calculated value is a point estimation of the near-surface heat flow and the map provides estimations at the country scale, making comparison difficult.

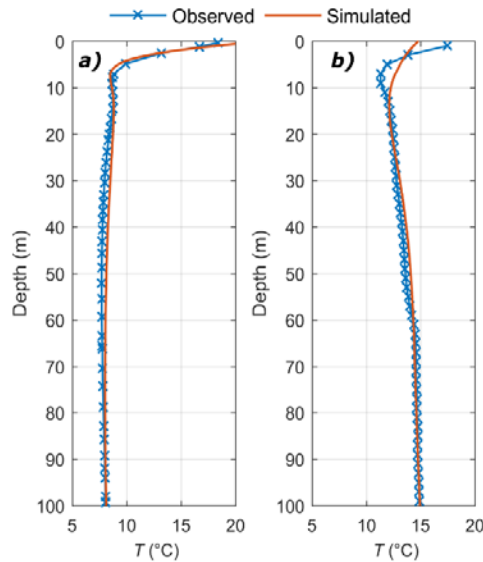


**Figure 3.8. Simulated temperature matched with observed temperature for the sites a) in Quebec City and b) in Orléans.**

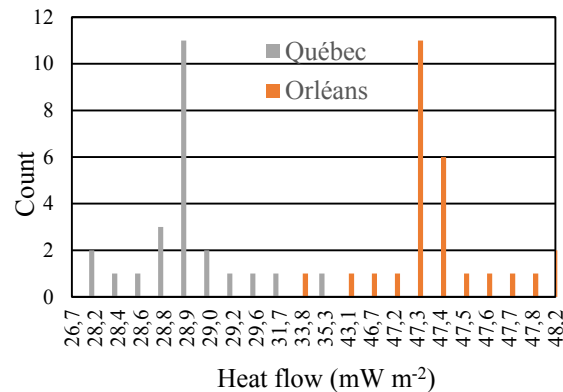


**Figure 3.9. The histogram of basal heat flow values tried by the coordinate search solver to find the solution that best reproduces temperature measurements for the sites a) in Quebec City and b) in Orléans.**

### 3.4 Discussion

A method, relying on thermal response tests (TRT) and undisturbed temperature profiles in ground heat exchangers was presented in this work, to extend the use of TRT for the evaluation

of heat flow essential for deep geothermal resource assessment. The proposed analysis provides a preliminary estimation of the Earth heat flow in the near-surface with relatively shallow boreholes. A depth of approximately 100 m is typically not deep enough to infer ground surface temperature history with inverse simulations of heat transfer to reproduce temperature measured in such a short borehole (Jessop, 1990). A borehole unaffected by paleoclimates in its deeper part is needed to infer both the site heat flow and temperature history in a single optimization sequence. A depth of more than 3000 m seems to be optimal to resolve the temperature rise after the glacial period adequately. Nevertheless, undisturbed temperature logs of that deep are rare (Hartmann & Rath, 2005). In the circumstance of a shallow borehole, ground surface temperature can be evaluated from other paleoclimate studies with deeper boreholes and taken into account to correct the temperature measurement of shallower boreholes. A depth of about 300 to 500 m is suitable to derive a mean temperature for the last 1000 years (Hartmann & Rath, 2005). The observed temperature profiles measured in the studied ground heat exchangers were corrected analytically according to the paleoclimate effects of the quaternary glaciations in North America and Europe with forward calculations since the boreholes analyzed were relatively short. The surface temperature perturbation due to the recent climate warming was treated afterward with numerical simulations because atmospheric temperature record of sufficient time was not available.

In fact, the undisturbed temperature profiles reported for this study were reproduced with an inverse numerical model simulating conductive heat transfer to estimate the site heat flow through the optimization of the bottom boundary condition. The historic ground surface temperature affected by the recent climate warming was used to define the magnitude of temperature changes at the model upper boundary. Data recorded at weather stations constrained simulations to cope with the shallow depth of the 100 m boreholes that is not sufficient to accurately infer the ground surface temperature history. The historic surface temperatures near the experimental site in Orléans were not available before 1996. Therefore, surface temperature history of France was used from 1901 to 1996. This value may not represent the exact temperature variation in the study area and can explain the poor temperature match near the surface. A more accurate estimation of the heat flow at this site would require a better definition of the upper boundary condition. Nevertheless, the heat flow estimated at both sites is small and the potential for deep geothermal resources is low.

The approach presented in this work can be used for the preliminary evaluation of heat flow with TRT and ground heat exchangers, aiming at the exploration of deep geothermal resources of

urban areas. This can reduce exploration risks, where deep wells are sparse and geothermal heat pump system common, which is the case of cities. Deep boreholes suitable for heat flow assessment are rarely drilled in populated towns, although energy needs and potential to develop geothermal direct use can be significant due to the population density.

### 3. 5 Conclusion

An inverse numerical model based on inferred thermal conductivity profiles from thermal response test and temperature profiles measured in ground heat exchangers has been developed to estimate terrestrial heat flux near-surface. This methodology helps to fill the lack of heat flux observations in urban areas. It could be combined in future work with heat flux observations on deep boreholes, outside but close to cities, in order to define the potential of deep geothermal resources of urban areas where the demand for heat is high. The direct use of geothermal resources for heating purposes is generally restricted to one or two kilometers of the pumping and injection wells, a location which must coincide with adjacent energy markets. The analysis of TRTs and temperature profiles is a tangible way to better define the heat flux and geothermal resources of these urban energy markets.

Further work can now be envisioned to collect TRT dataset from private companies and use the approach described in this paper to better define heat flow distribution. For example, more than 100 TRTs have been inventoried in the St. Lawrence Lowlands hosting populated cites of Montreal and Québec (Bédard *et al.*, 2018), while only three deep wells are available for this region to evaluate heat flow (Fou, 1969; Saull *et al.*, 1962). In fact, the Earth heat flow could be estimated where temperature profiles have been measured in ground heat exchangers before doing TRT to improve current geothermal resources assessment based on bottom-hole temperature that is not in equilibrium with the host rock (Bédard *et al.*, 2012; Majorowicz and Minea, 2012). In the absence of equilibrium temperature profiles in deep boreholes, theses authors have used public bottom hole temperature records which can contain mistakes and can be difficult to accurately correct for drilling disturbance, resulting in significant uncertainty about geothermal potential (Bédard *et al.*, 2014). Analysis of equilibrium temperature in ground heat exchangers, although shallow, can help reduce this uncertainty to eventually justify the drilling of a deep borehole for equilibrium temperature profiling. Such invasive exploration work that is more accurate, but has a greater environmental impact, needs to be better justified because of its important cost.

### **III. Conclusions**



## 1 Synthèse des résultats

La première partie du projet de maîtrise concerne les tests de réponse thermique avec câbles chauffants, une méthode développée par Raymond *et al.* (2010) comme une alternative aux tests de réponse thermique conventionnels. Deux tests avec deux câbles chauffants différents et des systèmes de mesure distribuée de la température avec une fibre optique ont été effectués dans deux sites expérimentaux à l'INRS et au BRGM, où des TRT conventionnels avaient été déjà effectués.

La conductivité thermique du sous-sol a été estimée à différentes profondeurs dans les deux forages expérimentaux. Avec le câble chauffant en sections, la conductivité estimée varie de 1.72 à 2.19 W m<sup>-1</sup>K<sup>-1</sup>, avec une moyenne de 2.02 W m<sup>-1</sup>K<sup>-1</sup>. Ces résultats montrent une surestimation de la conductivité thermique par rapport à la valeur estimée lors du test conventionnel (1.75 W m<sup>-1</sup>K<sup>-1</sup>). Cette surestimation est probablement due à l'effet de convection naturelle généré dans le tuyau de l'échangeur de chaleur durant la période d'injection de chaleur.

La convection naturelle a été évaluée en utilisant le critère de stabilité du nombre de Rayleigh (Love *et al.*, 2007) qui permet d'inférer la présence de convection dans des puits d'eau souterraine. Ce critère a été calculé en utilisant les données de température mesurées de façon distribuée. Les résultats ont montré que des mouvements de convection naturelle peuvent être générés pendant l'injection de chaleur quand le câble chauffant en sections est utilisé.

Le deuxième TRT, effectué avec un câble chauffant continu et un taux d'injection chaleur plus bas que dans le test précédent, soit 10 W m<sup>-1</sup> K<sup>-1</sup>, a permis d'évaluer la possibilité de réduire au minimum le taux d'injection chaleur requis pour réaliser le test. Une réduction du taux d'injection de chaleur implique une augmentation de température moins importante et exige une période d'injection de chaleur plus longue. La réduction du taux d'injection de chaleur a pu être effectuée grâce à l'amélioration de la résolution des capteurs de température au cours des dernières années. Des capteurs de température avec une résolution de +/- 0.032 °C ont été utilisés dans cette étude.

La conductivité thermique estimée lors de ce test a été comparée avec la valeur estimée lors d'un test conventionnel. Des différences qui varient entre -48.30 % et +26.53 % ont été trouvées. Néanmoins la valeur moyenne du profil de conductivité thermique estimée avec le câble chauffant correspond à la conductivité thermique globale déterminée avec le test

conventionnel. La réduction du taux d'injection chaleur permettra d'effectuer le TRT avec le câble continu sur des périodes de temps plus longues.

L'incertitude associée à l'estimation de la conductivité thermique lors des deux tests a été évaluée. La méthode proposée par Witte (2013) pour estimer l'incertitude des tests de réponse thermique conventionnels a été adaptée pour les câbles chauffants. Pour le câble chauffant en sections, la méthodologie proposé par Simon (2016), pour un test avec une seule section chauffante, a été utilisée et appliquée aux dix sections chauffantes utilisées lors de l'essai. Une incertitude qui varie entre 14.6 % et 18.4 % a été déterminée. Ces valeurs sont supérieures à l'incertitude estimée pour les tests conventionnels et pour le câble continu. En effet, l'incertitude rapportée par Witte (2013) pour un test conventionnel avec circulation d'eau est d'environ 5.1 % alors qu'avec le câble chauffant continu elle varie entre 2.1 et 2.2 %. Cette incertitude plus élevée pour le TRT avec le câble chauffant en sections, est due à la difficulté d'évaluer avec exactitude le taux d'injection de chaleur pour les essais avec des sections chauffantes. Néanmoins, ces erreurs sont inférieures à l'erreur de 25 % rapporté par Simon (2016) pour l'évaluation de la conductivité thermique à petite échelle avec un test ayant une seule section chauffante. L'incertitude d'un TRT est fortement influencée par l'incertitude associée à l'évaluation du taux d'injection de chaleur, laquelle est mesurée avec plus d'exactitude pour un test avec un câble chauffant continu, qu'avec circulation d'eau et, finalement, qu'avec un câble chauffant en sections.

Dans la deuxième partie du projet de maîtrise, un modèle numérique inverse basé sur les profils de conductivité thermique inférée a été développé pour estimer le flux de chaleur terrestre près de la surface. La conductivité thermique estimée lors des TRT est utilisée comme intrant dans les modèles afin de reproduire les profils de température à l'équilibre mesurés avant les TRT. Le flux de chaleur près de la surface a été estimé pour les deux sites expérimentaux. Au LISTE de l'INRS, un flux de chaleur de  $28.9 \text{ mW m}^{-2}$  a été inféré, cette valeur est cohérente avec l'intervalle de flux de chaleur entre  $30 - 40 \text{ mW m}^{-2}$  défini par (Mareschal & Jaupart, 2004, Mareschal *et al.*, 2000) dans la carte du flux de chaleur du bouclier canadien (Figure 1).

Au BRGM, un flux de chaleur de  $47.3 \text{ mW m}^{-2}$  a été estimé. Cette valeur est faible par rapport à l'intervalle de  $100 - 110 \text{ mW m}^{-2}$  définie pour la ville d'Orléans sur la carte du flux de chaleur de la France (Figure 2; SIG Mines France, 2007). Néanmoins, la comparaison entre les valeurs estimées avec le modèle et les cartes de flux de chaleur est difficile. L'échelle de l'estimation est ponctuelle dans les cas du modèle numérique et une estimation ou interpolation à grande

échelle est effectuée dans les cas de la carte de flux de chaleur et aucun point de mesure sont disponibles pour les villes concernées.

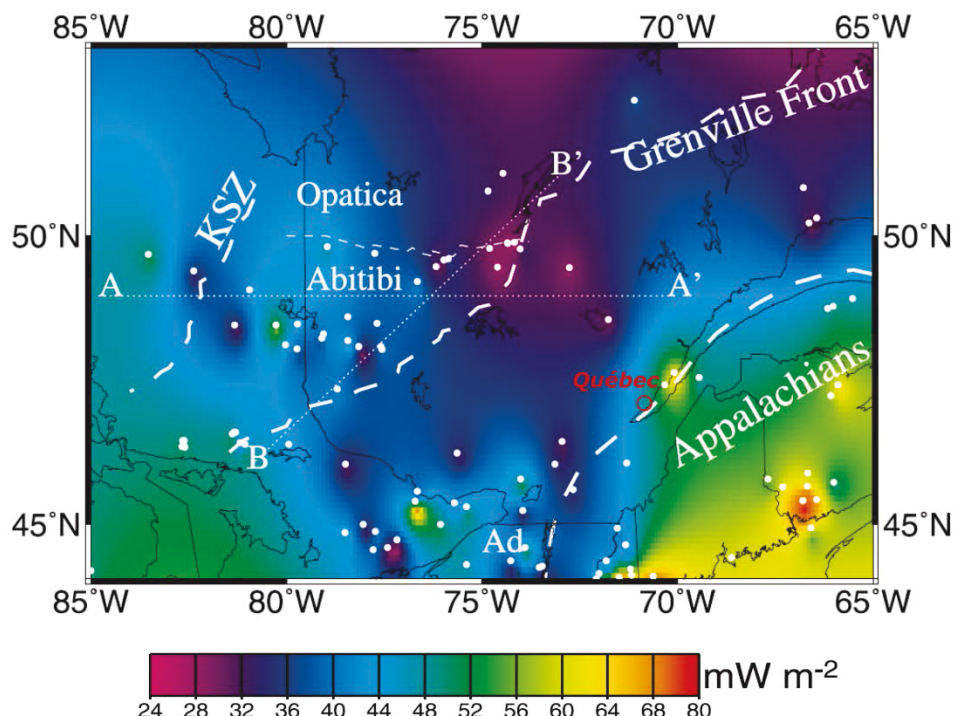


**Figure 1. Carte de flux de chaleur de l'est du Canada. Les points blancs représentent les sites où le flux de chaleur a été évalué avec des mesures en forages généralement plus profonds que ceux utilisés pour les TRT (modifiée de Mareschal *et al.*, 2000).**

Cette étude a permis d'utiliser des câbles chauffants en sections et continus, combinés avec un système de mesure distribuée de la température, pour mieux comprendre les phénomènes de transfert de chaleur lors des TRT. La conductivité thermique du sous-sol sur deux sites expérimentaux et l'incertitude associée à cette estimation a été évaluée. Les deux types de câbles chauffants permettent de réduire la puissance nécessaire pour effectuer un TRT. Avec un câble chauffant continu, l'erreur du test est réduite par rapport à l'erreur d'un test conventionnel (Witte *et al.*, 2002) et d'un test avec des sections chauffantes (Simon, 2016).

Le temps requis pour réaliser un TRT avec des câbles chauffants est plus long qu'un TRT conventionnel (Raymond *et al.*, 2015, Raymond *et al.*, 2010). En utilisant des câbles chauffants, le suivi de la température pendant la période de restitution thermique est nécessaire pour déduire la conductivité thermique (Raymond *et al.*, 2015), ce qui rend le test plus long que les 50 à 80 h recommandées pour les TRT conventionnels (Kavanaugh, 2001). Cependant, l'estimation de la conductivité thermique basée sur la période de restitution thermique est plus exacte qu'avec la période d'injection de chaleur (Raymond *et al.*, 2011c).

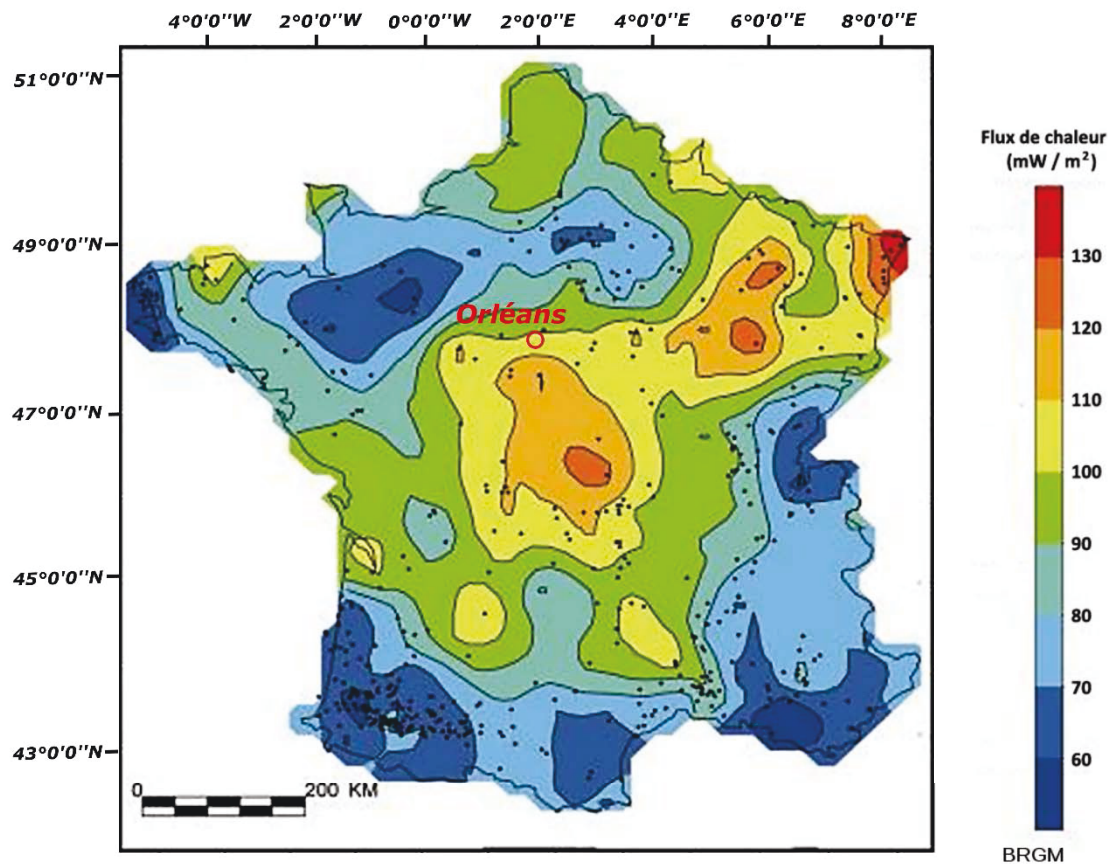


**Figure 2. Carte de flux de chaleur de la France.** Les points noirs représentent les sites où le flux de chaleur a été évalué avec des mesures en forages généralement plus profonds que ceux utilisés pour les TRT (modifiée de SIG Mines France, 2007).

En utilisant un câble chauffant continu d'environ 100 m de longueur, l'expérience de terrain démontre que le taux d'injection de chaleur par longueur unitaire doit être assez faible pour effectuer l'essai avec une puissance électrique inférieure à 1200 W. Une longue période d'injection de chaleur est conséquemment nécessaire pour atteindre une différence de température d'au moins 3 °C dans le tuyau de l'échangeur de chaleur. Le temps total d'un TRT avec un câble chauffant continu est ainsi plus long que celui d'un test avec des sections chauffantes et que celui d'un test conventionnel. Néanmoins, la réduction de l'incertitude du test et les manipulations du terrain simplifiées sont des avantages du test avec un seul câble chauffant continu.

Les mesures de température distribuées avec le FO-DTS et les capteurs de température submersibles permettent d'évaluer la conductivité thermique en fonction de la profondeur, considérant l'hétérogénéité du sol (Fujii *et al.*, 2009), et d'évaluer éventuellement l'influence de l'écoulement d'eau souterraine sur la conductivité thermique à différentes profondeurs (Molina-

Giraldo *et al.*, 2011, Raymond *et al.*, 2011b). Ce dernier aspect pourrait être développé davantage dans des travaux futurs. Un modèle numérique basé sur les données d'un TRT a été proposé pour estimer le flux de chaleur près de la surface. Cette application permettra d'élargir l'utilisation des TRT pour des explorations préliminaires des ressources géothermiques profondes.

## 2 Conclusions

Les résultats des deux TRT effectués avec des câbles chauffants ont montré qu'il est préférable d'utiliser la méthodologie associée au câble continu plutôt qu'en sections pour réaliser l'essai dans des forages de 100 m de profondeur. Ceci est possible en utilisant un taux d'injection de chaleur faible lorsque la résolution des capteurs de température est suffisante, soit +/- 0.1 °C pour cette étude.

Le critère de stabilité du nombre de Rayleigh a suggéré la présence de convection naturelle pendant la période d'injection de chaleur dans le TRT avec le câble chauffant en sections. L'évaluation de la convection naturelle et l'analyse d'incertitude indiquent que le test avec le câble chauffant continu est plus exact que le test avec le câble chauffant en sections. En utilisant le câble chauffant continu, l'hypothèse des transferts de chaleur par conduction est validée et l'incertitude totale de l'essai est plus faible lorsque comparée au TRT avec sections chauffantes.

Le câble en sections permet toutefois d'effectuer l'essai dans des forages de plus de 100 m sans augmenter le taux d'injection de chaleur. Cependant, l'analyse du TRT avec le câble chauffant en sections est limitée par l'effet de la convection naturelle qui n'est pas incluse dans le modèle analytique. Une analyse plus poussée est nécessaire pour évaluer le rapport entre le transfert de chaleur par conduction et par convection afin d'ajuster la méthodologie d'analyse du test avec le câble chauffant en sections. La longueur chauffante définie pour effectuer l'analyse, ainsi que l'inclusion de la convection naturelle dans le modèle analytique pourraient être réévalués. L'analyse du TRT avec sections chauffantes pourrait aussi être effectuée avec un modèle numérique, facilitant la simulation des transferts thermiques par convection naturelle.

L'utilisation du câble chauffant continu dans des forages profonds est limitée par l'incrément de la résistance électrique du câble avec sa longueur, imposant une diminution du taux d'injection de chaleur. Dans des travaux futurs, un TRT avec un câble chauffant en sections couplé à un système distribué de mesure de la température (FO-DTS) et un taux d'injection de chaleur faible (tel qu'il a été fait avec le câble chauffant continu) pourrait être effectué afin de vérifier si

l'effet de convection naturelle est minimisé par la réduction du taux d'injection chaleur. Un TRT avec un câble chauffant continu de plus de 100 m, et des capteurs de température de haute résolution devrait aussi être effectué afin de vérifier l'applicabilité du câble chauffant continu dans des forages d'environ 150 m de profondeur couramment utilisés pour les échangeurs de chaleur géothermique.

L'analyse des profils de température mesurée dans les échangeurs de chaleur couplés aux données de conductivité thermique issue des TRT fournit une estimation préliminaire du flux de chaleur terrestre près de la surface. Les estimations du flux de chaleur sont généralement éparses et non uniformément réparties, en particulier dans les zones urbaines où les forages profonds sont inhabituels. Cette méthodologie contribue à combler le manque d'observations de flux de chaleur dans les zones urbaines. Elle pourrait être combinée dans des travaux futurs aux observations de flux de chaleur sur les forages profonds afin de définir le potentiel des ressources géothermiques profondes au niveau des villes où la demande en chauffage est élevée. L'utilisation directe des ressources géothermiques pour des fins de chauffage se fait dans un rayon généralement restreint, soit un ou deux kilomètres des puits de pompage dont la localisation doit coïncider avec des marchés énergétiques limitrophes. L'analyse des TRT et des profils de température apparaît une avenue tangible pour mieux définir le flux de chaleur et les ressources géothermiques de ces marchés énergétiques urbains. Cette analyse fournit une estimation préliminaire du flux de chaleur avant de procéder à des travaux d'exploration plus invasifs qui sont bien entendu plus exacts, mais dont l'impact environnemental et le coût sont plus importants.

## RÉFÉRENCES

- Acuña J, Palm B. (2013). Distributed thermal response tests on pipe-in-pipe borehole heat exchangers. *Applied Energy* 109:312-320. doi:10.1016/j.apenergy.2013.01.024.
- Allis RG. (1978). The effect of Pleistocene climatic variations on the geothermal regime in Ontario: a reassessment. *Canadian Journal of Earth Sciences* 16(7):1517-1517. doi:10.1139/e79-137.
- Asselin S. (2014). Manuel d'utilisation: Appareil de lecture de conductivité thermique. Internal report, Institut national de la recherche scientifique, Quebec City.
- Austin III WA. (1998). Development of an in situ system for measuring ground thermal properties. Master thesis, Oklahoma State University, Oklahoma City.
- Ballard JM, Koubikana C, Raymond J. (2016). Développement des tests de réponse thermique automatisés et vérification de la performance des forages géothermiques d'un diamètre de 4,5 po. Internal report R1601, Institut national de la recherche scientifique, Quebec City.
- Beck AE, Anglin FM, Sass JH. (1971). Analysis of Heat Flow Data—in situ Thermal Conductivity Measurements. *Canadian Journal of Earth Sciences* 8(1):1-19. doi:10.1139/e71-001.
- Beck AE. (1977). Climatically perturbed temperature gradients and their effect on regional and continental heat-flow means. *Tectonophysics*, 41(1), 17-39. doi:[https://doi.org/10.1016/0040-1951\(77\)90178-0](https://doi.org/10.1016/0040-1951(77)90178-0).
- Bédard K, Comeau FA, Raymond J, Gloaguen E, Comeau G, Millet E, Foy S. (2018). Cartographie de la conductivité thermique des Basses-Terres du Saint-Laurent. Rapport de recherche (R1789). INRS, Centre Eau Terre Environnement, Québec.
- Bédard K, Comeau F-A, Raymond J, Malo M, Nasr M. (2017). Geothermal Characterization of the St. Lawrence Lowlands Sedimentary Basin, Québec, Canada. *Natural Resources Research* 10.1007/s11053-017-9363-2. doi:10.1007/s11053-017-9363-2.

Bédard K, Raymond J, Malo M, Konstantinovskaya E, Minea V. (2014). St. Lawrence Lowlands bottom-hole temperature: various correction methods. GRC Trans. 38, 351–355.

Beier RA, Acuña J, Mogensen P, Palm B. (2012). Vertical temperature profiles and borehole resistance in a U-tube borehole heat exchanger. Geothermics 44:23-32. doi:10.1016/j.geothermics.2012.06.001.

Bense VF, Read T, Bour O, Le Borgne T, Coleman T, Krause S, Chalari A, Mondanos M, Ciocca F, Selker JS. (2016). Distributed Temperature Sensing as a downhole tool in hydrogeology. Water Resources Research 52(12):9259-9273. doi:10.1002/2016WR018869.

Berthold S, Resagk C. (2012). Investigation of thermal convection in water columns using particle image velocimetry. Experiments in Fluids, 52(6), 1465-1474. doi:<https://doi.org/10.1007/s00348-012-1267-7>.

Bi Y, Wang X, Liu Y, Zhang H, Chen L. (2009). Comprehensive exergy analysis of a ground-source heat pump system for both building heating and cooling modes. Applied Energy 86(12):2560-2565. doi:10.1016/j.apenergy.2009.04.005.

BIPM, IEC, IFCC, ILAC, ISO, & IUPAC. (2008). Evaluation of Measurement Data—Supplement 1 to the Guide to the Expression of Uncertainty in Measurement,” Propagation of Distributions Using a Monte Carlo Method, Joint Committee for Guides in Metrology. Bureau International des Poids et Mesures, JCGM, 101.

Bodri L, Cermak V. (2007). CHAPTER 2 - Climate Change and Subsurface Temperature. in *Borehole Climatology* (pp 37-173). Oxford: Elsevier.

Bozdağ Ş, Turgut B, Paksoy H, Dikici D, Mazman M, Evliya H. (2008). Ground water level influence on thermal response test in Adana, Turkey. International Journal of Energy Research 32(7):629-633. doi:10.1002/er.1378.

Carslaw HS. (1945). Introduction to the mathematical theory of the conduction of heat in solids. Macmillan: London, England, 1921..

Chang KS, Kim MJ. (2016). Thermal performance evaluation of vertical U-loop ground heat exchanger using in-situ thermal response test. *Renewable Energy* 87(Part 1):585-591. doi:10.1016/j.renene.2015.10.059.

COMSOL AB. (2016). COMSOL Multiphysics Reference Manual. Stockholm.

COMSOL AB. (2013). Optimization Module User's Guide, version 4.4. Stockholm.

Conn AR, Scheinberg K. Vicente LN. (2009). Introduction to derivative-free optimization (Vol. 8). Philadelphia: Siam.

Davies JH (2013) Global map of solid Earth surface heat flow. *Geochemistry, Geophysics, Geosystems* 14(10):4608-4622. doi:10.1002/ggge.20271.

Davies JH, Davies DR. (2011) Earth's surface heat flux. *Solid Earth*, 1(1):5-24. doi:10.5194/se-1-5-2010.

Eklöf C, Gehlin S. (1996). TED-a mobile equipment for thermal response test: testing and evaluation. Master thesis, Luleå University of Technology, Luleå.

Ellison S, Williams A. (2012). Eurachem/CITAC guide: Quantifying Uncertainty in Analytical Measurement. Laboratory of the Government Chemist, London.

Freifeld BM, Finsterle S, Onstott TC, Toole P, Pratt LM. (2008). Ground surface temperature reconstructions: Using in situ estimates for thermal conductivity acquired with a fiber-optic distributed thermal perturbation sensor. *Geophysical Research Letters*, 35(14). doi:10.1029/2008GL034762.

Fou JTK. (1969). Thermal conductivity and heat flow at St. Jérôme, Quebec (M.Sc. Thesis). McGill University, Montreal, Canada.

Fujii H, Okubo H, Nishi K, Itoi R, Ohyama K, Shibata K. (2009). An improved thermal response test for U-tube ground heat exchanger based on optical fiber thermometers. *Geothermics* 38(4):399-406. doi:10.1016/j.geothermics.2009.06.002.

Fujii H, Okubo H, Itoi R. (2006). Thermal response tests using optical fiber thermometers. *GRC transactions* 30:545-551.

- Gehlin S, Hellström G. (2003). Influence on thermal response test by groundwater flow in vertical fractures in hard rock. *Renewable Energy* 28(14):2221-2238. doi:10.1016/S0960-1481(03)00128-9.
- Gehlin S. (2002). Thermal response test method development and evaluation. Doctoral dissertation, Luleå University of Technology, Luleå.
- Gehlin S. (1998). Thermal response test: in situ measurements of thermal properties in hard rock. Licentiate dissertation, Luleå University of Technology, Luleå.
- Golovanova IV, Sal'manova RY, Tagirova CD. (2014). Method for deep temperature estimation with regard to the paleoclimate influence on heat flow. *Russian Geology and Geophysics* 55(9):1130-1137. doi:<https://doi.org/10.1016/j.rgg.2014.08.008>.
- Gustafsson AM, Westerlund L. (2011). Heat extraction thermal response test in groundwater-filled borehole heat exchanger – Investigation of the borehole thermal resistance. *Renewable Energy* 36(9):2388-2394. doi: 10.1016/j.renene.2010.12.023.
- Hartmann A, & Rath V. (2005). Uncertainties and shortcomings of ground surface temperature histories derived from inversion of temperature logs. *Journal of Geophysics and Engineering*, 2(4), 299.
- Ingersoll LR, Plass HJ. (1948). Theory of the ground heat pipe heat source for the heat pump. *Transactions of the American Society of Heating and Ventilating Engineers* 20, 119–122.
- IPCC. (2011). Summary for Policymakers. In: IPCC Special Report on Renewable Energy Sources and Climate Change Mitigation. Édit [O. Edenhofer, R. Pichs-Madruga, Y. Sokona, K. Seyboth, P. Matschoss, S. Kadner, T. Zwickel, P. Eickemeier, G. Hansen, S. Schlömer & (Eds)]. CVSCambridge University Press, Cambridge and New York.
- Jessop AM. (1990). Chapter 3 - Analysis and Correction of Heat Flow on Land. *Thermal Geophysics* (pp 57-85). Vol.17. Amsterdam: Elsevier.
- Kavanaugh S. (2001). Investigation of methods for determining soil formation thermal characteristics from short term field tests. American Society of Heating, Refrigerating and Air-Conditioning Engineers, Atlanta.

Klepikova M, Roques C, Loew S., Selker, J. (2018). Improved Characterization of Groundwater Flow in Heterogeneous Aquifers Using Granular Polyacrylamide (PAM) Gel as Temporary Grout. *Water Resources Research* 54, 1410–1419. doi:10.1002/2017WR022259.

Lasdon LS, Waren AD, Jain A, Ratner M. (1978). Design and testing of a generalized reduced gradient code for nonlinear programming. *ACM Transactions on Mathematical Software* 4(1):34-50. doi:10.1145/355769.355773.

Love AJ, Simmons CT, Nield DA. (2007). Double-diffusive convection in groundwater wells. *Water resources research* 43(8). doi:10.1029/2007WR006001.

Majorowicz JA, Minea V. (2012). Geothermal energy potential in the St-Lawrence River area, Québec. *Geothermics* 43, 25–36. <https://doi.org/10.1016/j.geothermics.2012.03.002>.

Majorowicz J, Wybraniec S. (2011). New terrestrial heat flow map of Europe after regional paleoclimatic correction application. *International Journal of Earth Sciences* 100(4):881-887. doi:10.1007/s00531-010-0526-1.

Majorowicz J, Šafanda J. (2008). Heat flow variation with depth in Poland: evidence from equilibrium temperature logs in 2.9-km-deep well Torun-1. *International Journal of Earth Sciences* 97(2):307-315. doi:10.1007/s00531-007-0210-2.

Maragna C. (2014). Analyse d'un test de réponse thermique. Internal report, Division Géothermie, Bureau de Recherche Géologique et Minières de France, Orléans.

Marcotte D, Pasquier P. (2008). On the estimation of thermal resistance in borehole thermal conductivity test. *Renewable Energy* 33(11):2407-2415. doi:10.1016/j.renene.2008.01.021.

Mareschal JC, Jaupart C. (2004). Variations of surface heat flow and lithospheric thermal structure beneath the North American craton. *Earth and Planetary Science Letters* 223(1):65-77. doi: 10.1016/j.epsl.2004.04.002.

Mareschal JC, Jaupart C, Gariépy C, Cheng LZ, Guillou-Frottier L, Bienfait G, Lapointe R. (2000). Heat flow and deep thermal structure near the southeastern edge of the Canadian Shield. *Canadian Journal of Earth Sciences* 37(2-3):399-414.doi: 10.1139/e98-106.

Mogensen P. (1983). Fluid to duct wall heat transfer in duct system heat storages. International Conference on Subsurface Heat Storage in Theory and Practice, Stockholm.

Molina-Giraldo N, Blum P, Zhu K, Bayer P, Fang Z. (2011). A moving finite line source model to simulate borehole heat exchangers with groundwater advection. International Journal of Thermal Sciences 50(12):2506-2513.doi:10.1016/j.ijthermalsci.2011.06.012.

Mustafa Omer A. (2008). Ground-source heat pumps systems and applications. Renewable and Sustainable Energy Reviews 12(2):344-371. doi:10.1016/j.rser.2006.10.003.

Ouzzane M, Eslami-Nejad P, Badache M, Aidoun Z. (2015). New correlations for the prediction of the undisturbed ground temperature. Geothermics 53:379-384. doi:10.1016/j.geothermics.2014.08.001.

Pehme P, Greenhouse J, Parker BL. (2007a). The Active Line Source (ALS) technique, a method to improve detection of hydraulically active fractures and estimate rock thermal conductivity. 60th Canadian Geotechnical Conf. & 8th Joint CGS/IAH-CNC Groundwater Conference, Ottawa.

Pehme PE, Greenhouse JP, Parker BL. (2007b). The active line source temperature logging technique and its application in fractured rock hydrogeology. Journal of Environmental & Engineering Geophysics 12(4):307-322. doi:10.2113/jegg12.4.307.

Philippe M. (2010). Development and experimental validation of vertical and horizontal ground heat exchangers for residential buildings heating. Thèse de doctorat, École Nationale Supérieure des Mines de Paris, Paris.

Raymond J. (2018). Colloquium 2016: Assessment of the subsurface thermal conductivity for geothermal applications. Canadian Geotechnical Journal, 55(9), 1209-1229. doi:10.1139/cgj-2017-0447.

Raymond J, Ballard J-M, Koubikana Pambou CH. (2017). Field assessment of a ground heat exchanger performance with a reduced borehole diameter. in 70th Canadian Geotechnical Conference and the 12th Joint CGS/IAH-CNC Groundwater Conference, Ottawa.

Raymond J, Lamarche L, Malo M. (2016). Extending thermal response test assessments with inverse numerical modeling of temperature profiles measured in ground heat exchangers. Renewable Energy 99:614-621. doi:10.1016/j.renene.2016.07.005.

Raymond J, Lamarche L, Malo M. (2015). Field demonstration of a first thermal response test with a low power source. Applied Energy 147:30-39. doi:10.1016/j.apenergy.2015.01.117.

Raymond J, Lamarche L. (2014). Development and numerical validation of a novel thermal response test with a low power source. Geothermics 51:434-444. doi:10.1016/j.geothermics.2014.02.004.

Raymond J, Therrien R, Gosselin L. (2011a). Borehole temperature evolution during thermal response tests. Geothermics 40(1):69-78. doi:10.1016/j.geothermics.2010.12.002.

Raymond J, Therrien R, Gosselin L, Lefebvre R. (2011b). Numerical analysis of thermal response tests with a groundwater flow and heat transfer model. Renewable Energy 36(1):315-324. doi: 10.1016/j.renene.2010.06.044.

Raymond J, Therrien R, Gosselin L, Lefebvre R. (2011c). A review of thermal response test analysis using pumping test concepts. Ground Water 49(6):932-945. doi: 10.1111/j.1745-6584.2010.00791x.

Raymond J, Robert G, Therrien R, Gosselin L. (2010). A novel thermal response test using heating cables. World Geothermal Congress, Bali.

Sanner B, Hellström G, Spitler J, Gehlin S. (2013). More than 15 years of mobile Thermal Response Test—a summary of experiences and prospects. European Geothermal Congress, Pisa.

Sanner B, Hellström G, Spitler J, Gehlin S. (2005). Thermal response test—current status and world-wide application. World geothermal congress, Antalya.

Sarbu I, Sebarchievici C. (2014). General review of ground-source heat pump systems for heating and cooling of buildings. Energy and Buildings 70(Supplement C):441-454. doi:10.1016/j.enbuild.2013.11.068.

Sass JH, Beardmore G. (2011). Heat Flow Measurements, Continental. *Encyclopedia of Solid Earth Geophysics* (pp 569-573). Dordrecht: Springer. doi:10.1007/978-90-481-8702-7\_72.

Saull VA, Clark TH, Doig RP, Butler RB. (1962). Terrestrial Heat Flow in the St. Lawrence Lowland of Québec. *Can. Min. Metall. Bull.* 65, 63–66.

Self SJ, Reddy BV, Rosen MA. (2012). Geothermal heat pump systems: Status review and comparison with other heating options. *Applied Energy* 101(Supplement C):341-348. doi:10.1016/j.apenergy.2012.01.048.

SIG Mines France. (2007). Données thermiques (flux de chaleur et température). Bureau de recherches géologiques et minières, Orléans. [http://sigminesfrance.brgm.fr/geophy\\_flux.asp](http://sigminesfrance.brgm.fr/geophy_flux.asp). (Consulté le 15 mai 2018).

Simon F. (2016) Développement d'une approche nouvelle pour les tests de réponse thermique en géothermie. Mémoire de maîtrise, École de technologie supérieure, Montréal.

Spitler JD, Gehlin S. (2015). Thermal response testing for ground source heat pump systems—An historical review. *Renewable and Sustainable Energy Reviews* 50:1125-1137. doi:10.1016/j.rser.2015.05.061.

van de Giesen N, Steele-Dunne S C, Jansen J, Hoes O, Hausner M B, Tyler S, Selker J. (2012). Double-Ended Calibration of Fiber-Optic Raman Spectra Distributed Temperature Sensing Data. *Sensors* (Basel, Switzerland), 12(5), 5471-5485. doi:10.3390/s120505471.

Velez-Marquez MI, Raymond J, Blessent D, Philippe M, Simon N, Bour O, Lamarche L. (2018). Distributed thermal response tests using a heating cable and fiber optic temperature sensing. *Energies* 2018, 11(11), 3059; <https://doi.org/10.3390/en11113059>

Westaway R, Younger PL. (2013). Accounting for paleoclimate and topography: A rigorous approach to correction of the British geothermal dataset. *Geothermics* 48:31-51. doi:10.1016/j.geothermics.2013.03.009.

Witte HJL. (2013). Error analysis of thermal response tests. *Applied Energy* 109(Supplement C):302-311. doi: 10.1016/j.apenergy.2012.11.060.

Witte HJL, van Gelder G, Spitler JD. (2002). In-situ thermal conductivity testing: A dutch perspective. *ASHRAE Transactions* 108(1):263–272.

Zhang C, Guo Z, Liu Y, Cong X, Peng D. (2014). A review on thermal response test of ground-coupled heat pump systems. *Renewable and Sustainable Energy Reviews* 40:851-867.  
doi:10.1016/j.rser.2014.08.018.